Part 2 Open-type Wharves on Piles (Semi Draft)

June 2025

1. Technical Notes

Reference

1-1. Characteristics of Open-type Wharves on Piles

The open-type wharves on piles are mooring facilities composed of the main wharf body and the retaining seawall behind the wharf. The retaining seawall consists of a slope and a retaining wall and is often structured to resist earth pressure and sliding from behind. The open-type wharves on piles are lightweight structures with a concrete deck placed on top of pillars such as vertical piles and raking piles.

Raking piles are more stable than vertical piles and can minimize displacement of the pile heads, making them more resistant to earthquakes and suitable for deep water and soft ground conditions. However, raking piles are often combined with vertical piles, which may make construction management more complicated, and may require higher material and labor costs than the vertical piles. The design example of raking piles is introduced in Part 5 Platform and Dolphin section.

1-2. Basic Policy for Performance Verification

All open-type wharves on piles shall satisfy serviceability requirements on variable states such as ship actions, surcharge load, earthquake motions, and wave impacts. The standard performance verification procedure for open-type wharves on piles is shown in Figure 1.1.

When evaluating the performance of open-type wharves on piles, the following points should be taken into consideration:

- ✓ The performance verification flow shown in Figure 1.1 omits an assessment of the impact of liquefaction due to earthquake
- ✓ Since the performance verification of the wharf is based on the principle that the deformation of the retaining wall will not transmit its effects to the wharf structure. Therefore, the structural specifications and/or construction shall take this principle into consideration.
- ✓ When installing cargo handling equipment such as container cranes, it is generally desirable to install them independently either on the wharf deck or on the retaining wall. If the crane legs must straddle the wharf deck and the retaining wall, sufficient foundation work, such as pile foundations, should be provided to prevent differential settlement.
- ✓ When installing cargo handling equipment such as container cranes, it is necessary to perform seismic response analysis considering the resonance phenomenon of the cargo handling equipment and the wharf.
- ✓ Open-type wharves on piles are in harsh environments, and due to material degradation, such as salt damage to concrete members and corrosion of steel materials, the performance of members is prone to decline. Therefore, sufficient consideration should be given to maintenance during the service life at the design stage.
- ✓ In evaluating the actions, if it is deemed necessary to consider the rotation of the deck blocks, the additional study should take this into account.

Three-dimensional analysis enables the consideration of normal directional continuity and the torsion of blocks resulting from eccentric loads, facilitating more realistic evaluations. In contrast, two-dimensional analysis offers the advantage of using simplified

models comparable to those in three-dimensional analysis, with the clarity of the calculation process enhancing its versatility. Given the increasing prevalence of three-dimensional modeling in the world, the example presented in this Casebook is invaluable for both validating three-dimensional models and enhancing engineers' comprehension of design methodologies.

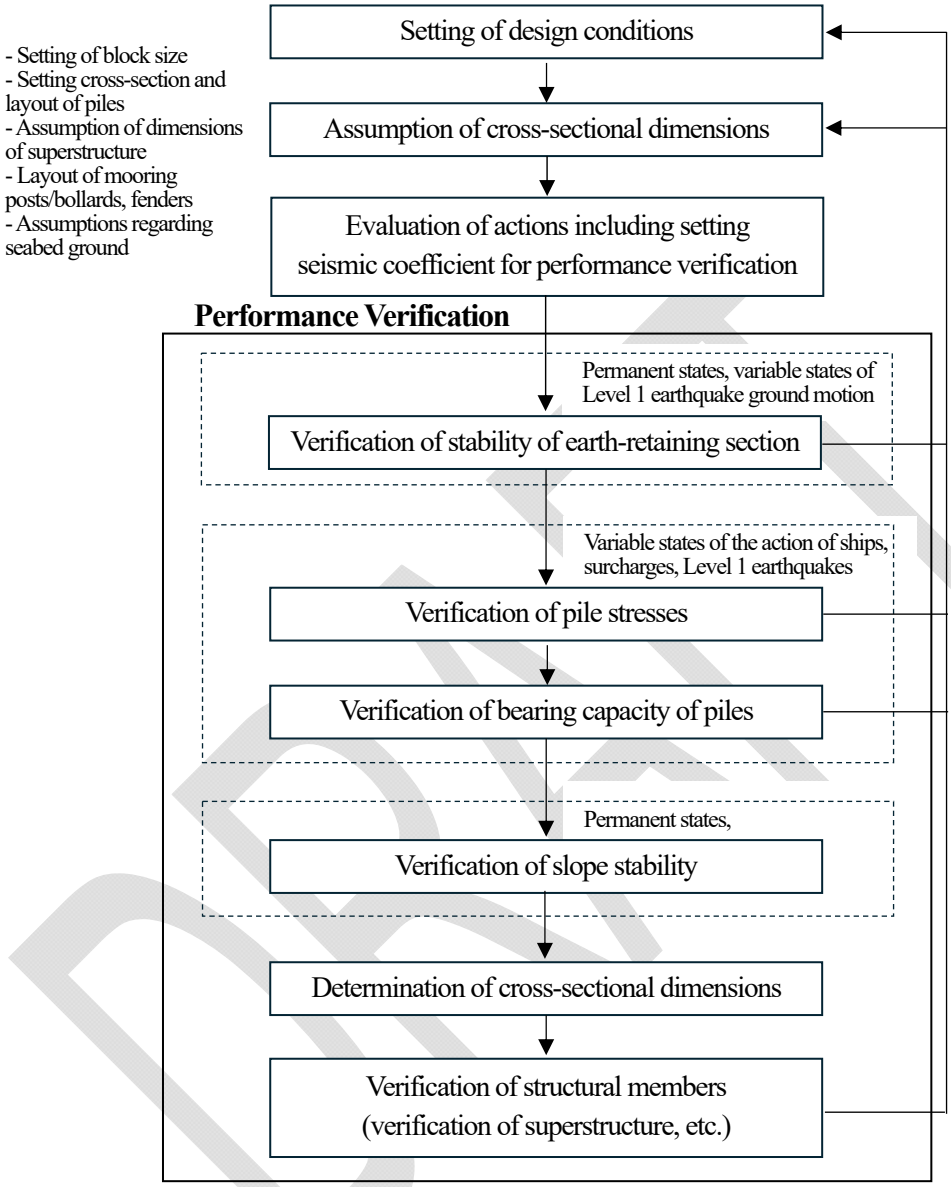

Note: Evaluation of the effect of liquefaction and settlement is not shown in the diagram; therefore, it is necessary these effects separately. Verification shall be carried out for high earthquake-resistance facilities against Level 2 earthquake ground motion.

Source: Modified from TCVN 11820-5-2021

Figure 1.1- Flow Chart of Performance verification

Modified from TCVN 11820 Part 5: 2021, Hinh 3

1-3. Design Conditions

(1) Setting of Block Size

The size of deck block is determined by considering the following factors:

- ✓ Ground conditions, such as slope stability of seawall
- ✓ Static loads and live loads
- ✓ Distances between piles and pile rows, and the shape and dimensions of piles
- ✓ Easiness of form work and timbering

- ✓ Tide level
- ✓ Arrangement of bollards, and/or shape and dimensions of fenders

(2) Specifications of Piles

Open-type wharves on piles normally use one or combination of other types of pile.

1) Pretensioned Spun High Strength Concrete Piles (PHC piles)

- ✓ The maximum length per pile in Vietnam as of 2024 is approximately 60m or more. However, the unit length may be determined based on handling capacity during lifting and driving operations.
- ✓ PHC piles differ from reinforced precast piles in that they are better able to resist tensile stresses during handling, driving and in service than reinforced piles.
- ✓ Pile joints should have the necessary bending moment capacity and be protected against corrosion.
- ✓ Recent research findings suggest that, in addition to the internal reinforcement rebar, when cutting off the head of PHC pile, only the concrete above the cutting level should be removed, leaving some of the rebar/PC bar in place to anchor it firmly to the superstructure.

PHC pile is commonly used in Vietnam, and engineers have addressed various design issues. However, construction challenges such as pile cutting due to high refusal and the occurrence of cracks in the piles can present significant problems. Below, examples of how to address these construction challenges are provided.

i) Pile cutting due to high refusal

The cutting of PHC piles leads to a localized reduction in prestress, therefore, reinforcement in the impacted sections is necessary. The area of localized reduction is referred to the following study results. The range of localized reductions in prestress due to cut-off of PHC piles is approximately 20 to 30 times the diameter of the PC steel bar in the cut-off tests in Figure 1.20 and Table 1.15.

Specifications for Highway Bridges: 2012

In addition, according to the Japan Road Association's 'Specifications for Highway Bridges', when cutting off the head of a PHC pile, the area within 50φ (φ is the diameter of the PC steel bar) from the cut-off point loses prestress and is treated as a cross section of reinforced concrete. In other words, when cutting off the head of a pile, it must be fully embedded in the deck or reinforced with reinforced concrete and other methods.

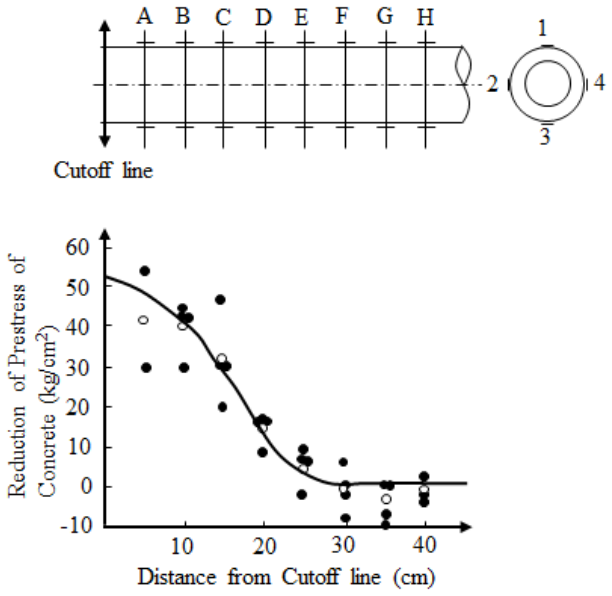

Source: Q&A for design and construction prefabricated concrete pile: 2009

Figure 1.2- Cut-off Test Results

Table 1.1- Summary Table of Cut-off Test Results

No	1	2	3	4	Average
A	135 (54)	- (-)	75 (30)	- (-)	105 (42)
B	110 (44)	105 (42)	105 (42)	75 (30)	99 (40)
C	75 (30)	115 (46)	75 (30)	50 (20)	79 (32)
D	40 (16)	40 (16)	35 (14)	20 (8)	34 (14)
E	15 (6)	20 (8)	15 (6)	-5 (-2)	11 (4)
F	15 (6)	-5 (-2)	-20 (-8)	0 (0)	-3 (-1)
G	0 (0)	-20 (-8)	-25 (-10)	0 (0)	-11 (-4)
H	5 (2)	-10 (-4)	-5 (-2)	0 (0)	-3 (-1)

Note: Unit: μ, ( ) is kg·cm^2 as the reduction of prestress, Age: 21days,
Diameter of PC steel bar: 9.0mm, Effective prestress: 53kg/cm^2

Source: Q&A for design and construction prefabricated concrete pile: 2009

ii) Cracks during construction

Cracking during construction is generally not permitted, for the following reasons:

- ✓ Difficulty in controlling the width of cracks occurring during construction
- ✓ Difficulty in controlling deformation after loss of rigidity due to cracking
- ✓ Lack of data concerning shrinkage and creep behavior in the compressive zone of cracked concrete at the serviceability limit state

When all of the above issues have been adequately resolved, cracking during construction may be permitted.

2) Bored Piles

- ✓ Bored cast in-situ piles are particularly suitable for use as non-displacement friction piles in stiff clay or weak rock, or to achieve large load-bearing capacities by means of the large shaft diameters available or by under-reaming the toe.
- ✓ Construction and acceptance requirements shall be compliant TCVN 9395.
- ✓ Examination of resistance of bored piles shall be compliant TCVN 11820-4-1: 2019.

3) Steel Piles

- ✓ Steel piles are relatively light and easy to handle, and can be driven in most types of ground, including many types of weathered rock.
- ✓ H-piles are also useful as tension piles because of the large penetrations which can be achieved. Circular piles are more suitable where large axial and bending effects are to be resisted. In weathered rock condition, the advantages of each type may be employed in a composite pile comprising a bottom H-section, driven to achieve uplift resistance and welded to the inside of a tubular upper section which is used to resist vertical and horizontal actions.
- ✓ Steel piles have good energy-absorption properties and may therefore be used, when installed vertically, to resist horizontally applied actions. If a concrete encasement is added for corrosion protection, the necessary limitations on maximum strain might require the permissible energy absorption to be reduced.
- ✓ When the bearing layer is shallow, the tip of the steel pipe pile can be reinforced with an underreaming method to ensure pull-out bearing capacity as shown in Figure 1.3. Anchor and socket types are available and are installed by drilling into the steel pipe pile.

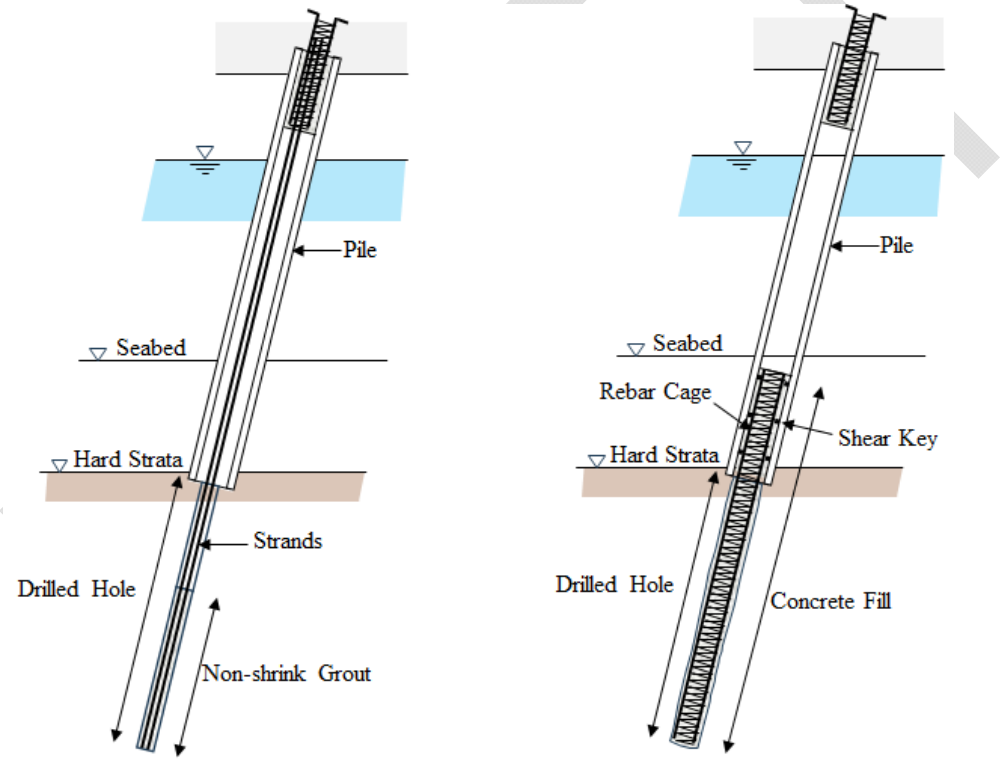

Source: JICA Team

Figure 1.3- Underreaming Methods

(3) Specifications of Superstructure

The specifications of the superstructure are determined by considering the following factors:

- ✓ Pile spacing and pile row spacing, along with the shape and dimensions of the piles
- ✓ Dead load and live load
- ✓ Tide levels and wave condition such as uplift force
- ✓ Construction issues related to formwork and scaffolding
- ✓ Arrangement of mooring bollards
- ✓ Arrangement, shape, and dimensions of fenders

The superstructure of the wharf typically adopts a cast-in-place reinforced concrete structure. According to past records, for general wharves (targeting ships around 10,000 tons) where cranes are loaded, the standard dimensions of the wharf superstructure are as follows:

- ✓ Pavement thickness: 10 cm (concrete pavement)
- ✓ Deck thickness: 25 to 40 cm
- ✓ Girder height: 100 to 200 cm
- ✓ Girder width: approximately the width of the pile
- ✓ Overhang: 1.5 to 2.0 meters from the center of the support pile

Precast concrete units may be used for part of the superstructure in Vietnam. The dimension of superstructure varies depending on site conditions such as handling capacity and pile spacing. Therefore, this design example will not include a precast superstructure. However, examples of precast systems are shown in Figure 1.4 and 1.5. The precast longitudinal beam and/or precast transverse beam can be used as temporary members by reducing the concrete cover. There is a risk of concrete spalling and internal cracks progressing due to corrosion of reinforcement bar. If the precast longitudinal beam and/or precast transverse beam can be used as permanent members, it is necessary to sufficiently consider its handling capacity, bond ability with cast-in-place concrete, continuity of reinforcing bars at span joints and cracking of the precast beam.

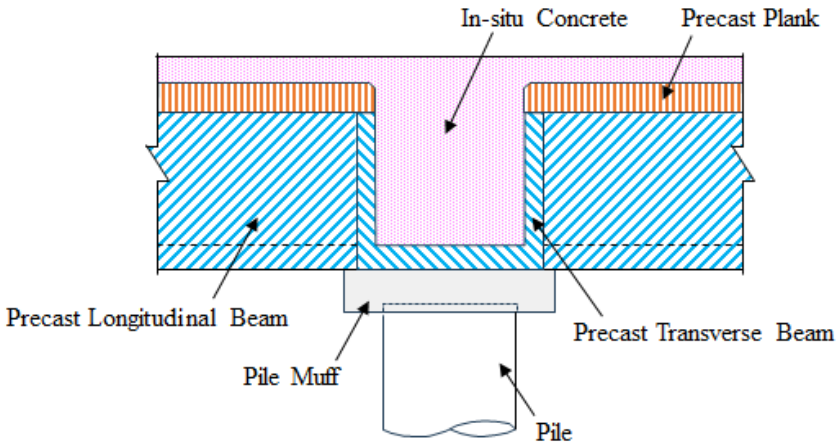

Figure 1.4- Typical Concrete Members of Precast System

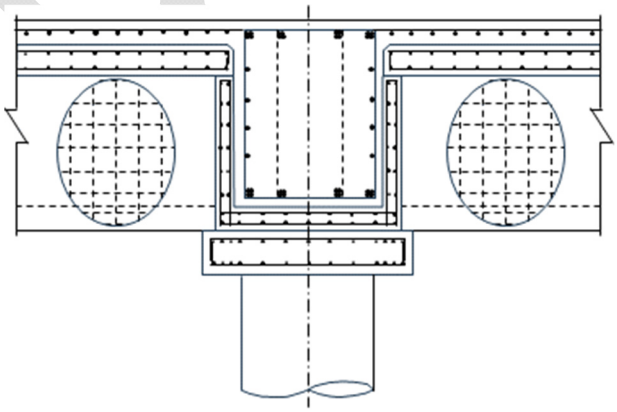

Source: JICA Team

Figure 1.5- Typical Reinforcement Arrangement of Precast System

(4) Arrangement of Accessories (cast-in-place reinforced concrete superstructure)

Fenders and mooring posts / bollards should be arranged to minimize eccentric external forces acting on one deck block as much as possible. Generally, one mooring post / bollard is installed per block, and two rubber fenders as shock-absorbing structures are installed per block (20 to 30 meters in length).

(5) Assumptions of the Seabed Ground

1) Determination of Slope Inclination

When placing retaining structures behind a slope, their position should be appropriately determined considering the stability of the slope. In the case of soft ground, the stability of the slope should also be evaluated for circular slip failure. The slopes for open-type wharves are rarely composed of weak clay layers but are instead composed of sandy soil or riprap.

When placing retaining structures behind the slope, it is desirable to avoid placing them in front of the slope drawn at the gradient indicated by Equation (1.1).

$$\alpha=\phi-\epsilon \qquad (1.1)$$

TCVN 11820 Part 5: 2021 Equation (69)

Where:

α : inclination angle of the slope relative to the horizontal plane (°)

ϕ : shear resistance angle of the main constituent material of the slope (°)

ϵ : $\tan^{-1}k_h'$

k_h' : horizontal seismic coefficient for underwater conditions

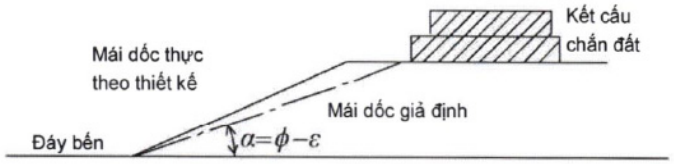

Source: TCVN 11820-5-2021

TCVN 11820 Part 5: 2021 Hinh 61

Figure 1.6- Position of Earth retaining Structure behind Slope

Note:

Equation (1.1) may not be applied to hard strata or bedrock slopes.

The angle set in Equation (1.1) is a restriction when a structure is constructed behind the top of the slope. The slant angle as an actual design cross section is usually steeper than α. For example, if the foundation of earth retaining section and the slope face comprise rubbles, the ratio is usually set to be approximately 1:1.5 to 1:2. This is to ensure sufficient slope at the front of the earth retaining structure as much as possible so that the effects of scouring and local collapse do not reach to the front toe of structure.

2) Virtual Ground Surface

In calculation of the lateral resistance and bearing capacity of piles, a virtual ground surface shall be assumed at an appropriate level for each pile.

The calculation method for lateral resistance used in the analysis of open-type wharves on straight piles is originally intended for horizontal ground surfaces. Therefore, when calculating the lateral resistance of piles driven into slopes, some correction is necessary.

For simplicity in calculating lateral resistance or bearing capacity, the virtual ground surface for each pile can be set at the height halfway between the front water depth and

the actual slope along the pile axis (see Figure 1.7). However, for wide wharves exceeding 20 meters or extremely long slopes, this method may not be appropriate, and other methods should be used for calculation.

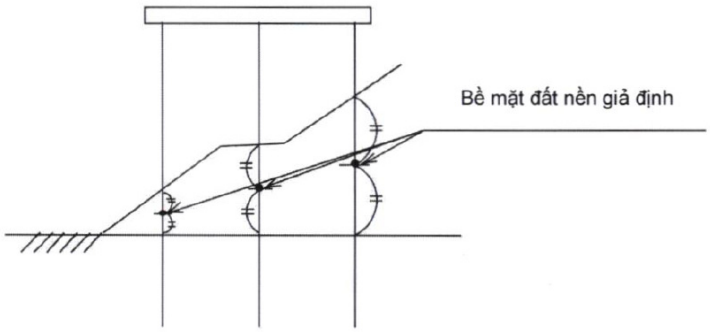

TCVN 11820 Part 5: 2021 Hinh 62

Source: TCVN 11820-5-2021

Figure 1.7- Virtual Ground Surface

3) Coefficient of Horizontal Subgrade Reaction

In calculation of the lateral resistance of piles, it is desirable to obtain the coefficient of subgrade reaction of the subsoil through lateral loading tests of piles in situ. When lateral loading tests of piles are not carried out, the coefficient can be obtained using appropriate calculation methods derived from lateral resistance test results.

For piles such as those in open-type wharves, where horizontal forces are applied up to near the yield point of the piles, some empirical values of the coefficient of horizontal subgrade reaction related to *N*-values exist. However, accurately estimating the subgrade reaction coefficient from *N*-values is challenging, so it is preferable to obtain it through lateral loading tests in situ.

If loading tests cannot be performed, the mid-point between the lower limit and median values obtained by back-calculating from pile lateral resistance tests should be used. When using Chang's method, Equation (1.2) may be applied.

However, field observations indicate that the coefficient of horizontal subgrade reaction for rubble mound is lower than the value obtained by Equation (1.2). According to Chang's method, the coefficient of horizontal subgrade reaction is considered to be 3,000 to 4,000 kN/m³.

$$k_{CH}=1500N \quad (1.2)$$

TCVN 11820 Part 5: 2021 Equation (70)

Where:

k_{CH} : coefficient of horizontal subgrade reaction (kN/m³)
N : *N*-value of the ground from the surface to about $1/\beta$
β : refer to the virtual fixed point

Reference:

The following *N* values can be applied when calculating the coefficient of horizontal subgrade reaction:

- ✓ Rubble mound: N=2 to 10
- ✓ Sandy ground: SPT results
- ✓ Clayey ground: q_u =33.3N (for coefficient of horizontal subgrade reaction)

The coefficient of horizontal subgrade reaction calculated using Equation (1.2) is a static value and can be used when verifying the stress on piles through static frame

analysis. However, it cannot be applied to liquefied ground. Additionally, there are reports suggesting that doubling the value obtained from Equation (1.2) and using the actual ground surface instead of the virtual ground surface when calculating the natural period of the wharf provides results closer to the actual values.

Since soil is not an elastic material, the horizontal force-displacement relationship for piles is generally nonlinear, and as the horizontal force increases, the value of k_{CH} decreases. When deriving Equation (1.2) from lateral resistance test results, it is advisable to set a lower value for k_{CH} to account for this characteristic.

4) Virtual Fixed Point

In open-type wharves on vertical piles, the virtual fixed point of the pile can be assumed to be at a position $1/\beta$ below the virtual ground surface. β can be calculated using Equation (1.3).

$$\beta = \sqrt[4]{\frac{k_{CH}D}{4EI}} \qquad (1.3)$$

TCVN 11820 Part 5: 2021 Equation (71)

Where:

β : characteristic value of the pile (m^{-1})
k_{CH} : coefficient of horizontal subgrade reaction (kN/m^3)
D : diameter or width of the pile (m)
E : elastic modules of the pile material (kN/m^2)
I : inertia moment of the pile section (m^4)

The method of using a virtual fixed point has traditionally been used to conveniently determine the pile head moment, although there is no clear rationale behind this method. Therefore, other methods to set the virtual fixed point can be proposed, or the pile head moment and other parameters can be determined without using the virtual fixed point.

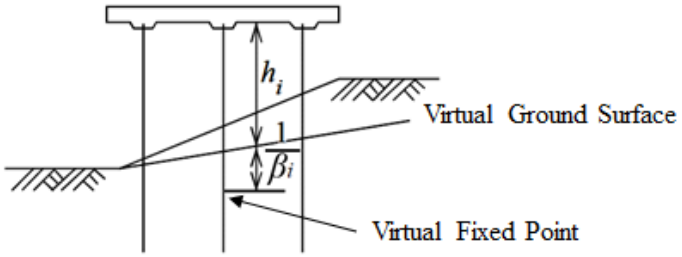

OCDI 2020 Part III Chapter 5 Fig. 5.2.8

Source: OCDI 2020

Figure 1.8- Virtual Fixed Point

In areas at risk of scour, it is advisable to install scour prevention materials such as gravel mats, asphalt mats, and others at the toe of the slope. Furthermore, in areas at risk of suction of the seabed, laying suction prevention materials like geotextiles on top of the seabed is recommended.

1-4. Loads and Actions

(1) Loads to be Considered

The loads acting on the retaining structure should be appropriately estimated by referring to gravity-type quaywall or sheet pile quaywall depending on the structure type. The loads acting on the open-type wharves need to be set according to operation conditions. The typical design loads and actions to be considered are as shown in Table

1.2.

Table 1.2- Design Loads and Actions

Vertical load and action	Horizontal load and action
1) Self-weight (Superstructure and piles) 2) The loads on the berth: - Surcharge; - Train load; - Vehicle load; - Cargo handling equipment load; - Sidewalk live load 3) Tractive force of vessel 4) Uplift 5) Negative friction forces on piles	1) Earthquake forces acting on the superstructure and piles 2) Earthquake forces acting on the surcharge 3) Earthquake forces acting on the vehicles, cargo handling equipment 4) Wave loads, wind loads and current loads 5) Reaction force of the fender 6) Tractive force of vessel

The self-weight in Table 1.2 and the inertia force includes the self-weight of each pile and the earthquake force acting on the pile's self-weight. To calculate the self-weight of the reinforced concrete superstructure, dimensions of the superstructure should be assumed, the volume calculated and then multiplied by the unit weight.

Since the performance verification of piles of the open-type wharves should be finalized based on multiple trial calculations, and the superstructure dimensions are determined through performance verification of structural calculations, the self-weight of the reinforced concrete superstructure can be assumed to be 21 kN per 1.0 m^2. The unit weight of 21 kN/m^2 is based on records from large ship mooring facilities. When the pile spacing is wider than usual, when large cargo handling equipment is to be installed on the deck as in a container terminal, or when continuous steel pipe piles are used as retaining structures for the land side piles of the wharf, it is advisable to calculate the volume separately to determine the self-weight of the superstructure.

The earthquake force due to live loads is typically considered to act on the deck surface. However, if particularly heavy loads with a high center of gravity are to be loaded, it is important to consider the horizontal inertial force acting at the height of the center of gravity. The live load of earthquake motion on rail-mounted cranes is assumed to be calculated by multiplying the seismic coefficient for self-weight. The horizontal load can be considered to be transmitted from the wheels to the wharf deck.

(2) Fender Reaction Force

The reaction force of the fendering structure can generally be calculated by assuming absorption of the berthing energy at one location of the fender. Since the absorption of energy due to the displacement of the wharf itself is often less than 10% of the total berthing energy, the energy absorption due to the displacement of the wharf itself is generally not considered.

The typical displacement-absorption energy curve and a displacement-reaction force curve for rubber fenders is shown in Figure 1.9.

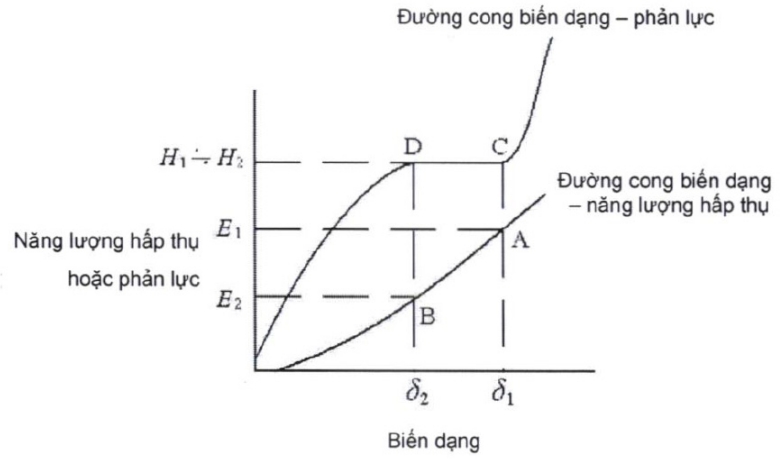

Source: TCVN 11820-5-2021

Figure 1.9- Performance Curves of Rubber Fenders

The pair of "displacement - energy curve" and "displacement - reaction force curve" of a rubber fender. If a single fender absorbs a berthing energy of E_1, the corresponding fender deformation, δ_1 is obtained. Then, using the other curve, the corresponding reaction force acting on the pier is obtained as H_1 ($\delta_1 \rightarrow C \rightarrow H_1$). However, if fenders are deployed too close to each other and the berthing energy is absorbed by two fenders, the approaching energy acting on one fender becomes $E_2 = E_1/2$ and this causes the corresponding fender deformation δ_2. As can be seen from the Figure 1.9 ($\delta_2 \rightarrow D \rightarrow H2$), the reaction force acting on the pier is almost the same as that generated in the single fender case because of the characteristics of rubber fender. Thus, the horizontal reaction force acting on the pier becomes $2H_2=2H_1$, which means that the horizontal force to be used in the design is twofold. When using fenders that have such characteristics, therefore, it is desirable to give careful consideration to this behavior of reaction force in the designing and locating fenders.

1) Berthing Energy of Ships

The actions caused by ship berthing shall be calculated from the berthing energy of ships in general. The berthing energy of a ship can be calculated with Equation (1.4) by using the mass of the ship, the berthing velocity of the ship, the virtual mass factor, the eccentricity factor, the flexibility factor, and the berth configuration factor. In the Equation, the subscript k indicates the characteristic values.

$$E_{f_k} = \frac{1}{2} M_{s_k} V_{b_k}{}^2 C_{m_k} C_{e_k} C_{s_k} C_{c_k} \qquad (1.4)$$

Where:

E_f : berthing energy of the ship (kJ)
M_s : mass of the ship (t)
V_b : berthing velocity of the ship (m/s)
C_m : virtual mass factor
C_e : eccentricity factor
C_s : flexibility factor
C_c : berth configuration factor
k : characteristic value

2) Mass of the ship

Equation (1.5) can be used as relational equations between the characteristic values of the full-load displacement tonnage (DT) of the respective types of ships and deadweight tonnages (DWT) or gross tonnages (GT) of the ships.

Cargo ships: $DT_k = 2.920DWT^{0.924}$
Container ships: $DT_k = 1.634DWT^{0.986}$
Tankers: $DT_k = 1.688DWT^{0.976}$
Roll-on roll-off (RORO) ships: $DT_k = 8.728GT^{0.790}$
Pure car carriers (PCC): $DT_k = 1.946GT^{0.898}$
LPG carriers: $DT_k = 4.268GT^{0.914}$
LNG carriers: $DT_k = 1.601GT^{0.970}$ (1.5)
Passenger ships: $DT_k = 2.730GT^{0.871}$
Short-to-medium distance ferries (navigation distance of less than 300 km):
$DT_k = 4.980GT^{0.855}$
Long distance ferries (navigation distance of 300 km or more):
$DT_k = 15.409GT^{0.735}$

TCVN 11820 Part 2: 2025 Equation (270)

Where:

DT : full-load displacement tonnage of the ship (ton)
DWT : deadweight tonnage of the ship (ton)
GT : gross tonnage of the ship (ton)

3) Berthing velocity

- ✓ The berthing velocities of ships shall be determined on the basis of actual measurements or the existing measurement data of berthing velocities by taking into consideration the types and loading conditions of design ships, locations and structures of mooring facilities, presence or absence of tugboat assistance, the sizes, and meteorological and oceanographical conditions.
- ✓ Large cargo ships and tankers berth at mooring facilities in a manner that temporarily stop at positions parallel to the mooring facilities at certain distances from them and then come alongside the mooring facilities with a few tugboats gently pushing them. If strong winds are blowing against mooring facilities, there may be cases wherein large cargo ships or tankers come alongside the mooring facilities with tugboats pulling them. When adopting the tugboat-assisted berthing method as mentioned above, the berthing velocities are normally set at approximately 10 to 15 cm/s on the basis of the existing performance records.
- ✓ Special ships such as ferries, RORO ships, or small cargo ships may require berthing methods that are different from those used with large ships, e.g., berthing without the assistance of tugboats or approaching mooring facilities in the direction parallel to their normal lines when ships have ramps at their bows or sterns. Therefore, the berthing velocities of special ships should be carefully determined on the basis of actual measurements and others with particular focus on their berthing methods.
- ✓ Considering that small ships, such as small cargo ships, berth at mooring facilities under their own power without tugboat assistance, it shall be noted that their berthing velocities are generally larger than those of large ships and may exceed 30 cm/s. Therefore, the berthing velocities of small ships should be carefully determined on the basis of actual measurements and others.
- ✓ For the berthing velocities of medium and small ships, in anticipation of indiscreet

berthing or berthing at mooring facilities subject to currents, it is necessary to determine the berthing velocities on the basis of the existing measurement data by taking into consideration the drift velocities of ships.

✓ Figure 1.10 shows the relationship among ship maneuvering conditions, ship sizes, and berthing velocities established on the basis of the empirical data. This figure suggests that larger berthing velocities should be set when ships berth at the mooring facilities that are not sheltered by breakwaters or when the sizes of design ships become smaller.

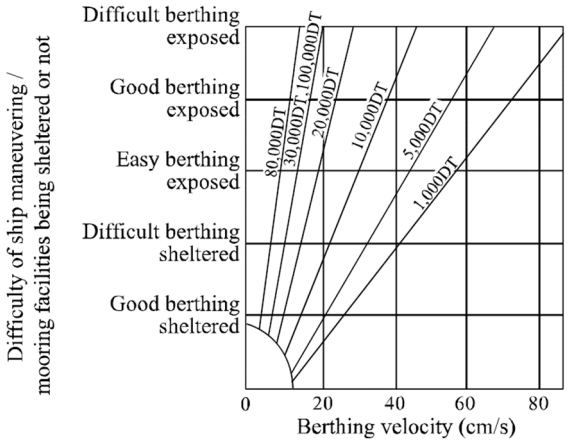

TCVN 11820 Part 2: 2025 Hinh 132

Source: TCVN 11820-2-2025

Figure 1.10- Relationship among Ship Maneuvering Conditions, Ship Sizes, and Berthing Velocities

✓ Study reports on berthing velocities show that ships' loading conditions significantly impact their speeds. Berthing velocities decrease with full loads and small keel clearances and increase with light loads and large clearances.

✓ The relationship between berthing velocities and ship sizes was studied using measurement data collected in the previous studies on the berthing velocities of ships. Figure 1.11 shows the relationship between the measurement values of berthing velocities and ship sizes for the respective types of ships. The figure shows that there is an overall trend of decreasing berthing velocities with increasing ship sizes and that berthing velocities are approximately 20 cm/s at a maximum and are distributed widely from 5 to 15 cm/s with a large variance.

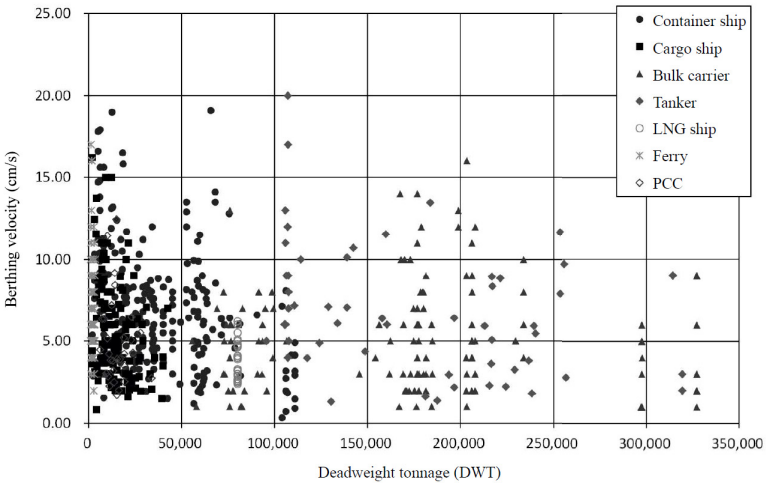

TCVN 11820 Part 2: 2025 Hinh 133

Source: TCVN 11820-2-2025

Figure 1.11- Measurement Values of Berthing Velocities (by Ship Type)

✓ Regarding the relationship between berthing velocities and ship sizes, the regression equations considering the coverage ratios were also proposed. Figure 1.12 shows the regression equations with different coverage ratios overlaid on the graph of the relationship between the measurement values of berthing velocities and ship sizes. The probability distribution of the berthing velocities of ships generally shows the logarithmic normal distribution, and the relationship between berthing velocities and ship sizes can be expressed by regression equations in the form of power functions. It shall be noted that these regression equations show extremely large berthing velocities for small ships with deadweight tonnages less than 10,000 tons.

TCVN 11820 Part 2: 2025 Hinh 134

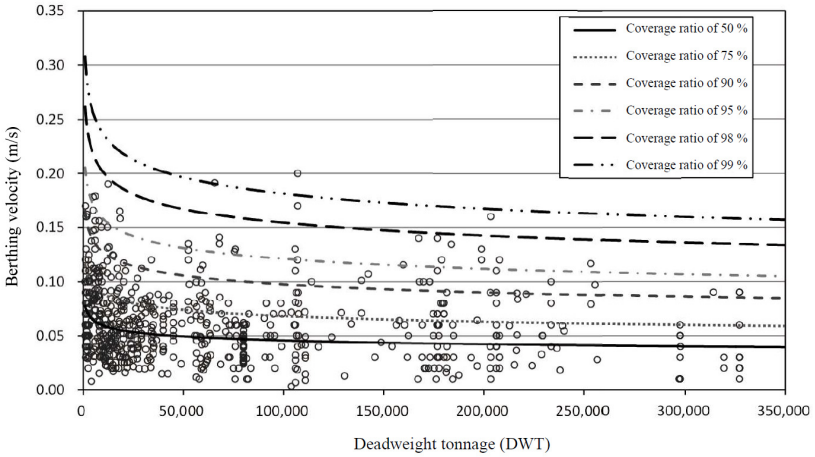

Source: TCVN 11820-2-2025

Figure 1.12- Relationship between Measurement Values of Berthing Velocities of Ships and Regression Equations

4) Virtual mass factor

The virtual mass factor C_m can be calculated by the following equation:

TCVN 11820 Part 2: 2025 Equation (271) (272)

$$C_m = 1 + \frac{\pi}{2C_b}\frac{d}{B} \quad (1.6)$$

$$C_b = \frac{\nabla}{L_{pp}Bd} \quad (1.7)$$

Where:

C_m : virtual mass factor
C_b : block coefficient
∇ : displacement volume of the ship (m^3)
L_{pp} : length between perpendiculars (m)
B : molded breadth (m)
d : full-load draft (m)

When a ship berths, the velocities of not only the mass of the ship M_s but also the mass of the water body around the ship M_w are reduced simultaneously. Therefore, the inertia force due to the mass of the water body needs to be added to the motion of the ship. For this reason, the virtual mass factor can be defined by Equation (1.8).

TCVN 11820 Part 2: 2025 Equation

$$C_m = \frac{M_s + M_w}{M_s} \quad (1.8)$$

Where:

C_m : virtual mass factor

M_s : mass of the ship (t)
M_w : mass of the water body around the ship (added mass) (t)

(273)

Ueda et al. proposed Equation (1.6) on the basis of the results of the hydraulic model tests and field measurements. The second term of the equation corresponds to M_w/M_s in Equation (1.8).

5) Eccentricity Factor

The eccentricity factors C_e can be calculated by the following equation:

$$C_e = \frac{1}{1+\left(\frac{l}{r}\right)^2} \quad (1.9)$$

TCVN 11820 Part 2: 2025 Equation (274)

Where:

C_e : eccentricity factor
l : distance measured from the ship's contact point to the center of gravity of the ship in the direction parallel to the normal line of the mooring facility (m)
r : radius of rotation around the vertical axis passing through the center of gravity of the ship (m)

During berthing, ships approach mooring facilities that are not perfectly alongside them. Therefore, ships start yawing in horizontal planes and rolling around their longitudinal axes when they come into contact with mooring facilities (fenders). As a result, the yawing and rolling partially consume the kinetic energy of the ships. Considering that the amount of energy consumed by rolling is negligibly smaller than that by yawing, Equation (1.9) considers kinetic energy consumption only by yawing.

r/L_{pp} is a function of the block coefficient C_b and can be obtained from Figure 1.13, Equation (1.10), which is a linear approximation of the curve in the figure, may also be used.

$$r = (0.19C_b + 0.11)L_{pp} \quad (1.10)$$

TCVN 11820 Part 2: 2025 Equation (275)

Where:

r : radius of rotation (also called radius of gyration with the relationship of $I_z = M_s r^2$ with the moment of inertia I_z around the vertical axis of the ship)
C_b : block coefficient
L_{pp} : length between perpendiculars (m)

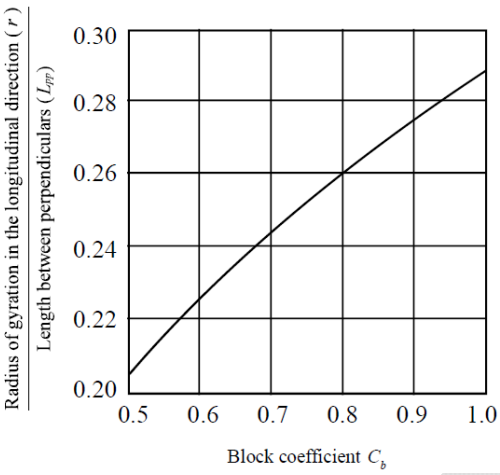

TCVN 11820 Part 2: 2025 Hinh 135

Source: TCVN 11820-2-2025

Figure 1.13- Relationship between Radii of Gyration in the Longitudinal Direction and Block Coefficients

As shown in Figure. 1.14, when a ship comes closest to a mooring facility at point P and into contact with fenders F_1 and F_2, the distance l measured from a point of contact to the center of gravity of the ship in the direction parallel to the mooring facility can be calculated by using Equation (1.11) or (1.12). Here, the value of l needs to be L_1 when $k > 0.5$, L_2 when $k < 0.5$, and either L_1 or L_2 when $k = 0.5$ depending on which variable makes the value of C_e in Equation (1.9) larger.

$$L_1 = \{0.5\alpha + e(1-k)\}L_{pp}\cos\theta \quad (1.11)$$

$$L_2 = \{0.5\alpha - ek)\}L_{pp}\cos\theta \quad (1.12)$$

TCVN 11820 Part 2: 2025 Equation (276) (277)

Where:

- L_1 : distance measured from the point of contact to the center of gravity of the ship in the direction parallel to the mooring facility when the ship comes into contact with the fender F_1 (m)
- L_2 : distance measured from the point of contact to the center of gravity of the ship in the direction parallel to the mooring facility when the ship comes into contact with the fender F_2 (m)
- θ : berthing angle (generally set at around 0 to 10°)
- e : ratio of the interval of fenders measured in the longitudinal direction of the ship to the length between perpendiculars
- α : ratio of the length of the parallel side of the ship at the height of the point of contact with the fender to the length between perpendiculars (differs depending on the types of ships and block coefficients but is generally set at 1/3 to 1/2 or may be set at approximately 1/3 for ships with small breadths, such as container and passenger ships, or approximately 1/2 for ships with wide breadths, such as cargo ships and tankers)
- k : parameter representing the point between fenders F_1 and F_2, where the ship comes closest to the mooring facility (set in the range of $0 < k < 1$ or may be set at 0.5 in general)

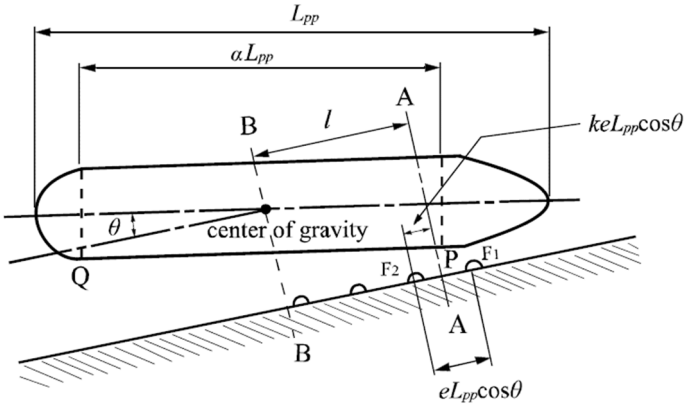

TCVN 11820 Part 2: 2025 Hinh 136

Source: TCVN 11820-2-2025

Figure 1.14- Schematic Illustration of Ship Berthing

6) Flexibility Factor

The flexibility factor C_s is the ratio of the berthing energy absorbed by the deformation of a ship hull to the berthing energy of the ship. Assuming that there is no energy absorption by the deformation of ship hull, the characteristic value of the flexibility factor C_{sk} can generally be set at 1.0.

7) Berth Configuration Factor

The water mass compressed between a berthing ship and a mooring facility behaves like a cushion and produces an effect to decrease the kinetic energy of the ship to be finally absorbed by fenders. The berth configuration factor C_c needs to be determined by taking into account this effect. Furthermore, the behavior of water mass is considered to be affected by berthing angles, shapes of ship hulls, under-keel clearances (distances between ship bottoms and the seafloor), and berthing velocities. However, the characteristic value of the berth configuration factor C_{ck} can generally be set at 1.0.

8) Selection of Fenders

Rubber and pneumatic fenders are selected considering the following:

- ✓ Ensure that the reaction force of the fender stays within the allowable load of the ship's hull.
- ✓ Consider the movement of the moored ship, especially in areas affected by waves. Select appropriate fenders based on the berthing angle and other berthing conditions.
- ✓ Consider not only the characteristics of the fender itself but also the overall structural properties of the mooring facility when selecting suitable fenders.

The absorbed energy of the fenders is calculated using Equation (1.13), where the subscript "*d*" indicates design values.

$$E_{sd} = \varphi E_{cat} \geqq E_{fd} \quad (1.13)$$

OCDI 2020 Part III Chapter 5 Equation (9.2.4)

Where:

E_s : absorbed energy of the fenders (kN·m)
φ : manufacturing tolerance of the fenders (10% in general)
E_{cat} : standard value of absorbed energy of the fenders (kN·m)
E_f : berthing energy of the ship (kN·m)

In addition, if the mooring facility has a structural type that is significantly affected by

the fender reaction force, or if the allowable hull pressure on the target ship is limited to less than 700 kN/m^2, it is necessary to take into account factors that affect the performance of the rubber fender (inclination, velocity, temperature, and aging factor).

Reference:

The PIANC guideline recommends multiplying the effective berthing energy by 1.1 to 2.0 as the factor for abnormal impact when the absorbed energy exceeds the effective berthing energy due to ship operation errors, unexpected strong winds or currents, etc. PIANC guideline also recommends using velocity and temperature correction factors to adjust the energy absorption and reaction force of fenders. These factors account for variations due to different ship berthing velocities, ambient temperatures, and rubber types used in the fenders. The guidelines suggest that the maximum allowable surface pressure should be between 200 to 400 kN/m^2. PIANC MarCom WG33: 2002

BS 6349 Part 4 also recommends multiplying the berthing energy factor by 1.5 to 2.0 as a risk-based approach. BS 6349 Part 4: 2014

Similar to PIANC guidelines, BS6349 also provides guidance on hull pressures, but the recommended values are more conservative than those in PIANC guidelines.

(3) Seismic Coefficient

For structures with relatively long natural periods and flexibility (e.g., Vertical pile-type piers, etc.), it is possible to pay attention to the vibration characteristics, appropriately calculate the natural period of the low-order vibration mode that is expected to affect damage, and use the method described in TCVN 9386-1: 2012. TCVN 11820 Part 2: 2025 5.13.4 4)

The seismic coefficient is determined depending on geological conditions and ground acceleration according to the earthquake classification criteria of TCVN 9386-1: 2012.

Notes:

In many countries, including Vietnam, three-dimensional structural analysis is conducted on open-type wharves on piles. The seismic motion is mostly input in the directions of the longitudinal and transverse directions using the spectrum shown below. Since Vietnam has few earthquake records, when performing time history response analysis, it is crucial to verify the analysis with input seismic motions of various periods and frequencies.

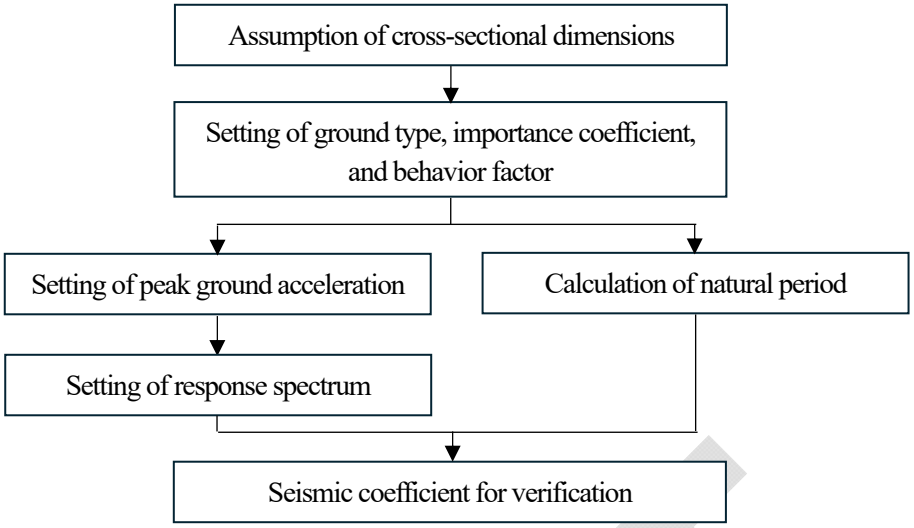

Figure 1.15- Example Flow for Setting Seismic Coefficient

1) Ground Type

Ground types A, B, C, D, and E, described by the stratigraphic profiles and parameters given in Table 1.3 and described hereafter, may be used to account for the influence of local ground conditions on seismic action.

Table 1.3- Identification of Ground Types

TCVN 9386-1: 2012 Bang 3.1

Ground Type	Description of Stratigraphic profile	Parameters		
		$V_{s,30}$ (m/s)	N_{SPT} (blows/ 30cm)	c_u(kPa)
A	Rock or other rock-like geological formation, including at most 5 m of weaker material at the surface	> 800	-	-
B	Deposits of very dense sand, gravel, or very stiff clay at least several tens of metres in thickness, characterised by a gradual increase of mechanical properties with depth	360 - 800	> 50	> 250
C	Deep deposits of dense or medium-dense sand, gravel or stiff clay with thickness from several tens to many hundreds of metres	180 - 360	15-50	70-250
D	Deposits of loose-to-medium cohesionless soil (with or without some soft cohesive layers), or of predominantly soft-to-firm cohesive soil.	< 180	< 15	< 70
E	A soil profile consisting of a surface alluvium layer with V_S values of type C or D and thickness varying between 5m and 20 m underlain by stiffer material with V_S > 800 m/s			

S_1	Deposits consisting, or containing a layer at least 10 m thick, of soft clays/silts with a high plasticity index (PI > 40) and high-water content	<100 (indicative)	-	10-20
S_2	Deposits of liquefiable soils, of sensitive clays, or any other soil profile not included in types A-E or S_1			

Source: TCVN 9386-1-2012

2) Importance Coefficient

Reliability differentiation is implemented by classifying structures into different importance classes. An importance coefficient γ_I is assigned to each importance class. Wherever feasible this coefficient should be derived so as to correspond to a higher or lower value of the return period of the seismic event (with regard to the reference return period) as appropriate for the design of the specific category of structures. Terms to coefficients and importance coefficients are given in TCVN 9386-1: 2012 Annex E, Part 1.

Table 1.4- Level and Coefficient of Importance

Modified from TCVN 9386-1: 2012 Phu luk E

Important Level		Structure	Importance coefficient γI
Special	Structure has special importance, not allow being damaged by seismic	N/A	Designed with the biggest acceleration can happen
I	Structure has survival importance with community protection, function cannot be discontinued during seismic process	Storage or pipe-line relative to toxic substance, flammable substance, substance easy to explode	1.25
II	Structure has importance in preventing seismic consequence, if it is collapse causing big damage of person and property	Traffic structure III-3, III-5 in ANNEX F III-5 Waterway structure a) Wharf b) Harbor for ship, ship building and repairment factory c) Dock for ship d), e)	1.0
III	Structure not belong to special level and level I, II, IV	N/A	0.75
IV	Structure has secondary Importance for safety of person life	N/A	Not require to calculate anti-seismic

Source: Modified from TCVN 9386-1-2012

3) Behavior Factor

The resistance and energy-dissipation capacity to be assigned to the structure are related to the extent to which its non-linear response is to be exploited. In operational terms such balance between resistance and energy-dissipation capacity is characterized by the values of the behavior factor q and the associated ductility classification, which are given in the relevant Parts of this standard. As a limiting case, for the design of structures classified as low-dissipative, no account is taken of any hysteretic energy dissipation and the behavior factor may not be taken, in general, as being greater than the value of 1.5 considered to account for overstrength.

The behavior factor shall be carefully determined based on engineering justification and in reference to appropriate standards. When selecting behavior factors, it is imperative that sections be categorized either as compact sections in accordance with ASCE or as Class 1/Class 2 sections as per Eurocode. Confinement reinforcement is required for the expected plastic hinge zones in concrete piles, and it is crucial to preserve the shear capacity of the pile. Additionally, the capacity of the superstructure must also be safeguarded. Consequently, engineers shall adhere to the supplementary requirements stipulated by the adopted codes and standards.

Reference:

Eurocode 8-2: 2005 introduces the maximum values of the behavior factor on bridge piers as Table 1.5.

Table 1.5- Maximum Values of the Behavior Factor

Eurocode 8-2 Bridge: 2005 Table 4.1

Type of Ductile Members	Seismic Behavior	
	Limited Ductile	Ductile
Reinforced concrete piers:		
Vertical piers in bending	1.5	3.5 $\lambda(\alpha_s)$
Inclined struts in bending	1.2	2.1 $\lambda(\alpha_s)$
Steel piers:		
Vertical piers in bending	1.5	3.5
Inclined struts in bending	1.2	2.0
Piers with normal bracing	1.5	2.5
Piers with eccentric bracing	-	3.5
Abutments rigidly connected to the deck:		
In general	1.5	1.5
Locked in structures	1.0	1.0
Arches	1.2	2.0
$\alpha_s = L_s/h$ is the shear span ratio of the pier, where L_s is the distance from the plastic hinge to the point of zero moment and h is the depth of the cross-section in the direction of flexure of the plastic hinge. For $\alpha_s \geq 3 \quad \lambda(\alpha_s) = 1.0, \quad 3 > \alpha_s \geq 1.0 \quad \lambda(\alpha_s) = \sqrt{(\alpha_s/3)}$		

Source: Eurocode 8-2-2005

Reference:

ASCE 61-14 introduces a response modification factor similar to behavior factor. The response modification factor for solid prestressed concrete piles and steel pipe piles is 2.0, but batter pile is 1.0. Example open-type wharves on piles with batter piles are shown in Figure 1.16 and Table 1.6.

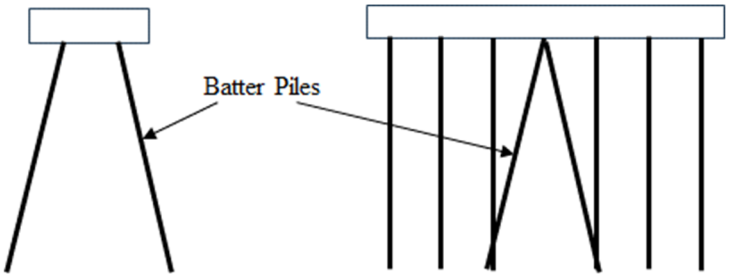

Source: ASCE 61-14-2014

Figure 1.16- Example Open-type Wharves with Batter Piles

Table 1.6- Design Coefficients for Various Elements

Modified from ASCE 61-14: 2014 Table 5-1

Ductile Element	Response Modification Factor *R*	Deflection Amplification Factor C_s
Solid Prestressed Concrete Piles	2	2
Steel Pipe Piles	2	2
Connections not meeting Chapter 7 (pile to deck connections) in ASCE 61-14 provisions	1	1
Batter Piles	1	1

Source: Modified from ASCE 61-14-2014

4) Peak Ground Acceleration

The reference peak ground acceleration on type A ground, a_gR, for use in Vietnam given in TCVN 9386-1:2012, Annex G, Part 1 or may be derived from zonation maps found in some regions approved by the relevant authorities.

However, Figure 1.17 indicates acceleration for a return period of 500 years, and for a Level 1 performance verification with a return period of 75 years, the acceleration for a may be reduced. Since there are no acceleration maps with a return period of 75 years in Vietnam, Consultants are expected to set the design background acceleration after careful consideration and/or consultation with seismic experts.

Reference:

The PIANC WG34 report "Seismic Design Guidelines for Port Structures" recommends the application of seismic loading at two levels:

✓ Level 1:

The structures should not have significant residual deflections after the earthquake and should be immediately operational. The return period for the Level 1 event is 75 years, corresponding to a 50% probability aof exceedance over the design life of 50 years.

✓ Level 2:

The structures should be operational following repairs. The structures should not buckle, collapse or overturn. The return period for the Level 2 event is 475 years, corresponding to a 10% probability of exceedance over the design life of 50 years.

TCVN 9386-1: 2012 Phu luk G

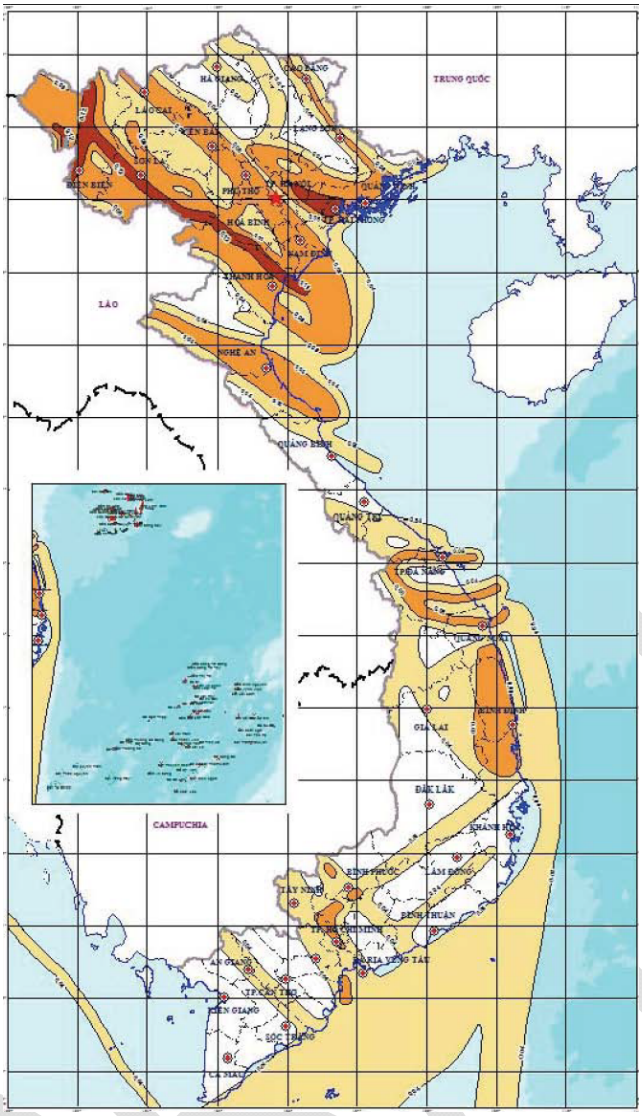

Source: TCVN 9386-1-2012

Figure 1.17- Zoning Maps of Background Acceleration on Viet Nam Territory (Return period: 500 years)

5) Response Spectrum

For the horizontal components of the seismic action, the design elastic response spectrum $S_d(T)$ is defined by the following equations and Figure. 1.18.

TCVN 9386-1: 2012 Equation (3.13), (3.14), (3.15), (3.16)

$$0 \le T \le T_B : S_d(T) = \alpha_g \cdot S \left[\frac{2}{3} + \frac{T}{T_B} \cdot \left(\frac{2.5}{q} - \frac{2}{3} \right) \right]$$

$$T_B \le T \le T_C : S_d(T) = \alpha_g \cdot S \cdot \frac{2.5}{q} \qquad (1.14)$$

$$T_C \le T \le T_D : S_d(T) \begin{cases} = \alpha_g \cdot S \cdot \dfrac{2.5}{q} \cdot \left[\dfrac{T_C}{T} \right] \\ \ge \beta \cdot \alpha_g \end{cases}$$

$$T_D \le T : S_d(T) \begin{cases} = \alpha_g \cdot S \cdot \dfrac{2.5}{q} \cdot \left[\dfrac{T_C T_D}{T^2}\right] \\ \ge \beta \cdot \alpha_g \end{cases}$$

Where:

$S_d(T)$: design elastic response spectrum
T : natural period of a linear single-degree-of-freedom system
a_g : design ground acceleration on type A ground
T_B : lower limit of the period of the constant spectral acceleration branch
T_C : upper limit of the period of the constant spectral acceleration branch
T_D : value defining the beginning of the constant displacement response range of the spectrum
S : soil factor
q : behavior factor
β : lower bound factor for the horizontal design spectrum

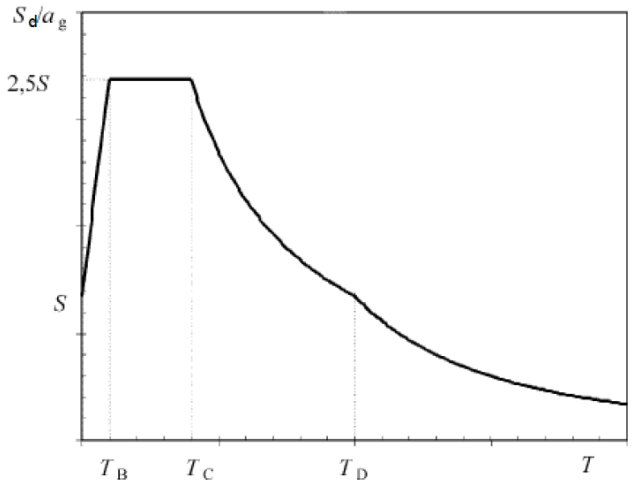

TCVN 9386-1: 2012 Hinh 3.1

Source: modified TCVN 9386-1-2012

Figure 1.18- Shape of the Elastic Response Spectrum

Table 1.7- Values of the Parameters Describing the Elastic Response Spectra

TCVN 9386-1: 2012 Bang 3.2

Ground type	S	T_B (s)	T_C (s)	T_D (s)
A	1,0	0,15	0,4	2,0
B	1,2	0,15	0,5	2,0
C	1,15	0,20	0,6	2,0
D	1,35	0,20	0,8	2,0
E	1,4	0,15	0,5	2,0

Source: TCVN 9386-1-2012

6) Natural Period

The calculation of the open-type wharf's natural period can be obtained by setting the spring constant from the relationship between action and deformation obtained through frame analysis and using Equation (1.15).

$$T_s = 2\pi \sqrt{\frac{W}{gK}} \quad (1.15)$$

OCDI 2020 Part III Chapter 5 Equation (5.2.5)

Where:

T_s : natural period of the piled pier
W : total weight of the superstructure of the pier and the load during seismic events (kN)
g : gravitational acceleration (m/s²)
K : spring constant of the piled pier (kN/m)

The natural period of the piled pier shall be calculated as the maximum acceleration among the following case:

Case 1: Actual ground surface + $2k_{CH}$
Case 2: Actual ground surface + k_{CH}
Case 3: Virtual ground surface + $2k_{CH}$
Case 4: Virtual ground surface + k_{CH}
k_{CH}: Equation (1.2)

The natural period of the pile pier can be calculated by setting the spring constant based on the relationship between force and deformation obtained from frame analysis, and the natural period can be obtained using Equation (1.15). In the case of dynamic behavior such as during an earthquake, $2k_{CH}$ of Case 1 is approximated, but in the case of static behavior, k_{CH} must be used.

(4) Wave Force

Structural members such as piles that have a small diameter relative to the wavelength hardly disturb the propagation of waves. The wave force acting on such members can be obtained using the Morison's formula as shown in Equation (1.16), in which the wave force is expressed as the sum of a drag force that is proportional to the square of the velocity of the water particles and an inertia force that is proportional to the acceleration.

$$\vec{f_n} = \frac{1}{2} C_D \rho_0 |\vec{u_n}| \vec{u_n} D \Delta S + C_M \rho_0 \vec{a_n} A \Delta S \quad (1.16)$$

TCVN 11820 Part 2: 2025 Equation (225)

Where:

$\vec{f_n}$: force that acts on a small length ΔS (m) in the axial direction of the member, where the direction of this force lies in the plane containing the member axis and the direction of motion of the water particles and is perpendicular to the member axis (kN)
$\vec{u_n}$, $\vec{a_n}$: components of the water particle velocity (m/s) and acceleration (m/s²), respectively, in the direction perpendicular to the member axis that lies within the plane containing the member axis and the direction of motion of the water particles (i.e., the same direction as $\rightarrow f_n$) (these components are for incident waves that are not disturbed by the presence of member)
$|\vec{u_n}|$: absolute value of $\rightarrow u_n$ (m/s)
C_D : drag coefficient
C_M : inertia coefficient
D : width of the member in the direction perpendicular to the member axis as viewed from the direction of $\rightarrow f_n$(m)

A : cross-sectional area of the member along a plane perpendicular to member axis (m^2)
ρ_0 : density of seawater (normally 1.03 t/m^3)

Although the total wave pressure changes due to the phase differences among the waves, it is acceptable to calculate the wave force without considering the phase difference.

(5) Current Force

The force caused by the flow, acting on structures and structures on submerged pile foundations or near the water surface such as bridge piers, pipes, or rubble foundation covering materials, is proportional to the square value of the velocity.

$$F_D = \frac{1}{2} C_D \rho_0 A U^2 \qquad (1.17)$$

TCVN 11820 Part 2: 2025 Equation (36)

Where:

F_D : drag force acting on the object in the flow direction (kN)
C_D : drag coefficient
ρ_0 : density of seawater (normally 1.03 t/m^3)
A : projected area of the object in the direction of flow (m^2)
U : flow velocity (m/s)

(6) Uplift Acting on Piled Pier

In the case of facilities near still water surface, such as the superstructure of piled piers or pile-type dolphins, and in particular those facilities that are roughly parallel to the water surface, there is a risk that a rising wave surface will strike on the bottom surface of the facilities and an impulsive wave force (uplift) will act on. In particular, it becomes a large impact load when the wave height is large and the clearance with the still water surface is small. In addition, in a case where there is a reflecting wall at the rear as in the case of open type wharf, and the waves become standing waves and act on this, the wave surface rise rate increases and so does the impact load. If there is a risk of an impact load, the impulsive uplift should be calculated by a suitable method such as a hydraulic model test. Due attention should also be paid to the fact that ordinary uplift that is not an impact load also acts on the bottom surface of such structures, in addition to the impulsive uplift.

Various calculation methods for uplift force are introduced in TCVN11820-2: 2025, so the most suitable method should be selected while taking into consideration the installation conditions of the facility and the wave conditions.

(7) Temperature Load

Temperature constraints may be considered to assess the effects of long-term creep and shrinkage of concrete, and temperature differences (both positive and negative) between the top and bottom surfaces of the deck may be considered to assess bending stresses within the slab. When conducting three-dimensional FEM structural analysis, it is relatively easy to input temperature conditions, making it possible to set detailed environmental parameters depending on the software used.

Foreign standards such as British Standards contain detailed analysis methods that can be useful as references.

1-4. Performance Verification

(1) Stability Verification

For the performance verification of a vertical piled pier, appropriate items from Table 1.8 to 1.11 should be selected and reviewed.

For the performance verification of a vertical piled pier concerning Level 1 earthquake motion, the principle is generally that there is no transmission of actions from the retaining structure.

In addition, the seismic coefficient is calculated from the acceleration response spectrum value corresponding to the natural period of the pier. However, the natural period of the pier cannot be determined unless the pile parameters are determined. Therefore, a calculation process is required in which the pile parameters are assumed, the seismic coefficient is calculated from the acceleration response spectrum corresponding to the assumed natural period, performance verification is performed, and if the results are not satisfactory, the pile parameters are revised.

Although the deformation of the pier is not specified, it is acceptable to set limits considering deformations of the pier, such as ensuring that the access bridge does not fall.

Table 1.8- Performance Verification Items and Standard Indexes to Provide Limit Values in Each Design Situation Concerning Superstructure of Piled Piers

OCDI 2020 Part III Chapter 5 Attached Table 11-22

Performance requirements	Design situation			Verification item	Standard index to provide limit value
	Situation	Dominating action	Non-dominating action		
Serviceability	Variable	Berthing and traction by ships	Self-weight, surcharges	Cross-sectional failure of superstructure	Design cross sectional resistance
		Level 1 earthquake ground motion	Self-weight, surcharges		
		Surcharges (including surcharges during cargo handling)	Self-weight, wind acting on cargo handling equipment and ships		
		Surcharges (including surcharges during cargo handling)	Self-weight, surcharges	Crack width of superstructure cross-section	Limit value of bending crack width
		Repeatedly applied surcharges	Self-weight	Fatigue failure of superstructure	Design fatigue strength
		Variable waves	Self-weight	Cross-sectional failure of superstructure	Design cross-sectional resistance

Source: Modified from OCDI 2020

Table 1.9- Performance Verification Items and Standard Indexes to Provide Limit Values in Each Design Situation Concerning Piles of Piled Piers

OCDI 2020 Part III Chapter 5 Attached Table 11-23

Performance requirements	Design situation			Verification item	Standard index to provide limit value
	Situation	Dominating action	Non-dominating action		
Serviceability	Variable	Berthing, traction by ships	Self-weight, surcharges	Axial forces in piles	Action-resistance ratio concerning bearing capacity of piles
		Level 1 earthquake ground motion	Self-weight, surcharges		
		Surcharges (including surcharges during cargo handling)	Self-weight, wind acting on cargo handling equipment and ships		
		Berthing, traction by ships	Self-weight, surcharges	Yielding of piles	Design yield stress of piles
		Level 1 earthquake ground motion	Self-weight, surcharges		
		Surcharges (including surcharges during cargo handling)	Self-weight, wind acting on cargo handling equipment and ships		
		Variable waves	Self-weight	Axial forces acting in piles	Action-resistance ratio concerning bearing capacity of piles

Source: Modified from OCDI 2020

Table 1.10- Performance Verification Items and Standard Indexes to Provide Limit Values in Each Design Situation Concerning Access Bridges of Piled Piers

OCDI 2020 Part III Chapter 5 Attached Table 11-24

Performance requirements	Design situation			Verification item	Standard index to provide limit value
	Situation	Dominating action	Non-dominating action		
Serviceability	Variable	Variable waves	Self-weight	Uplift force on access bridge	Design cross-sectional resistance

Source: Modified from OCDI 2020

Table 1.11- Performance Verification Items and Standard Indexes to Provide Limit Values in Each Design Situation Concerning Piled Piers of Structures with Stiffening Members

OCDI 2020 Part III Chapter 5 Attached Table 11-25

Performance requirements	Design situation			Verification item	Standard index to provide limit value
	Situation	Dominating action	Non-dominating action		
Serviceability	Variable	Berthing, traction by ships	Self-weight, surcharges	Yielding of stiffening members	Design yield stress and design shear force resistance
		Level 1 earthquake ground motion	Self-weight, surcharges	Failure of connections at joints	Design shear force resistance
		Surcharges (including surcharges during cargo handling)	Self-weight, surcharges, wind acting on ships	Punching shear failure at joints	Design shear force resistance
		Repeatedly acting surcharges	Self-weight	Fatigue failure of joints	Design fatigue strength
		Variable waves	Self-weight	Failure of connections at joints	Design shear force resistance

Source: Modified from OCDI 2020

(2) Performance Verification for the Stresses in the Piles

Performance verification for the stresses in the piles under variable situation (surcharge, ship berthing force, tractive force by ship, and earthquake ground motion)

The stresses occurring in the piles of a piled pier may be verified using Equation (1.18). In the following equations, denotes the partial factor corresponding to the suffix, where the suffixes k and d indicate the characteristic value and the design value, respectively. As for the partial factors in the relevant equations, the values shown in Table 1.12 can be used. The values shown as "-" in Table 1.12 indicates that the values may be verified using the values enclosed in parentheses ( ) to ensure convenience. If the axial forces are tensile, S_k and R_k can be calculated using Equations (1.18 (b)) and (1.18 (c)), respectively, and each value should satisfy Equation (1.18).

$$m \cdot \frac{S_d}{R_d} \le 1.0 \quad R_d = \gamma_R R_k \quad S_d = \gamma_S S_k \tag{1.18}$$

OCDI 2020 Part III Chapter 5 Equation (5.2.6) (5.2.6(a)) (5.2.6(b-1))

✓ When the axial forces are compressive,

$$S_k = \left(\frac{\sigma_{c_k}}{\gamma ed} + \sigma_{bc_k}\right) \quad R_k = \sigma_{by_k} \tag{1.18(a)}$$

✓ When the axial forces are tensile,

$$S_k = \sigma_{t_k} + \sigma_{bt_k} \quad R_k = \sigma_{ty_k} \tag{1.18(b)}$$

$$S_k = -\sigma_{t_k} + \sigma_{bc_k} \qquad R_k = \sigma_{by_k} \tag{1.18(c)}$$

(5.2.6(b-2))

Where:

γed : coefficient defined as the value of the axial compressive yield stress (refer to Table 1.14) divided by the characteristic value of the yield stress

σ_t and σ_c : tensile stress due to the axial tensile forces acting on the cross-section and compressive stress due to the axial compressive forces, respectively (N/mm^2)

σ_{bt} and σ_{bc} : maximum tensile stress and maximum compressive stress because of the flexural moment acting on the cross-section, respectively (N/mm^2)

σ_{ty} and σ_{cy} : axial tensile yield stress and axial compressive yield stress, respectively (N/mm^2)

σ_{by} : bending compressive yield stress (N/mm^2)

R : resistance term (N/mm^2)

S : load term (N/mm^2)

γ_R : partial factor that is to be multiplied with the resistance term

γ_S : partial factor that is to be multiplied with the load term

m : adjustment factor

Table 1.12- Partial Factor Used for Verification of the Stresses Occurring in the Piles of a Piled Pier

OCDI 2020 Part III Chapter 5 Table 5.2.1

Verification target	Installation water depth	Partial factor to be multiplied with resistance term: γ_R	Partial factor to be multiplied with load term: γ_S	Adjustment factor: m
Stress occurring in the piles of a piled pier (variable action due to surcharge (during work))	All water depth	- (1.00)	- (1.00)	1.67
Stress occurring in the piles of a piled pier (variable action due to surcharge (during storm))	All water depth	- (1.00)	- (1.00)	1.12
Stress occurring in the piles of a piled pier (variable action due to tractive force by ship)	All water depth	- (1.00)	- (1.00)	1.67
Compressive stress occurring in the piles of a piled pier (variable action due to ship berthing force)	Less than 12.0m	0.97	1.34	- (1.00)
	12.0m and above	1.01	1.29	
Tensile stress occurring in the piles of a piled pier (variable action due to ship berthing)	All water depth	- (1.00)	- (1.00)	1.67
Stress occurring in the piles of a piled pier (variable action due to Level 1 earthquake ground motion)	All water depth	- (1.00)	- (1.00)	1.12

Source: Modified from OCDI 2020

The partial factors are used for the verification of the compressive stresses occurring in the piers of a piled pier at the time when a ship berth in Table 1.12 is the coefficient obtained by the conducted code calibrations so that the obtained dimensions are averagely equivalent as the cross-sections of open-type wharves on vertical piles designed using the previous design methods. In addition, partial factors related to other design states set by referring to the allowable stresses of the steel members in the previous design methods.

The design values in Equation (1.18) are calculated according to Equation (1.19).

$$\sigma_{t_k}=\frac{P_k}{A},\ \sigma_{c_k}=\frac{P_k}{A}$$

$$\sigma_{bt_k}=\frac{M_k}{Z},\ \sigma_{bc_k}=\frac{M_k}{Z} \quad (1.19)$$

OCDI 2020 Part III Chapter 5 Equation (5.2.7)

Where:

A : cross-sectional area of the piles (mm^2)
P : axial force on the pile (N)
Z : section modulus of the piles (mm^3)
M : flexural moment of the piles (N·mm)

Table 1.13- Characteristic Values of Yield Strength for Steel Pile

Steel / Grade / Type of Stress	TCVN 9245: 2012	TCVN 9246: 2012
	SPP400	SPP490
Axial tensile stress (per net cross-sectional area)	235	315
Bending tensile stress (per net cross-sectional area)	235	315
Bending compression stress (per total cross-sectional area)	235	315
Shear stress (per total cross-sectional area)	136	182

Source: Modified from TCVN 11820-5-2015

TCVN 11820 Part 3: 2019 Table 5.5

Reference:

The axial compressive yield stress of typical steel pipe piles in Vietnam may be calculated by the equation given in Table 1.14 from OCDI 2020. As for the effective buckling length of the members, the distance from the lower end of the superstructure to $1/\beta$ under the virtual ground surface may be used as denoted in Figure 1.19.

Table 1.14- The Axial Compressive Yield Stresses

SPP400	SPP490
a) When $\frac{l}{r}\leq 19$ 235	a) When $\frac{l}{r}\leq 16$ 315
b) When $19<\frac{l}{r}\leq 93$ $235-1.4\left(\frac{l}{r}-19\right)$	b) When $16<\frac{l}{r}\leq 80$ $315-2.1\left(\frac{l}{r}-16\right)$
c) When $\frac{l}{r}>93$ $\frac{2.0\cdot 10^6}{6.7\cdot 10^3+\left(\frac{l}{r}\right)^2}$	c) When $\frac{l}{r}>80$ $\frac{2.0\cdot 10^6}{5.0\cdot 10^3+\left(\frac{l}{r}\right)^2}$

Source: Modified from OCDI 2020

Modified from OCDI 2020 Part III Chapter 5 Table 5.2.2

Where:

l : effective buckling length of the member (mm)
r : radius of gyration of the member gross cross-section (mm)

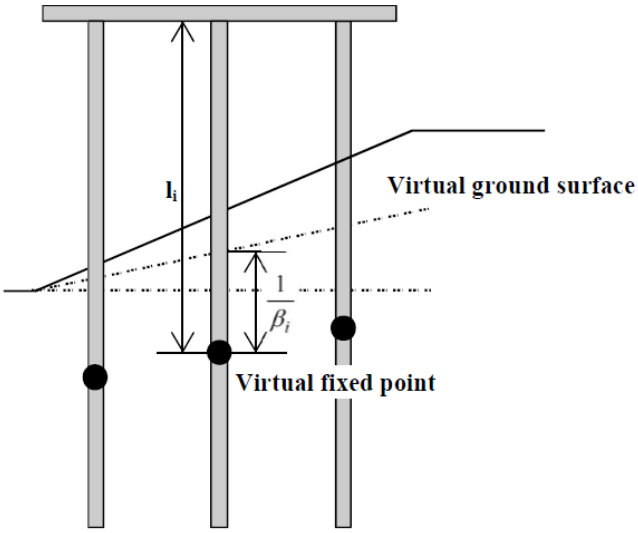

Source: OCDI 2020

Figure 1.19- Setting of the Effective Buckling Length

OCDI 2020 Part III Chapter 5 Fig 5.2.12

In an open-type wharf, typically, the piles are arranged in groups, and the piles are often rigidly connected to the superstructure. In such cases, it is common to analyze the structure as a framework structure evaluated by elastic springs representing the ground.

When evaluating the effects, if rotation of the wharf block must be considered, for example, in the case of horizontal eccentric loads due to fendering structure reaction forces, Equation (1.21) can be used. If combined with raking piles, TCVN 11820 Part 5, 8.5.4 is used or the calculation.

i. If there is no rotation of the pier block

$$H_i = \frac{K_{Hi}}{\sum_i K_{Hi}} H \tag{1.20}$$

ii. If there is a rotation of the pier block

$$H_i = \frac{K_{Hi}}{\sum_i K_{Hi}} H + \frac{K_{Hi} x_i}{\sum_i K_{Hi} x_i^2} eH \tag{1.21}$$

OCDI 2020 Part III Chapter 5 Equation (5.2.4)

Where:

H : horizontal force acting on the unit (kN)
H_i : horizontal force on pile (kN)
K_{Hi} : horizontal spring constant of pile (kN/m)

$$K_{Hi} = \frac{12EI_i}{\left(h_i + 1/\beta_i\right)^3} \tag{1.22}$$

Where:

h_i : vertical distance between the pile head and the virtual ground surface (m)
β_i : inverse of the distance between the virtual ground surface and the virtual fixed point of the pile (m^{-1})
EI_i : flexural rigidity of the pile ($kN \cdot m^2$)

e : distance between the block's symmetry axis and the horizontal force (m)

x_i : distance between the unit's symmetry axis and each pile (m)

The subscript i refers to the i-th pile

OCDI 2020 Part III Chapter 5 Fig. 5.2.7

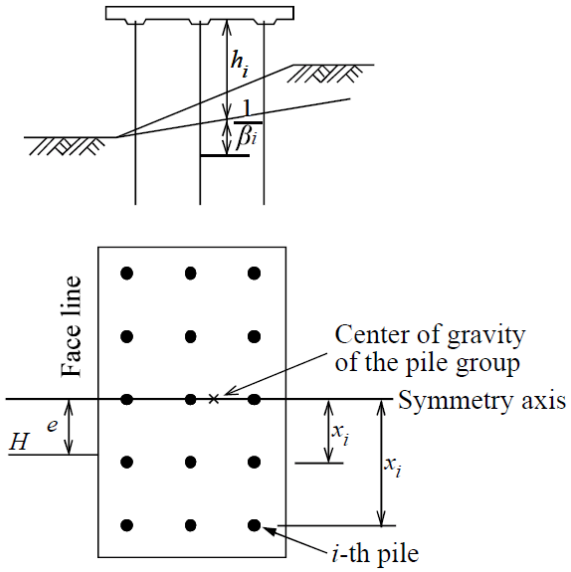

Source: OCDI 2020

Figure 1.20- Distance between the Center of Gravity of the Pile Group and Individual Piles

As for the cross-sectional stress of the pile, it is important to consider the impact stress during driving and buckling during driving, as well as negative friction where consolidation settlement is expected.

When using concrete piles, the bending moment listed in the catalogue is often not subject to axial force. The wharf piles are subject to large axial forces, so it is necessary to check whether axial force is present.

(3) Performance Verification of the Bearing Capacity in Piles under Design Situations

The bearing capacity of the piles in the piled piers can be verified using Equation (1.23). The symbol is the partial factor corresponding to the suffix, where the suffixes k and d indicate the characteristic value and the design value, respectively. As for the partial factors in the relevant equation, the values shown in Table 1.15 can be used. The values denoted as "-" in Table 1.15 indicate that the values may be verified using the values enclosed in parentheses ( ) to ensure convenience.

$$m \cdot \frac{S_d}{R_d} \leq 1.0 \quad R_d = \gamma_R R_k \quad S_d = \gamma_S S_k \tag{1.23}$$

OCDI 2020 Part III Chapter 5 Equation (5.2.8)

Where:

m : adjustment factor

S : characteristic value of load term (kN/m)

R : characteristic value of resistance term (kN/m)

γ_S : partial factor that is to be multiplied with the load term

γ_R : partial factor that is to be multiplied with the resistance term

The pile lateral resistance force can be calculated as an effective soil layer below the virtual ground surface, and in locations where waves are expected to hit the deck, it is desirable to take into account the pull-out resistance of the piles against the uplift pressure of the waves.

The axial resistance force should be determined by the pile loading test, but if it is difficult to perform the loading test in advance, it can be estimated based on the following estimation formula. However, even if the following estimation formula is used, a load test of the pile should be carried out during the construction stage.

Table 1.15- Partial Factors Used for Performance Verification Regarding the Bearing Capacity in Piles

OCDI 2020 Part III Chapter 5 Table 5.2.3

Verification target	Type of piles	Partial factor to be multiplied with resistance term: γ_R	Partial factor to be multiplied with load term: γ_S	Adjustment factor: m
Bearing capacity of the open-type wharves on vertical piles (variable situation for surcharges during ship actions)	Pulling pile	- (1.00)	- (1.00)	3.00
	Pushing pile	- (1.00)	- (1.00)	2.50
Bearing capacity of the open-type wharves on vertical piles (variable situation during storm, high waves, and Level 1 earthquake ground motion)	Pulling pile	- (1.00)	- (1.00)	2.50
	Pushing pile (bearing pile)	- (1.00)	- (1.00)	1.50
	Pushing pile (friction pile)	- (1.00)	- (1.00)	2.00

Source: Modified from OCDI 2020

1) Pushing Resistance Force of a Pile in its Axial Direction

As shown in Equation (1.24), the characteristic value of pushing resistance force of a pile in its axial direction is expressed as the sum of pile's characteristic values of base resistance and skin friction force.

$$R_{tk}=R_{pk}+R_{fk} \quad (1.24)$$

TCVN 11820 Part 2: 2025 Equation (A24)

Where:

R_{tk} : characteristic value of the pushing resistance force of a pile in its axial direction (kN)

R_{pk} : characteristic value of the base resistance force of a pile (kN)

R_{fk} : characteristic value of the skin friction force of a pile (kN)

i) Base resistance force in sandy ground

The characteristic value of the base resistance force of piles constructed with the hummer driving method and having sandy ground as the bearing stratum can be estimated with Equation (1.25).

$$R_{pk}= 300NA_p \quad (1.25)$$

TCVN 11820 Part 2: 2025 Equation (A26)

Where:

A_p : cross-sectional area at the pile bottom (m^2)
If pile's diameter is B,
$A_p = \pi B^2/4$

N : SPT-N value of the ground around the pile bottom

$$N = \frac{N_1 + \overline{N_2}}{2} \quad (1.26)$$

Where:

N_1 : SPT-N value of the ground at the pile bottom ($N_1 \leq 50$)

$\overline{N_2}$: mean SPT-N value in the range above the pile bottom to distance of $4B$ ($N_2 \leq 50$)

B : diameter or width of a pile (m)

ii) Base resistance force in clayey ground

The characteristic value of the base resistance force of piles constructed with the hummer driving method and the bottom of which is embedded in clayey ground can be estimated with Equation (1.27).

$$R_{pk} = 6 c_p A_p \quad (1.27)$$

TCVN 11820 Part 2: 2025 Equation (A27)

Where:

c_p : undrained shear strength in the ground at the pile bottom position (kN/m^2)

iii) Base resistance force in soft rock

If the bearing stratum is composed of soft rock, hard clay, bedrock, and others, the pushing resistance force of a pile in its axial direction shall be confirmed by the loading test as little knowledge is available concerning the base resistance force of piles constructed by the hummer driving method. Since little knowledge is available concerning the skin friction force of piles in such ground, the design in such ground needs not to expect the skin friction force or the skin friction force needs to be confirmed by the loading test.

Reference:

The base resistance and/or skin friction force can be estimated using the methods described in the following manual or report.

- ✓ Tomlinson MJ, Foundation Design and Construction
- ✓ CIRIA Report 181, Piled Foundation in Weak Rock

iv) Plugging ratio

The characteristic value of the base resistance force of a pile estimated from Equation (1.25) or (1.27) assumes that the pile bottom is completely closed. The characteristic values estimated by these equations are overmuch for an open-ended pile, which is the pile with its bottom opened, such as a steel pipe pile.

The behavior of the bottom of open-ended piles is quite different from that of closed-ended piles. However, the behavior of the ground in the vicinity of the bottom of open-end piles and interaction between piles and ground are still in the process of research, and no versatile estimation formula on the base resistance force of open-ended piles have been devised yet. As such, in practical use, the base resistance force of closed-ended piles estimated from Equation (1.25) or (1.27) is reduced by multiplying a coefficient called the plugging ratio, as shown in Equation (1.28) and used as the estimated value of the base resistance of open-ended piles.

$$R_{pok} = \eta \cdot R_{pk} \quad (1.28)$$

TCVN 11820 Part 2: 2025 Equation (A28)

Where:

R_{pok} : characteristic value of the base resistance force of open-end piles (kN)

η : plugging ratio

Plugging ratio is affected by different factors such as diameter of piles, embedment length of piles, characteristic of the ground, and construction methods. Although various methods to estimate the plugging ratio taking these factors into consideration are examined, currently, no standard method has been established. Therefore, when using open-ended piles, it is necessary to estimate the pushing resistance force of a pile in its axial direction by way of a loading test. The specifications of the pile bottom and construction conditions in the loading test must be as close as possible to actual piles

Past performance shows that the plugging ratio may be considered to be 100% provided that the pile diameter is 60cm or less for steel pipe piles and the short side is 40 cm or less for H-shaped steel piles. Large-diameter steel pipe piles frequently used in port facilities are reported to have significant effect of the pile diameter on the plugging ratio and may be referred to, as shown in Figure 1.21.

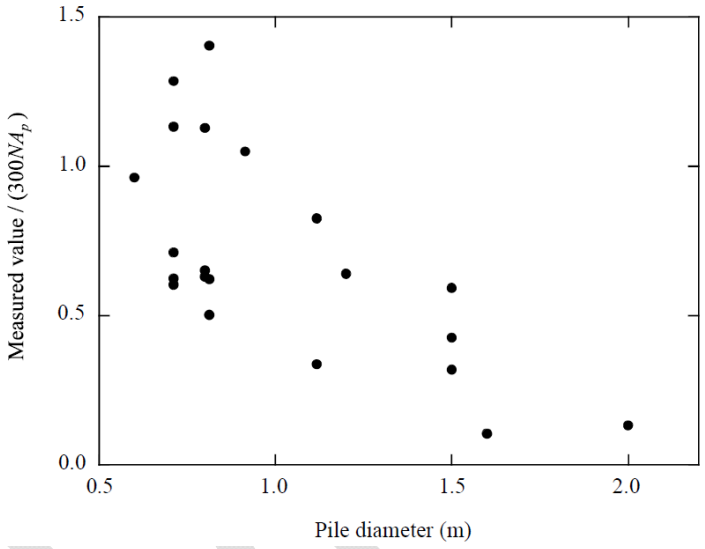

TCVN 11820 Part 2: 2025 Fig. A.13

Source: TCVN 11820-2-2025

Figure 1.21- Relation between Diameter of Open-ended Piles and Plugging Ratio (Kikuchi et al., added and altered)

Reference:

BS 8004 also indicates that for open ended driven tube or box piles in which a soil plug will not form during driving the full plan area A cannot be taken.

v) Skin friction force

As shown in Equation (1.29), the characteristic value of the skin friction force of a pile shall be considered to be determined by multiplying the skin friction force per unit contact area of the pile shaft and the ground by the perimeter surface area of the pile.

$$R_{fk} = \sum \overline{\gamma_{fki}} A_{si} \quad (1.29)$$

TCVN 11820 Part 2: 2025

Where:

γ_{fki} : mean skin friction force per unit contact area of pile and the

ground in the i-th layer (kN/m^2)

A_{si} : contact area of pile and the ground in the i-th layer (m^2)
$A_{si} = U_{si} \cdot l_i$

U_{si} : perimeter length of pile cross section in the i-th layer (m)

l_i : length of pile in the i-th layer (m)

Equation (A25)

v) For sandy soil ground:

$$\overline{\gamma_{fki}} = 2\overline{N} \quad (1.30)$$

TCVN 11820 Part 2: 2025 Equation (A29)

Where:

$\overline{N}$: mean SPT-N value in the i-th layer

vi) For cohesive soil ground:

$$\overline{\gamma_{fki}} = \overline{c_a} \quad (1.31)$$

TCVN 11820 Part 2: 2025 Equation (A30)

Where:

$\overline{c_a}$: mean adhesion of pile and the ground in the i-th layer

The adhesion value can be determined as follows:

$$\overline{c_a} = \begin{cases} c & c \le 100 \\ 100 & c > 100 \end{cases} \quad (1.32)$$

TCVN 11820 Part 2: 2025 Equation (A31)

Where:

c : undrained shear strength of the ground in the i-th layer (kN/m^2)

Additionally, if there is a risk of consolidation occurring around the piles, negative skin friction force should be considered separately when determining the static maximum axial resistance.

2) Pulling Resistance Force of a Pile in its Axial Direction

The characteristic value of the pulling resistance force of a pile in its axial direction is expressed by the sum of the characteristic value of skin friction force of the pile and the characteristic value of self-weight (underwater weight if in water) of the pile. The characteristic value of the skin friction force of a pile is considered to be determined by multiplying the skin friction force per unit contact area of the pile shaft and the ground by the perimeter surface area of the pile as in the case of the pushing resistance force of a pile in its axial direction (see Equation (1.29)).

3) Examination of the Embedment Length for Lateral Resistance

The embedment length of each vertical pile may be appropriately determined in accordance with the method of analysis of the pile lateral resistance. The embedment lengths of the vertical piles are generally set to be $3/\beta$ below the virtual ground surface based on the results of the pile lateral resistance analyses.

The method mentioned above in can be applied as an analysis method for a single pile receiving force from the perpendicular direction by setting $1/\beta$ in Chang's method as the virtual fixed point if stability analysis is conducted under horizontal force. Namely, Chang's method is the obtained solution if the pile length under the ground is assumed to be infinite. In addition, the range of finite underground pile length to which the method can be applied was examined, and it was observed that no large error occurs even if piles

with finite lengths are treated as those with infinite lengths if the embedment length of piles is $3/\beta$ or longer.

If the range of approximation between the piles with infinite lengths and the pile with finite lengths is widened in Chang's method, an embedment length of up to $2/\beta$ can be accepted for each vertical pile. However, it is preferable to avoid an embedment length shorter than $2/\beta$ using the virtual ground surface.

Even when Chang's method is used, if the solution method obtained using the boundary condition of finite embedment length is adopted, it does not have to be in accordance with the method.

If the lateral resistance of the piles is analyzed based on the PHRI method, the minimum embedment length of piles may become $1.5l_{ml}$. Here, l_{ml} is generally the depth from the ground surface to the flexural bending moment second zero point of the fixed head piles. (PHRI method: OCDI 2020 Part 3 Chapter 2 3.4.8)

4) Examination of the Pile Joints

When a pile joint is required in a pile, it is preferable to ensure that the pile can maintain its stability against the impact stress generated in the joint while driving.

The location of the pile joint shall be carefully determined to avoid the portion with excessive stress. It is recommended to position the splice at a depth deeper than the position of half of the maximum bending moment ($1/2M_{max}$ position) or at a depth deeper than the depth of the maximum bending moment l_{mF} is multiplied by 1.2 ($1.2l_{mF}$).

5) Change of the Plate Thickness or Material of Steel Pipe Pile

The strengths of the joints and portions with change in steel thickness should be examined carefully because there are some examples in which the piles of open-type wharves buckled at these portions because of ground deformation in a deep ground at which no bending stresses were generated under normal load conditions.

(4) Performance Verification for the Structural Members of the Superstructure

In principle, calculation of reinforcing bar arrangement of reinforced or prestressed concrete superstructures shall be made based on the limit state design method. Sufficient reinforcement should be provided against shear failure of the superstructure so that shear failure will not precede bending failure.

Since the superstructure is exposed to severe deterioration environment than other structures, it is necessary to take appropriate measures to satisfy the requirements for structural details such as the covering depth and the reinforcement required for the control of crack width under the serviceability limit state, so that a sufficient level of durability is retained.

1) Performance Verification for Pile Embedded Length

In the performance verification of the piled piers, the analysis is performed by assuming the formation of rigid connections between the pile heads and the concrete beams. Further, it is necessary that the pile head flexural moment can be smoothly distributed to the pile head and the concrete beam. The flexural moment that can be distributed to the beam M_{ud} may be calculated using Equation (1.33), ignoring the reinforcement connection plates or the vertical ribs that are provided, as necessary. In the following equation, the suffix d indicates the design value.

$$M_{ud} = \frac{DL^2 f'_{cd}}{6\gamma_b} \quad (1.33)$$

TCVN 11820 Part 11: 2025 Equation (4.3.10)

Where:

M_{ud} : bending moment transmitted by the pile embedded in the beam (N.mm)
D : diameter of pile (mm)
L : embedded length of pile (mm)
f'_{cd} : design value of the compressive strength of beam concrete (N/mm^2)
γ_b : member factor (may be considered to be 1.15)

Reference:

It is assumed that the axial forces are distributed by only the bond among the outer peripheral surface of the piles and the vertical ribs, which are provided, as necessary, as well as the concrete. In this case, the axial force that can be distributed, P_{ud}, can be calculated from Equation (1.34). In the following equation, the suffix d indicates the design value.

$$P_{ud} = \frac{1}{\gamma_b}\left(L\varphi + 2A_p\right) f_{bod} \quad (1.34)$$

OCDI 2020 Part III Chapter 5 Equation (5.2.13)

Where:

P_{ud} : axial force that can be distributed to the part of the pile embedded (N)
L : embedded length of the steel pipe pile (mm)
φ : outer perimeter of the steel pipe pile (mm)
f_{bod} : design value of the bond strength between the pile and the concrete (N/mm^2)
$f_{bod} = 0.11 f'^{2/3}_{ck} / \gamma_c$
f'_{ck} : characteristic value of the compressive strength of the concrete (N/mm^2)
γ_c : material coefficient of concrete (= 1.3)
A_p : area of vertical ribs that bonds with concrete (mm^2)
γ_b : member factor (may be considered to be 1.0)

It shall be verified that failure due to punching shear forces in the horizontal direction shall not occur in the beam at the end of which the steel pipe pile is embedded.

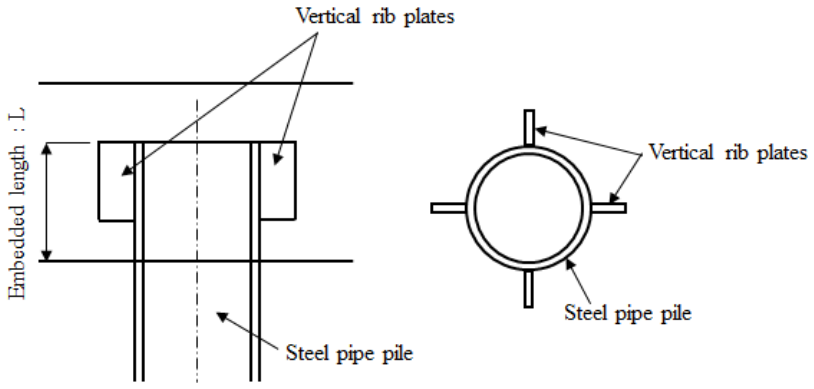

Figure 1.22- Pile Embedded Length and Rib Plates

2) Load Combinations and Partial Factor

The partial factors listed in Table 1.16 can be used for the verification of structural members. This table presents standard values for the partial factors; other methods may be used when appropriate for determining the partial factors.

3) Load Combinations for Superstructure Design

In the design of superstructure, the load combinations listed in Table 1.16 should be used and the superstructure should be safe against their actions.

i) Deck slab and access bridge
- deadweight and static load
- deadweight and live load
- deadweight and uplift

ii) Beam
- deadweight and static load
- deadweight and live load
- deadweight, moment generated at pile head due to the action of horizontal force, and static load when the horizontal force is acting
- load due to elastic settlement of the piles

Table 1.16- List of Partial Factors

TCVN 11820 Part 1: 2025 Bang.B.1

TCVN 11820 Part 6: 2023 Bang B.1

TCVN 11820 Part 11: 2025 Bang 4.1.1

OCDI 2020 Part III Chapter 5 Table 1.1.1

Partial factor		Cross-sectional failure	Fatigue failure	Other
Material factor γ_m	Concrete	1.3	1.3	1.0
	Reinforcing bars and PC steel members	1.0	1.05	1.0
	Other steel members	1.05	1.05	1.0
Load factor γ_f	Permanent actions	1.0–1.1 (0.9–1.0)	1.0	1.0
	Variable actions			
	Wave force	1.2	1.0	1.0
	Actions other than wave force	1.0–1.2 (0.8–1.0)	1.0	1.0
	Accidental actions	1.0	-	-
	Actions during construction	1.0	-	-
Structural analysis factor γ_a		1.0	1.0	1.0
Member factor γ_b		1.1–1.3	1.0–1.3	1.0
Structure factor γ_i		1.0–1.2	1.0–1.1	1.0

Note 1: The figures in parentheses in the table are applied when a smaller action results in a large risk.

Note 2: The values below may be used for the member factor when examining cross-sectional failure:
- When calculating bending and axial force: 1.1
- When calculating the maximum value of axial compressive force: 1.3
- When calculating shear capacity carried by concrete: 1.3
- When calculating shear capacitycarried by shear reinforcing bars: 1.1

Note 3: Since variations in the fatigue damage accumulated so far in the existing structural members need to be considered in designs for improvement, the member factor is set to an adequate value between 1.0 and 1.3 when examining the fatigue failure.

Note 4: When examining cross-sectional failure, the following values may be used as the structure factor:

		Permanent situation	Variable situation	Accidental situation
Superstructure of piled piers	Slab	1.2	1.2	1.0
	Beams	1.1	1.1	1.0
Breakwaters		1.0	1.1	1.0
Quay walls (caissons, etc.)		1.0	1.1 (only during earthquakes: 1.0)	1.0
Other (sheet pile superstructures, etc.)		1.0	1.0	1.0

Source: Modified from TCVN 11820-1-2025, TCVN 11820-6-2023, TCVN-11-2025, OCDI 2020

Table 1.17- Load Combination for Desk Slab and Access Bridge design

TCVN 11820 Part 11: 2025 Bang 4.3.7

Verification of cross-sectional failure	Verification of serviceability	Verification of fatigue failure
1.1(0.9)*D*+1.2(0.8)*S*	1.0*D*+0.5*S*	-
1.1(0.9)*D*+1.2(0.8)*L*	1.0*D*+0.5*L*	1.0*D*+1.0*L*
1.1(0.9)*D*+1.2(0.8)*S*+1.2(0.8)*B*	1.0*D*+0.5*S*+0.5*B*	-
0.9(1.1)*D*+1.0*U*	-	-
1.0*D*+1.0*S*+1.0*L*+1.0*E*	-	-

Where:

D: Dead weight, *S*: Surcharge load, *L*: Live load such as vehicle load and/or equipment load, *B*: Berthing force, *U*: Uplift force, *E*: Earthquake ground motion

Source: TCVN 11820-11-2025

4) Calculations of Sectional Forces

i) Calculation methods for concrete slab

The calculation method for concrete slab is as follows based on the ratio of the short span to the long span of the plate:

- Span ratio = short span/Long span < 0.4: slab supported by side walls
- Span ratio = short span/Long span ≥ 0.4: slab fixed on four sides

The effective width of slab supported by side walls is calculated by the following equation (refer to Figure 1.23).

$$b_e = a' + 2.4x\left(1 - \frac{x}{l'}\right) \qquad (1.35)$$

TCVN 11820 Part 11: 2025 Equation (4.3.2)

Where:

b_e : effective width (m)
a' : distribution width of the action (m)
x : distance from the point of concentrated load action to the nearest support (m)
l' : inflection point length (l'=0.8l) (m)
l : span length (m)
s : pavement thickness (m)

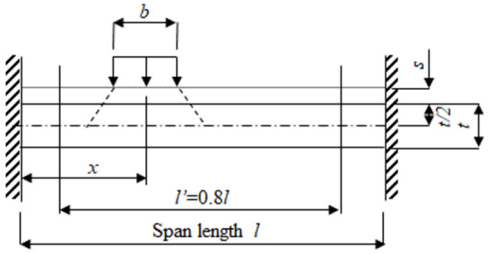

TCVN 11820 Part 11: 2025 Hinh 4.3.22

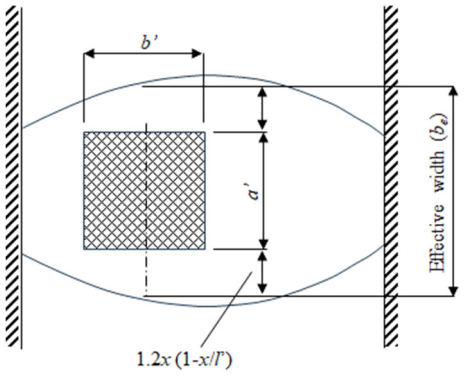

Source: TCVN 11820-11-2025

Figure 1.23- Effective Width of Slab Supported by Side Walls

ii) Sectional forces due to wheel loads

The bending moment on slab sections due to wheel loads from trucks, trailers, forklifts, etc., can be calculated using two methods: one method converts them into distributed loads and calculates the section from the calculation diagram of the section as a slab fixed on four sides, and the other method converts them into partial distributed loads and calculates them using Pigeaud's diagram.

The larger of the two calculated values can be considered as the design bending moment. It should be noted that conversion to distributed loads and conversion to partial distributed loads are converted into distributed loads as shown in Figures 1.24 and 1.25.

✓ Conversion to distributed loads

$$w_L = \frac{P}{(0.5L_1+0.25L_2)C} \quad (1.36)$$

TCVN 11820 Part 11: 2025 Equation (4.3.3)

Where:

w_L : equivalent distributed load (kN/m^2)
P : wheel load (kN)
C : width of one lane (vehicle width, m)
L_1 : long span length (m)
L_2 : short span length (m)

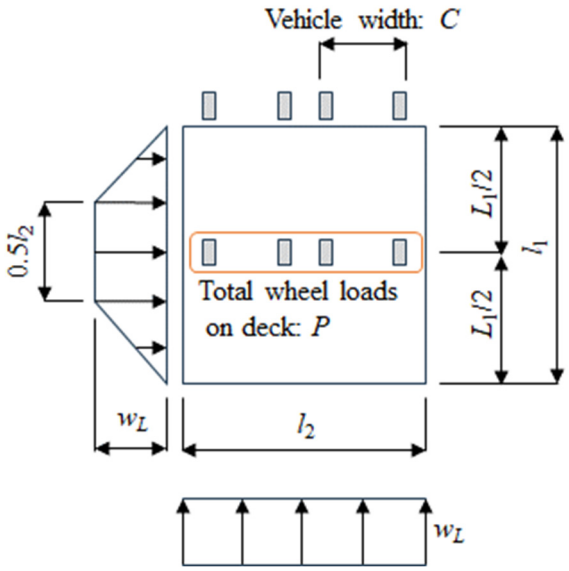

TCVN 11820 Part 11: 2025 Hinh 4.3.23

Source: TCVN 11820-11-2025

Figure 1.24- Conversion to Distributed Loads

✓ Conversion to partial distributed loads

$$\left.\begin{aligned} w &= \frac{P}{a' \times b'} \\ a' &= a + 2\left(s + \frac{t}{2}\right) \\ b' &= b + 2\left(s + \frac{t}{2}\right) \end{aligned}\right\} \quad (1.37)$$

TCVN 11820 Part 11: 2025 Equation (4.3.4)

here:

w : equivalent distributed load (kN/m^2)
P : wheel load (N)
a,b : width of load distribution (m)
s : pavement thickness (m)
t : slab thickness (m)
a',b' : converted distribution width of load (m)

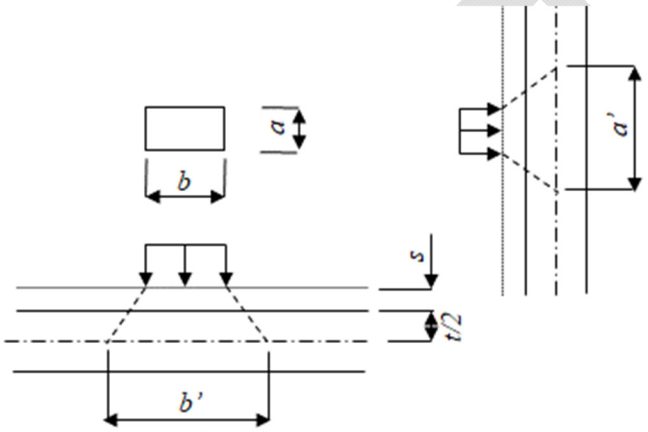

TCVN 11820 Part 11: 2025 Hinh 4.3.24

Source: TCVN 11820-11-2025

Figure 1.25- Conversion to Partial Distributed Loads

The bending moment on the slab due to the outrigger reaction force of a truck crane can be converted into a partial distributed load and may be determined from Pigeaud's diagram.

iii) Loads acting on beams

The live loads and dead loads acting on beams supporting slab fixed on four sides are considered with equivalent distributed loads as shown in Figure 1.24, and are calculated using the following formula:

✓ Equivalent distributed load for the short span

$$W = \frac{wL_s}{3} \quad (1.38)$$

✓ Equivalent distributed load for the long span

$$W = \frac{wL_s}{3}\left(1 - \frac{1}{3} \cdot \frac{L_s^2}{L_L^2}\right) \quad (1.39)$$

TCVN 11820 Part 11: 2025 Equation (4.3.8) (4.3.9)

Where:

W : equivalent distributed load acting on the beam (kN/m)
w : distributed load acting on the slab (kN/m^2)
L_s : short span length (m)
L_L : long span length (m)

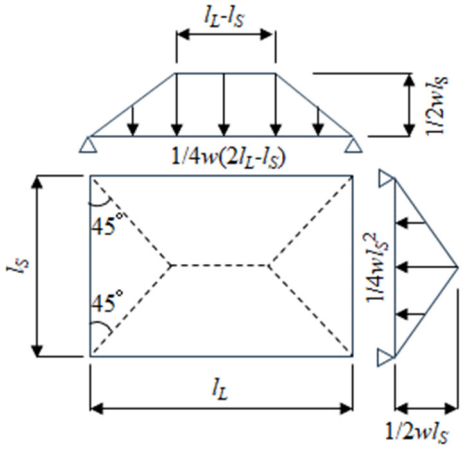

TCVN 11820 Part 11: 2025 Hinh 4.3.25

Source: TCVN 11820-11-2025

Figure 1.26- Live and Dead Loads Acting on Beams

5) Calculations of Bending Moment

i) Slab supported by side walls

$$\left.\begin{aligned} M_A &= \frac{wl^2}{12} \\ M_a &= \frac{wl^2}{24} \end{aligned}\right\} \quad (1.40)$$

TCVN 11820 Part 11: 2025 Equation (4.3.5)

Where:

M_A : bending moment at supports (kN·m)

M_a : maximum bending moment in the span (kN·m)

ii) Slab fixed on four sides

✓ $\lambda \leq 1$

$$\left.\begin{aligned} M_x &= Xql_x^2 \\ M_y &= Yql_x^2 \end{aligned}\right\} \quad (1.41)$$

TCVN 11820 Part 11: 2025 Equation (4.3.6)

✓ $\lambda > 1$

$$\left.\begin{aligned} M_x &= Xql_y^2 \\ M_y &= Yql_y^2 \end{aligned}\right\} \quad (1.42)$$

TCVN 11820 Part 11: 2025 Equation (4.3.7)

Where:

λ : l_x / l_y

M_x, M_y : bending moment in the x-direction and y-direction (kN·m/m)

X, Y : bending moment coefficients in the x-direction and y-direction

l_x, l_y : lengths of the slab in the x-direction and y-direction (m)

q : distributed load acting on the slab (kN/m^2)

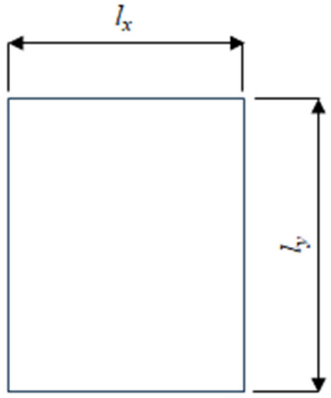

Figure 1.27- Span Length

(5) Corrosion Protection Design for Steel Members

1) General

The standard procedure in TCVN 11820 Part 3: 2019 is to apply protective covering/ coating method up to L.W.L. -1.0 (m) and cathodic protection method up to the M.L.W.L. (mean low water level). When the covering/coating method is used underwater it is necessary to pay attention to durability when selecting the covering/coating material and to watch for damage, such as during construction or from collisions with driftwood.

TCVN 11820 Part 3: 2019 Chapter 5.3.3.2

2) Cathodic Protection Method

Cathodic protection is a method of corrosion protection that involves applying an inflow of a protective current to a steel structure. The most common method is the galvanic anode method (installing aluminum alloy anodes on the steel surface) owing to its ease of maintenance. In this case, the electrons (e-) generated by dissolution of aluminum (Al) in the sea move through the steel, causing a reduction reaction of oxygen on the steel surface to start demonstrating the effect of cathodic protection.

Therefore, only the outer surface of steel pipe piles facing the seawater or soil below seabed is protected from corrosion. Based on survey results in Japan, the protective current density flowing into the steel surface is set at about 100 to 130 mA/m^2 in the sea and 20 to 26 mA/m^2 in soil below seabed.

In designing cathodic protection for port steel structures, the standard procedure is to set the corrosion control ratio at or below the M.L.W.L. (= (corrosion rate without corrosion protection − corrosion rate with corrosion protection) / corrosion rate without corrosion protection) to 90 %. In this case, when the corrosion rate without corrosion protection is 0.2 mm/yr, the corrosion rate with corrosion protection is 0.02 mm/yr. Note that when the anode is completely depleted (≈ when it reaches its design lifetime), it is necessary to renew the anode (install an additional one).

TCVN 11820 Part 3: 2019 Bang 4 Equation (1), (2)

3) Design of Protective Coating

Protective coating is a method that shields the protected material (steel) from corrosive environmental factors. There are generally five types of coating methods which are applied to port steel structures: (a) painting, (b) organic coating, (c) petrolatum coating, (d) inorganic coating and (e) metal coating. When designing protective coating, it is necessary to select the most appropriate method considering the ease of application, expected lifetime and any other relevant factors.

Currently in Vietnam, there is no sufficient data on the corrosion rate of steel in marine environment. So, can refer to the values about the corrosion rate of steel in Table 1.18.

Table 1.18- Standard Values of Corrosion Rates for Steel

Corrosive environment		Corrosion rate (mm/year)
Seaside	HWL or higher	0.3
	HWL to LWL -1m	0.1 - 0.3
	LWL -1m to seabed	0.1 - 0.2
	Below seabed	0.03
Landside	Above ground and exposed to air	0.1
	Underground (residual water level and above)	0.03
	Underground (residual water level and below)	0.02

Source: TCVN 11820-3-2019

(6) Pile Loading Test

1) General

Pile dynamic loading test, developed for supervising pile driving operations, applies dynamic loads such as hammer strikes to pile heads within a short time ($T_r < 5$). This brief loading induces wave phenomena inside the piles, creating different stress states compared to pushing and rapid loading tests. In the tests, dynamic resistance components form a larger fraction of the total ground resistance. The test involves installing strain gauges and accelerometers on pile heads to measure strain and acceleration waveforms generated by hammer impacts, analyzing the results using kinematic wave theory. Commonly, analysis employs the waveform matching method based on one-dimensional kinetic wave theory.

$$T_r = \frac{t_L}{2L/C} \tag{1.43}$$

Where:

T_r : relative loading time
t_L : loading time (sec)
L : pile length (m)
C : propagation velocity of the divergent wave

2) Timing of Dynamic Loading Tests

Pile dynamic loading tests for driven piles can be conducted in two ways due to their availability during construction: a post-construction dynamic loading test immediately after the piles are built, and a post-curing dynamic loading test after the predetermined curing periods have elapsed. The post-construction test is typically conducted right after pile driving work is complete, whereas the post-curing test occurs after allowing time for the ground disturbed by the pile driving to regain strength. This recovery is facilitated by the dissipation of excess pore water pressure, which increases the effective stress in the ground—a phenomenon known as "set-up." The increase in static resistance due to set-up can be quantified using a "set-up ratio" (refer to Figure 1.28), which helps estimate the static resistance after curing based on the results from the post-construction test alone.

Recommended curing periods are at least five days for sandy soil and 14 days for cohesive soil. However, extended curing periods can pose challenges due to insufficient hammer capacity for the restored ground resistance, leading to shorter practical curing periods of a few days to one week. The post-curing test may also be repeated with different curing periods for more accurate results.

When implementing the post-curing test on actual piles, it is advisable to check the allowances in overall pile lengths and the lengths of heavy-duty corrosion protection areas, especially if the elevations of the pile heads post-driving are lower than designed.

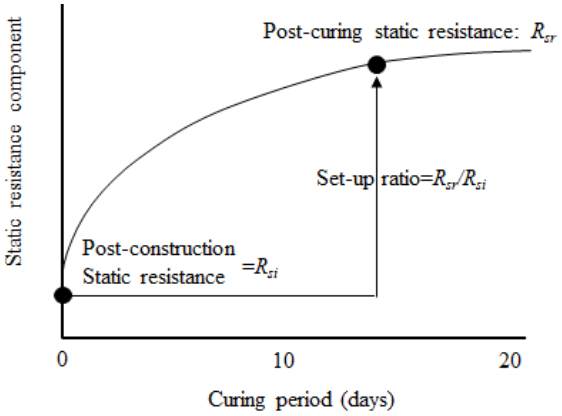

OCDI 2020 Part V Chapter 1 Fig. 3.10.18

Source: OCDI 2020

Figure 1.28- Concept of Set-up Ratio

3) Test Results

In dynamic loading tests, pile resistance is analytically determined using data from strain and acceleration measurements at the pile heads. These measurements help calculate axial forces, velocities, and displacements of the pile bodies. By applying one-dimensional kinetic wave theory, input and reflected waves in axial directions are derived from these values, representing hammer impact loads and ground resistance states, respectively.

Analysis methods such as the CASE method and waveform matching analysis such as CAPWAP are utilized to interpret these waveforms. The CASE method offers real-time ground resistance measurement during the test, though with lower accuracy. Conversely, waveform matching analysis models the piles and surrounding ground to simulate the test and performs inverse analyses to pinpoint static resistance components, allowing precise determination of friction forces across different soil layers.

While the dynamic loading test typically reports pile resistance values such as axial push resistance, base resistance, and skin friction, relationships between resistance and displacement are generally not illustrated. Advanced numerical analyses can estimate curves showing this relationship based on waveform analysis results, but such practices are rare, especially in pile loading tests for port facilities. Consequently, the detailed limit resistances often remain undefined.

Despite potential issues like insufficient impact energy, dynamic loading tests are still valuable for estimating axial pile resistance and are frequently repeated due to their simplicity. These tests are also used as construction confirmation tests, with ongoing efforts to enhance construction supervision accuracy through refined analysis of accumulated test data.

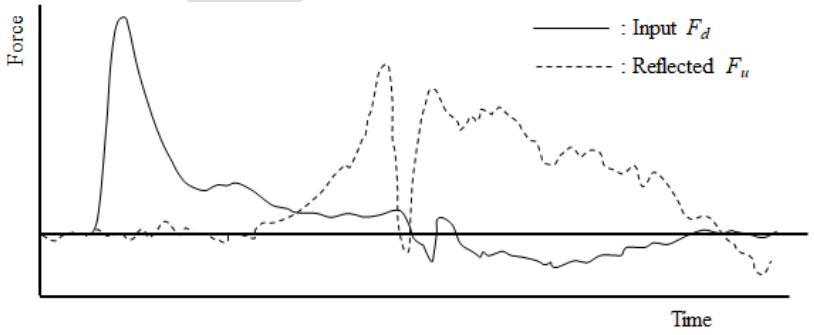

OCDI 2020 Part V Chapter 1 Fig. 3.10.23

Source: OCDI 2020

Figure 1.29- Example of Curves Representing the Relationships between Input Waves and Time, and between Reflected Waves and Time

2. Design Example

2-1. Typical Section for Performance Verification

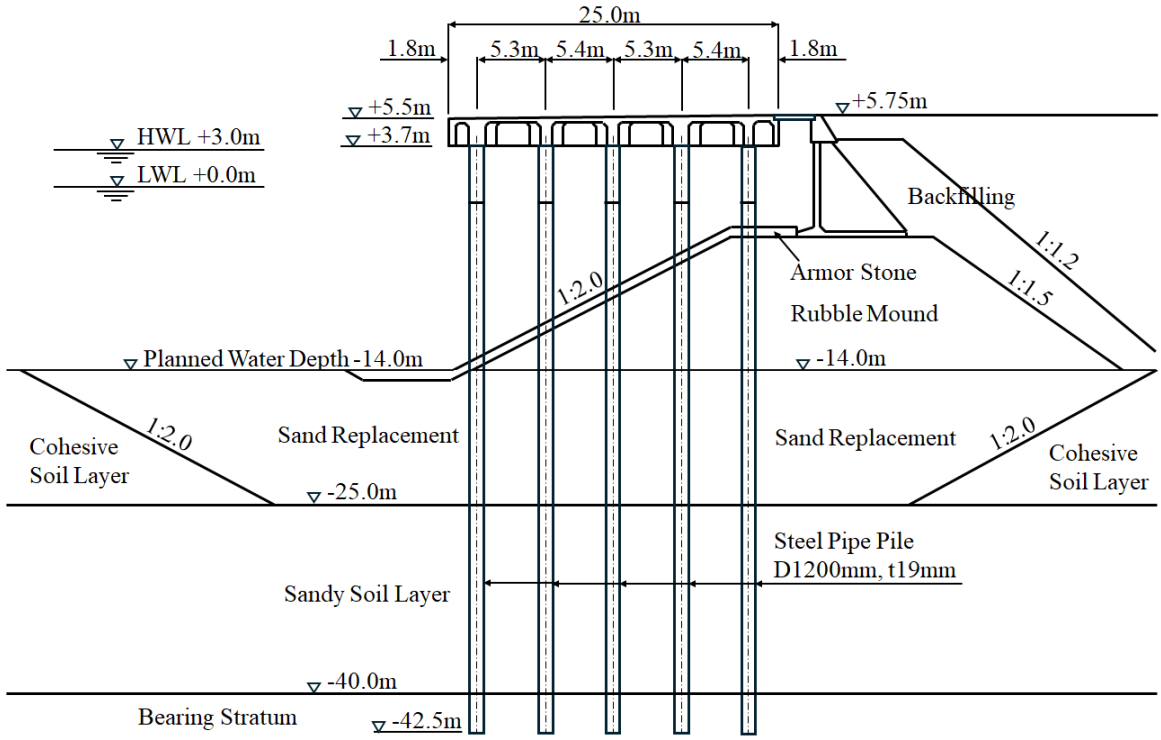

Figure 2.1- Typical Section of Design Example

2-2. Design Conditions

(1) Planning Conditions

- Planned water depth: *D.L.* – 14.00 m
- Design water depth: *D.L.* – 14.10 m
- Class: I (wall height is 19.5m)

Because installation of armor stones for scouring prevention is assumed on the front side of the wharf, the average of the accuracy of rough leveling of the stones (0 to -20 cm) is included in the calculation of the planned water depth.

- Crown height of deck: *D.L.* +5.50 m
- Deck length: $L = 20.00$ m per span
- Deck width: $B = 25.00$ m
- Deck gradient: $i = 1.00$ %

(2) Use Conditions

1) Dimensions of Design Vessel

- General cargo ship: 50,000 *DWT*
- Length overall: $Loa = 203.00$ m
- Beam: $B = 32.3$ m
- Loaded draft: $d = 12.60$ m
- Gross tonnage: $GT = 0.529DWT = 0.529 \times 50{,}000 = 26{,}450$ t

2) Design Service Life and Corrosion Countermeasures

- Design service life: 50 years
- Corrosion countermeasures

Cathodic protection:

50 years is assumed. The assumed corrosion control ratio is 90 %.

Protective coating:

Heavy anticorrosion coating is applied to the intertidal zone of steel pipe piles from L.W.L. -1.00 m to the bottom of the deck beams. The assumed corrosion protection efficiency in this case is 100 %.

(3) Natural Conditions

1) Tide Levels

- Design High Water Level: *D.L.* +3.00 m
- Mean Sea Level: *D.L.* +1.50 m
- Design Low Water Level: *D.L.* ±0.00 m

2) Ground Conditions

D.L. -14.00 m (Planned water depth)

Cohesive soil layer

$\gamma' = 6.0$ kN/m^3, $c = 20.0 + 3.0$ Z (kN/m^2)

D.L. -25.00 m

Sandy soil layer

$\gamma' = 10.0$ kN/m^3, $N = 20$, $\varphi = 33°$

D.L. -40.00 m

Sandy soil layer (bearing stratum)

$\gamma' = 10.0$ kN/m^3, $N = 50$, $\varphi = 40°$

- Sand replacement layer

  Sandy soil layer: $\gamma' = 10.0$ kN/m^3, $N = 8$, $\varphi = 30°$

- Rubble mound layer

  Gravel soil layer: $\gamma' = 10.0$ kN/m^3, $\varphi = 40°$

  When calculating the coefficient of the lateral subgrade reaction, $k_{CH} = 3{,}000$ kN/m^3 is assumed in the evaluation. Although there are various approaches to the skin friction of piles in rubble, including disregarding skin friction, in this example, N value = 2 (= 3,000/1,500) was set by back-calculation from $k_{CH} = 1{,}500\,N$ as conservative approach.

2-3. Seismic Coefficient

- Ground type: Type D
- Importance coefficient: 1.0 (Wharf)
- Background acceleration: 0.10g
- Behavior factor: 2 (Vertical piled wharf)

The seismic coefficient for verification in the variable situation is set by natural period estimated and shape of the elastic response spectrum shown in Figure 2.2.

Applied *N*-value is estimated as the average of the soil layer.

- Rubble mound layer: $N = 2$
- Sand replacement layer: $N = 8 \rightarrow N_{avg} = 5$

(1) Horizontal Spring Constant

The horizontal spring constant (k_{CH}) and inverse of the distance between the virtual ground surface and the virtual fixed point of the pile (β) for calculating the virtual fixed point ($1/\beta$) are calculated as follows:

$k_{CH} = 1500N_{avg} = 1500 \times 5 = 7{,}500$ kN/m³

$$\beta = \sqrt[4]{\frac{k_{CH}D}{4EI}}$$

$$= \sqrt[4]{\frac{7{,}500 \times 1.20}{4 \times 2.0 \times 10^{8} \times 1.16 \times 10^{-2}}}$$

$= 0.176$ m^{-1}

I: inertia moment of the pile section (m^4), includes 1.0mm corrosion

D1,200×t19mm with 1.0mm corrosion, $I = 1.16 \times 10^{-2}$ (m^4)

$1/\beta = 1/0.176 = 5.67$ m

Table 2.1- Virtual Fixed Point

Item	Row 1	Row 2	Row 3	Row 4	Row 5
Vertical distance between the pile head and the virtual ground surface h_i (m)	17.25	15.93	14.58	13.25	12.20
$1/\beta$ (m)	5.67	5.67	5.67	5.67	5.67
Cantilever length l_i (m)	22.92	21.60	20.25	18.92	17.87
Virtual fixed point (DL, m)	-19.22	-17.90	-16.55	-15.22	-14.17

The horizontal spring constants of each pile are calculated as follows:

$$K_{Hi} = \frac{12EI_i}{\left(h_i + 1/\beta_i\right)^3} = \frac{12EI_i}{l_i^3}$$

Row 1: $K_{H1} = \dfrac{12 \times 2.0 \times 10^{8} \times 1.16 \times 10^{-2}}{22.92^3} = 2{,}316$ kN/m

Row 2: $K_{H2} = \dfrac{12 \times 2.0 \times 10^{8} \times 1.16 \times 10^{-2}}{21.60^3} = 2{,}767$ kN/m

Row 3: $K_{H3} = \dfrac{12 \times 2.0 \times 10^{8} \times 1.16 \times 10^{-2}}{20.25^3} = 3{,}358$ kN/m

Row 4: $K_{H4} = \dfrac{12 \times 2.0 \times 10^{8} \times 1.16 \times 10^{-2}}{18.92^3} = 4{,}117$ kN/m

Row 5: $K_{H5} = \dfrac{12 \times 2.0 \times 10^{8} \times 1.16 \times 10^{-2}}{17.87^3} = 4{,}887$ kN/m

K_{Hi} per section = $\Sigma K_{Hi} = 17{,}445$ kN/m

K_{Hi} per span = $\Sigma K_{Hi} = 17{,}445 \times 5$ lines = 87,225 kN/m

(2) Natural Period

$$T = 2\pi\sqrt{\frac{W}{gK}}$$

Where:

T_s : natural period of the piled pier (sec)
W : total weight of the superstructure of the pier and the load during seismic events (kN)
g : gravitational acceleration (m/s²)
K : spring constant of the piled pier (kN/m)

1) Natural Period without Crane

W = 20.0(Span length) ×25.0(Span width) ×30 kN/m² + 20.0×25.0×10 kN/m²
= 20,000 kN

ΣK_{Hi} = 17,445 × 5 lines = 87,225 kN/m

$$T = 2\pi\sqrt{\frac{W}{gK}} = 2\pi\sqrt{\frac{20{,}000}{9.81\times 87{,}225}} = 0.96 \text{ sec}$$

2) Natural Period with Crane

W = 20.0×25.0×30 kN/m² + 20.0×25.0×10 kN/m² + 12,200 kN
= 32,200 kN

ΣK_{Hi} = 17,445 × 5 lines = 87,225 kN/m

$$T = 2\pi\sqrt{\frac{W}{gK}} = 2\pi\sqrt{\frac{32{,}200}{9.81\times 87{,}225}} = 1.22 \text{ sec}$$

(3) Seismic Coefficient

Peak acceleration: 0.10g ×2.820 = 0.282g
Ground type: Type D
Seismic coefficient: k_h = 0.282 / q (=2, behavior factor) = 0.141

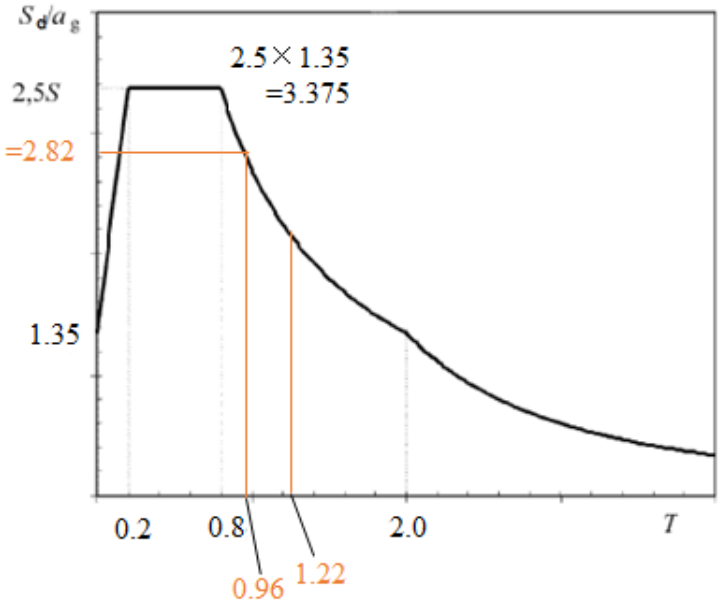

Figure 2.2- Shape of the Elastic Response Spectrum

2-4. Summary of Loads and Actions

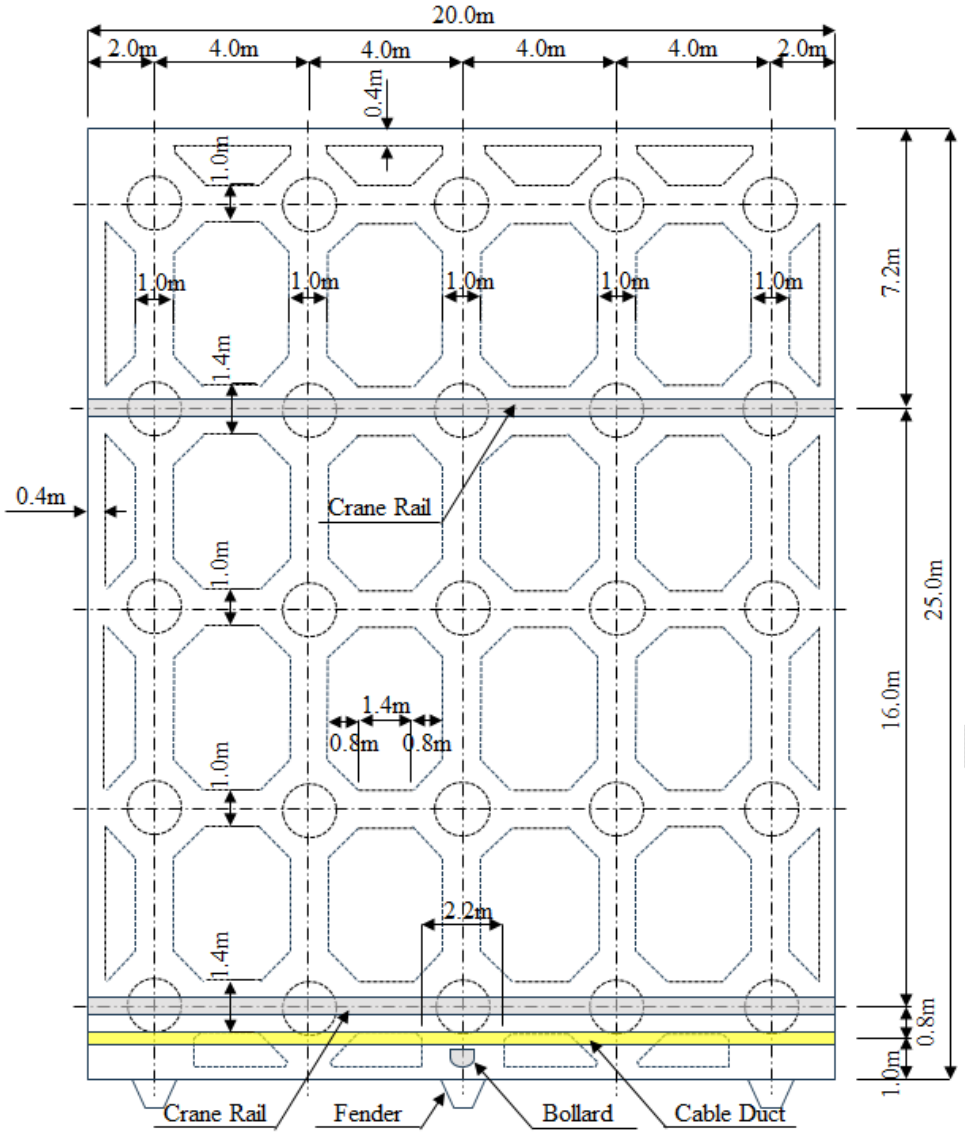

Figure 2.3- Dimensions of Superstructure of Piled Pier and Arrangement of Steel Pipe Piles

(1) Unit Weight of Concrete

- Unreinforced concrete: $\gamma_c = 22.6$ kN/m^3
- Reinforced concrete: $\gamma_c = 24.0$ kN/m^3
- Pavement concrete: $\gamma_c = 24.0$ kN/m^3

(Same as reinforced concrete because the pavement and slab are constructed as an integrated structure.)

TCVN 11820 Part 2: 2025 Bang 49

(2) Surcharges

- Permanent States (During operation): 20 kN/m^2
- Earthquake ground motion: 10 kN/m^2

(3) Live Loads

- Vehicle (truck) load
- Vehicle (trailer) load
- Forklift load
- Crane load

Type: Rail-mounted traveling bridge crane
Service weight: 11,000 kN
Rail gauge: 16.00 m
Wheelbase: 18.00 m
Number of wheels: 8 wheels × 2 legs (on both seaward side and harbor (land) side)
Length of 8 wheels/leg: 6.40 m
Wheel spacing: 800 mm
Closest approach distance of cranes: 3.40 m

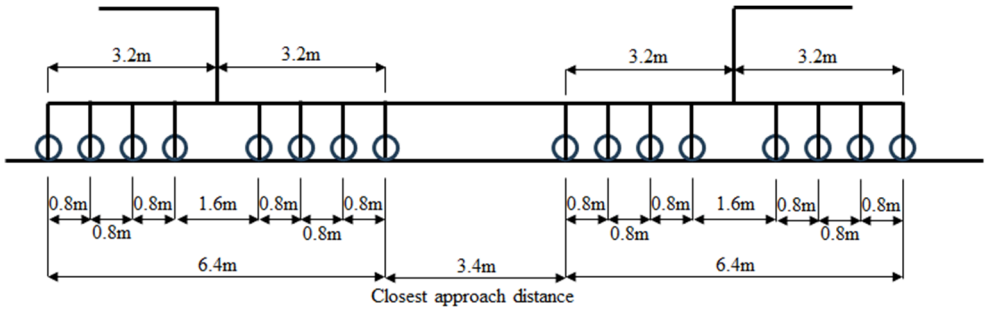

Figure 2.4- Arrangement of Crane Wheels

As the maximum wheel load used as an action in the static study, the value calculated based on the calculation standard for crane structural parts (JIS B 8821) or the crane structural standard (notification of the Ministry of Labor) can be used.

Table 2.2 shows the wheel loads set based on the above. In this example, the value (k_h = 0.20) of the wheel load during an earthquake calculated based on the crane structural standard, etc. by the wheel load set considering the dynamic interaction of the crane and the mooring facilities was larger than the seismic coefficient of verification (k_h = 0.14). Therefore, kh = 0.20 was adopted as a more conservative value.

Table 2.2- Crane Wheel Load

Unit: kN/wheel

Direction of action			Sea→Land	Land→Sea
Vertical load	During work (wind velocity 16 m/sec)	Sea side	346	523
		Land side	418	241
	During storm (wind velocity 55 m/sec)	Sea side	76	551
		Land side	635	160
	During earthquake (horizontal seismic coefficient kh=0.20)	Sea side	81	764
		Land side	683	-19
Horizontal load	During work (wind velocity 16 m/sec)	Sea side	35	52
		Land side	42	24
	During storm (wind velocity 55 m/sec)	Sea side	14	99
		Land side	114	29
	During earthquake (horizontal seismic coefficient kh=0.20)	Sea side	16	153
		Land side	137	-4

Source: Crane supplier

Among moving loads, the main load that affects the examination of the cross section of foundation piles is crane load. Here, the maximum support reaction force acting on the end support point A and its adjoining support point B in a 4-span continuous girder is

obtained.

For the variable situations related to work and earthquake ground motion, the value when the maximum influence value of the support reaction force occurs was obtained by a computer calculation, assuming one or two cranes are loaded on the wharf.

- Influence value of reaction force at support point A 5.665

Because the value for support point A is larger in this calculation result, the crane wheel load at support point A is used.

During work and during an earthquake, the wheel load is increased by an increment of 10 %, assuming a crane traveling speed of 1 m/s. An example of a calculation of the wheel load during work (sea → land) is shown below.

i. Vertical force during work (sea → land)
- Sea side 346 kN/wheel × 1.10 (extra) × 5.665 = 2,156.17 kN
- Land side 418 kN/wheel × 1.10 (extra) × 5.665 = 2,604.85 kN

ii. Horizontal force during work (sea → land)
- Sea side 35 kN/wheel × 1.10 (extra) × 5.665 = 218.11 kN
- Land side 42 kN/wheel × 1.10 (extra) × 5.665 = 261.73 kN

During a storm, the wheel load can be calculated as follows because the influence value of the maximum reaction force of piles when the crane is loaded at a fixed position is 5.384.

i. Vertical load during storm (sea → land)
- Sea side 76 kN/wheel × 5.665 = 430.55 kN
- Land side 635 kN/wheel × 5.665 = 3,597.39 kN

ii. Horizontal load during storm (sea → land)
- Sea side 14 kN/wheel × 5.665 = 79.31 kN
- Land side 114 kN/wheel × 5.665 = 645.83 kN

The characteristic values of the crane wheel load calculated by the method described above are shown in Table 2.3.

Table 2.3 Crane wheel load acting on piles (Wheel load at end position)

Table 2.3- Characteristic Value of Crane Wheel Load Unit: kN

Direction of action			Sea→Land	Land→Sea
Vertical force	During work (wind velocity 16 m/sec)	Sea side	2156.17	3259.18
		Land side	2604.85	1501.84
	During storm (wind velocity 55 m/sec)	Sea side	430.55	3121.51
		Land side	3597.39	906.43
	During earthquake (horizontal seismic coefficient kh=0.,20)	Sea side	504.77	4808.86
		Land side	4256.25	1.41
Horizontal force	During work (wind velocity 16 m/sec)	Sea side	218.11	-324.05
		Land side	261.73	-149.56
	During storm (wind velocity 55 m/sec)	Sea side	79.31	-560.85
		Land side	645.83	-164.29
	During earthquake (horizontal seismic coefficient kh=0.,20)	Sea side	99.71	-963.03
		Land side	853.74	-0.30

(4) Mooring Forces of Ships

Because the gross tonnage (*GT*) of the cargo vessel which is the design ship in this example is 26,450 t, the mooring force T_k of the ship is as shown below, assuming a value of 20,000 *GT* to 50,000 *GT*.

- Mooring force acting on bollard T_k = 1,000 kN

Table 2.4- Standard Values of Tractive Force by Ships

GT of ship (ton)					Tractive force acting on a bollard (kN)	Tractive force acting on a mooring post (kN)
Over	200	and	not more than	500	150	150
Over	500	and	not more than	1,000	250	250
Over	1,000	and	not more than	2,000	250	350
Over	2,000	and	not more than	3,000	350	350
Over	3,000	and	not more than	5,000	350	500
Over	5,000	and	not more than	10,000	500	700
Over	10,000	and	not more than	20,000	700	1,000
Over	20,000	and	not more than	50,000	1,000	1,500
Over	50,000	and	not more than	100,000	1,000	2,000

Source: TCVN 11820-2-2025

TCVN 11820 Part 2: 2025 Bang 48

(5) Berthing Force

1) Calculation of Berthing Energy

The characteristic value (E_{fk}) of the berthing energy of a vessel is obtained by the following equation (refer to Equation (1.4)).

$$E_{f_k} = \frac{1}{2} M_{s_k} V_{b_k}{}^2 C_{m_k} C_{e_k} C_{s_k} C_{c_k}$$

Where:

E_f : berthing energy of the ship (kJ)
M_s : mass of the ship (t)
V_b : berthing velocity of the ship (m/s)
C_m : virtual mass factor
C_e : eccentricity factor
C_s : flexibility factor =1.0
C_c : berth configuration factor =1.0

- Mass of ship
  $M_{sk} = DT = 2.920 \times 50{,}000^{0.924} = 64{,}155$ t

- Berthing velocity of the ship
  $V_{bk} = 0.10$ m/s

- Block coefficient
  Length between perpendiculars L_{pp} = 195.0 m
  The block coefficient (C_b) of the vessel is obtained by the following equation.

$$C_{bk} = \frac{\nabla}{L_{bb} B d} = \frac{64{,}155/1.03}{195.0 \times 32.3 \times 12.6} = 0.785$$

- Virtual mass factor

$$C_{mk} = 1 + \frac{\pi}{2 C_{bk}} \frac{d}{B} = 1 + \frac{\pi}{2 \times 0.785} \times \frac{12.6}{32.3} = 1.78$$

- Eccentricity factor
  Radius of gyration r

$$r = (0.19\, C_{bk} + 0.11)\, L_{pp} = (0.19 \times 0.785 + 0.11) \times 195.0 = 50.53 \text{ m}$$

Distance L_i from berthing point of vessel along the normal line of the mooring facility to the center of gravity of the vessel

$$L_1 = \{0.5\alpha + e\,(1-k)\}\, L_{pp}\cos\theta$$
$$= \{0.5 \times 0.50 + 0.051 \times (1-0.5)\} \times 195.0 \times \cos 3° = 53.65 \text{ m}$$

$$L_2 = (0.5\alpha - ek)\, L_{pp}\cos\theta$$
$$= (0.5 \times 0.50 - 0.051 \times 0.5) \times 195.0 \times \cos 3° = 43.72 \text{ m}$$

e = Fender pitch (here 10.0m) / $L_{pp}\cos\theta$
= 10.0 / (195.0× cos3°) = 0.051

Where:

- θ : berthing angle 3°
- e : ratio of fender interval and length between perpendiculars
- α : ratio of length of parallel side and length between perpendiculars (0.50)
  When it is assumed that the length of the parallel sides of a vessel is generally αL (L: ship length), a guideline of approximately 1/2 may be used for the parallel factor α when the design ship is a cargo ship.
  Therefore, $\alpha = 0.50$ was used here.
- k : parameter (0.50)

$$C_{ek} = \frac{1}{1+\left(\frac{l}{r}\right)^2} = \frac{1}{1+\left(\frac{43.72}{50.53}\right)^2} = 0.572$$

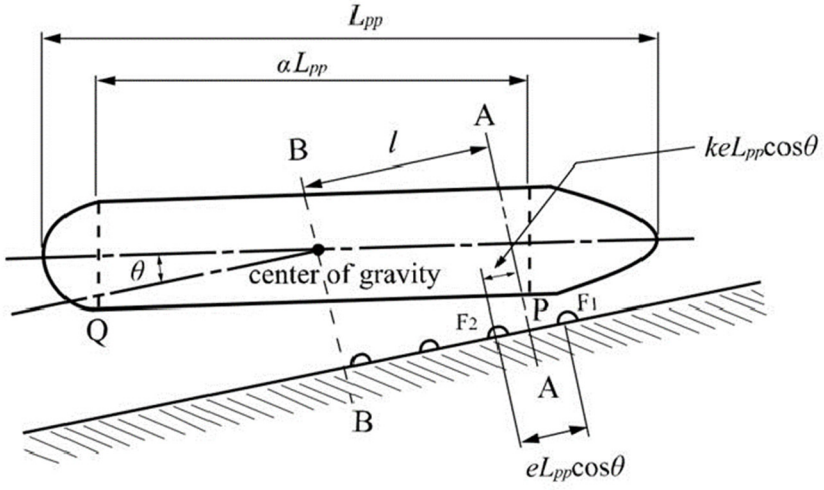

Source: TCVN 11820-2-2025

Figure 2.5- Schematic Illustration of Ship Berthing

Accordingly, the berthing energy E_f of the vessel is as follows.

$$E_{f_k} = \frac{1}{2} M_{s_k} V_{b_k}{}^2 C_{m_k} C_{e_k} C_{s_k} C_{c_k}$$
$$= \frac{1}{2} \times 64{,}155 \times 0.10^2 \times 1.78 \times 0.572 \times 1.0 \times 1.0$$

= 326.6 kN·m

2) Selection of Rubber Fender

Here, V-shaped rubber (natural rubber material) is used. The fenders are set so as to satisfy the following equation. The subscript *d* indicates a design value.

$E_{sd} = \varphi E_{cat} \geqq E_{fd}$

Where:

E_s : absorbed energy of the fenders (kN·m)
φ : manufacturing tolerance of the fenders (10% in general)
E_{cat} : standard value of absorbed energy of the fenders (kN·m)
E_f : berthing energy of the ship (kN·m)

$E_{cat} = K_e K H^2 L = 245 K H^2 L$

Where:

K_e : factor depending on shape (= 245)
K : factor depending on rubber material (= 0.7 to 1.3; here, K = 1.0)
H : height of fender (m)
L : length of fender (m)

The reaction force R_{cat} of the V-shaped rubber fender is obtained by the following equation.

$R_{cat} = K_f K H L = 735 K H L$

Where:

R_{cat} : maximum reaction force of fender (kN)
K_f : factor depending on shape (= 735)

The equation shown above is the case in which the design compression was set to 45 % of the fender height or less with a V-shaped fender (case of natural rubber material). Because the factors, etc. will differ depending on the type of fender, the manufacturer's catalog was used as reference. As manufacturing tolerances, in the selection of the rubber fender, φ = 0.9 was adopted for absorbed energy and φ = 1.1 was adopted for reaction force. The necessary length absorbed energy and reaction force of V-800H and V-1000H fenders were calculated by the following equations. The results are shown in Table 2.5.

- Absorbed energy of fender
  $E_s = 245\ H^2 L \bullet \varphi = 220.50\ H^2 L$ (kN·m)
- Reaction force of fender
  $R = 735.0\ HL \bullet \varphi = 808.5\ HL$ (kN)

Table 2.5- Verification of Fenders

Height	Length (m)	E_s (kN·m)	Judgement	Reaction force R (kN)
V-800 H	2.50	352.80	$\geq E_f$	1,617.00
V-1000 H	1.50	330.75	$\geq E_f$	1,212.75

The result of an economic comparison of the above-mentioned V-800 H and V-1000 H fenders showed that V-1000 H is more economical. Accordingly, V-1000 H × 1.50 m is used as the fender. If hull pressure is an issue, it is advisable to use a cone fender with a

larger steel frontal frame.

2-5. Structural Analysis

(1) Analysis Model

Linear frame analysis is performed based on the actions and structural conditions set above to calculate the sectional forces of the foundation piles. The analysis model is shown in Figure 2.6, and an example of input data is shown in Table 2.6. In this calculation example, the following items are not considered.

- ✓ The weight of water inside the pile and its inertia force.
- ✓ Hydrodynamic pressure acting on the pile.
- ✓ Buoyancy acting on the piles in the underwater part.
- ✓ Wave force and current force acting on the piles.

Furthermore, subsequent sections will present performance assessment results, using the steel pipe as a representative case after corrosion.

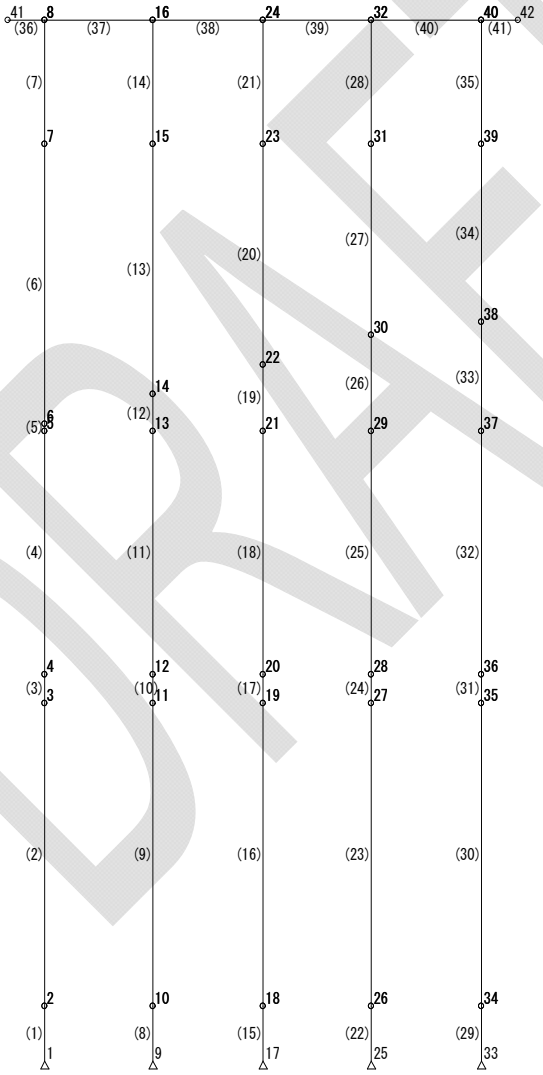

Figure 2.6- Model of Frame Analysis

(2) Sectional Forces

The calculated results of the sectional forces obtained from the frame analysis are shown in Table 2.7. As an example of the analysis results, the distribution diagram of displacement and bending moment during earthquake motion in the sea-to-land direction

is shown in Figure 2.7.

Table 2.6- Example of Input Section Data (After Corrosion)

Element	Point		Modulus of elasticity	Section Area	Inertial Moment
	i	j	E (kN/m^2)	A (m^2)	I (m^4)
1	1	2	2.0×10^{8}	6.673×10^{-2}	1.162×10^{-2}
2	2	3	2.0×10^{8}	6.673×10^{-2}	1.162×10^{-2}
3	3	4	2.0×10^{8}	6.673×10^{-2}	1.162×10^{-2}
4	4	5	2.0×10^{8}	6.673×10^{-2}	1.162×10^{-2}
5	5	6	2.0×10^{8}	6.673×10^{-2}	1.162×10^{-2}
6	6	7	2.0×10^{8}	6.673×10^{-2}	1.162×10^{-2}
7	7	8	2.0×10^{8}	6.673×10^{-2}	1.162×10^{-2}
8	9	10	2.0×10^{8}	6.673×10^{-2}	1.162×10^{-2}
9	10	11	2.0×10^{8}	6.673×10^{-2}	1.162×10^{-2}
10	11	12	2.0×10^{8}	6.673×10^{-2}	1.162×10^{-2}
11	12	13	2.0×10^{8}	6.673×10^{-2}	1.162×10^{-2}
12	13	14	2.0×10^{8}	6.673×10^{-2}	1.162×10^{-2}
13	14	15	2.0×10^{8}	6.673×10^{-2}	1.162×10^{-2}
14	15	16	2.0×10^{8}	6.673×10^{-2}	1.162×10^{-2}
15	17	18	2.0×10^{8}	6.673×10^{-2}	1.162×10^{-2}
16	18	19	2.0×10^{8}	6.673×10^{-2}	1.162×10^{-2}
17	19	20	2.0×10^{8}	6.673×10^{-2}	1.162×10^{-2}
18	20	21	2.0×10^{8}	6.673×10^{-2}	1.162×10^{-2}
19	21	22	2.0×10^{8}	6.673×10^{-2}	1.162×10^{-2}
20	22	23	2.0×10^{8}	6.673×10^{-2}	1.162×10^{-2}
21	23	24	2.0×10^{8}	6.673×10^{-2}	1.162×10^{-2}
22	25	26	2.0×10^{8}	6.673×10^{-2}	1.162×10^{-2}
23	26	27	2.0×10^{8}	6.673×10^{-2}	1.162×10^{-2}
24	27	28	2.0×10^{8}	6.673×10^{-2}	1.162×10^{-2}
25	28	29	2.0×10^{8}	6.673×10^{-2}	1.162×10^{-2}
26	29	30	2.0×10^{8}	6.673×10^{-2}	1.162×10^{-2}
27	30	31	2.0×10^{8}	6.673×10^{-2}	1.162×10^{-2}
28	31	32	2.0×10^{8}	6.673×10^{-2}	1.162×10^{-2}
29	33	34	2.0×10^{8}	6.673×10^{-2}	1.162×10^{-2}
30	34	35	2.0×10^{8}	6.673×10^{-2}	1.162×10^{-2}
31	35	36	2.0×10^{8}	6.673×10^{-2}	1.162×10^{-2}
32	36	37	2.0×10^{8}	6.673×10^{-2}	1.162×10^{-2}
33	37	38	2.0×10^{8}	6.673×10^{-2}	1.162×10^{-2}
34	38	39	2.0×10^{8}	6.673×10^{-2}	1.162×10^{-2}
35	39	40	2.0×10^{8}	6.673×10^{-2}	1.162×10^{-2}
36	41	8	2.8×10^{7}	2.310	8.489×10^{-1}
37	8	16	2.8×10^{7}	2.310	8.489×10^{-1}
38	16	24	2.8×10^{7}	2.310	8.489×10^{-1}
39	24	32	2.8×10^{7}	2.310	8.489×10^{-1}
40	32	40	2.8×10^{7}	2.310	8.489×10^{-1}
41	40	42	2.8×10^{7}	2.310	8.489×10^{-1}

Table 2.7- Summary Table of Sectional Forces

Acting Conditions		Items	Row 1	Row 2	Row 3	Row 4	Row 5
Operation (Surcharge)	Pile Head	Axial Force, N (kN)	917.802	1037.25	1078.61	1041.13	925.211
		Moment, M (kNm)	39.122	23.233	1.1	-19.782	-39.754
	Above Seabed	Axial Force, N (kN)	948.199	1067.65	1109	1071.52	955.608
		Moment, M (kNm)	25.119	14.677	0.521	-12.269	-24.129
	In ground	Axial Force, N (kN)	1027.51	1148.88	1186.87	1154.6	1029.11
		Moment, M (kNm)	-9.652	-5.729	-0.696	3.447	6.987

Earthquake (Sea-to-Land)	Pile Head	Axial Force, N (kN)	488.818	757.424	840.694	881.961	1031.1
		Moment, M (kNm)	-1081.23	-1187.75	-1301.81	-1400.43	-1415.53
	Above Seabed	Axial Force, N (kN)	519.215	787.821	871.091	912.357	1061.5
		Moment, M (kNm)	-575.885	-624.538	-662.756	-673.745	-654.246
	In ground	Axial Force, N (kN)	592.45	862.909	948.393	984.575	1131.74
		Moment, M (kNm)	744.339	764.114	768.047	754.237	741.091
Earthquake (Land-to-Sea)	Pile Head	Axial Force, N (kN)	979.666	902.181	885.075	783.843	449.235
		Moment, M (kNm)	1143.82	1224.92	1303.57	1368.77	1351.93
	Above Seabed	Axial Force, N (kN)	1010.06	932.578	915.472	814.24	479.632
		Moment, M (kNm)	616.076	648.021	663.589	654.115	615.64
	In ground	Axial Force, N (kN)	1083.18	1007.6	992.775	886.53	541.702
		Moment, M (kNm)	-759.291	-772.993	-769.16	-749.212	-731.549
Operating Crane (Sea-to-Land)	Pile Head	Axial Force, N (kN)	2306.48	1767.43	1791.87	2107	1788.23
		Moment, M (kNm)	-1061.3	-1030.84	-918.067	-1076.76	-1256.02
	Above Seabed	Axial Force, N (kN)	2336.88	1797.83	1822.27	2137.4	1818.63
		Moment, M (kNm)	-574.5	-539.561	-443.494	-505.721	-592.61
	In ground	Axial Force, N (kN)	2409.82	1872.83	1899.96	2209.74	1887.55
		Moment, M (kNm)	604.757	594.146	556.183	564.141	582.828
Operating Crane (Land-to-Sea)	Pile Head	Axial Force, N (kN)	3628.55	2108.6	1547.36	1502.74	973.771
		Moment, M (kNm)	617.54	824.902	1143.74	1214.58	1113.81
	Above Seabed	Axial Force, N (kN)	3658.94	2139	1577.76	1533.14	1004.17
		Moment, M (kNm)	268.986	387.864	562.343	563.968	479.199
	In ground	Axial Force, N (kN)	3733.44	2214.91	1655.29	1605.6	1067.57
		Moment, M (kNm)	-567.555	-612.848	-665.191	-652.092	-624.472
Earthquake + Crane (Sea-to-Land)	Pile Head	Axial Force, N (kN)	299.101	1093.19	1953.83	2771.67	2643.22
		Moment, M (kNm)	-2873.85	-3052.72	-3191.77	-3647.83	-3945.42
	Above Seabed	Axial Force, N (kN)	329.498	1123.59	1984.23	2802.07	2673.62
		Moment, M (kNm)	-1497.33	-1562.54	-1566.02	-1722.31	-1828.48
	In ground	Axial Force, N (kN)	402.881	1198.87	2061.83	2874.4	2743.47
		Moment, M (kNm)	1926.54	1958.06	1940.29	1948.62	1959.29
Earthquake + Crane (Land-to-Sea)	Pile Head	Axial Force, N (kN)	5188.86	2352.57	992.99	489.543	-213.689
		Moment, M (kNm)	2461.87	2883.88	3460.15	3824.49	3838.82
	Above Seabed	Axial Force, N (kN)	5219.25	2382.96	1023.39	519.94	-183.292
		Moment, M (kNm)	1208.64	1430.77	1707.69	1800	1731.9
	In ground	Axial Force, N (kN)	5293.11	2458.51	1100.92	592.306	-121.167
		Moment, M (kNm)	-1908.52	-1996.49	-2069.03	-2054.01	-2017.07
Mooring	Pile Head	Axial Force, N (kN)	1154.62	951.794	898.311	748.137	247.142
		Moment, M (kNm)	1940.8	2081.25	2219.31	2332.55	2310.62
	Above Seabed	Axial Force, N (kN)	1185.01	982.191	928.708	778.534	277.539
		Moment, M (kNm)	1006.67	1065.11	1097.69	1087.16	1027.91
	In ground	Axial Force, N (kN)	1258.41	1057.43	1006.18	850.955	339.982
		Moment, M (kNm)	-1250.15	-1275.23	-1272.38	-1242.41	-1215.94
Berthing	Pile Head	Axial Force, N (kN)	558.803	933.072	1048.35	1113.52	1346.26
		Moment, M (kNm)	-1591.59	-1738.28	-1893.44	-2025.29	-2040.18
	Above Seabed	Axial Force, N (kN)	589.2	963.469	1078.75	1143.91	1376.65
		Moment, M (kNm)	-817.415	-884.896	-936.551	-949.082	-918.446

	In ground	Axial Force, N (kN)	662.686	1038.76	1156.22	1216.28	1438.71
		Moment, M (kNm)	1051.96	1079.74	1085.45	1066.28	1048.32
Storm (Sea-to-Land)	Pile Head	Axial Force, N (kN)	610.882	1124.55	1806.67	2423.09	2062.75
		Moment, M (kNm)	-1330.42	-1391.62	-1417.43	-1725.44	-1980.62
	Above Seabed	Axial Force, N (kN)	641.279	1154.95	1837.07	2453.49	2093.14
		Moment, M (kNm)	-679.522	-696.303	-674.467	-807.364	-927.072
	In ground	Axial Force, N (kN)	714.813	1230.4	1914.9	2525.87	2162.41
		Moment, M (kNm)	891.712	902.29	887.638	911.341	935.967
Storm (Land-to-Sea)	Pile Head	Axial Force, N (kN)	3468.21	1849.98	1179.03	1023.09	507.634
		Moment, M (kNm)	1093.77	1329.64	1669.74	1807.43	1748.96
	Above Seabed	Axial Force, N (kN)	3498.61	1880.37	1209.42	1053.49	538.031
		Moment, M (kNm)	514.627	643.946	818.421	841.355	770.407
	In ground	Axial Force, N (kN)	3572.73	1956.08	1286.98	1125.92	600.774
		Moment, M (kNm)	-878.558	-928.97	-978.267	-965.28	-938.282

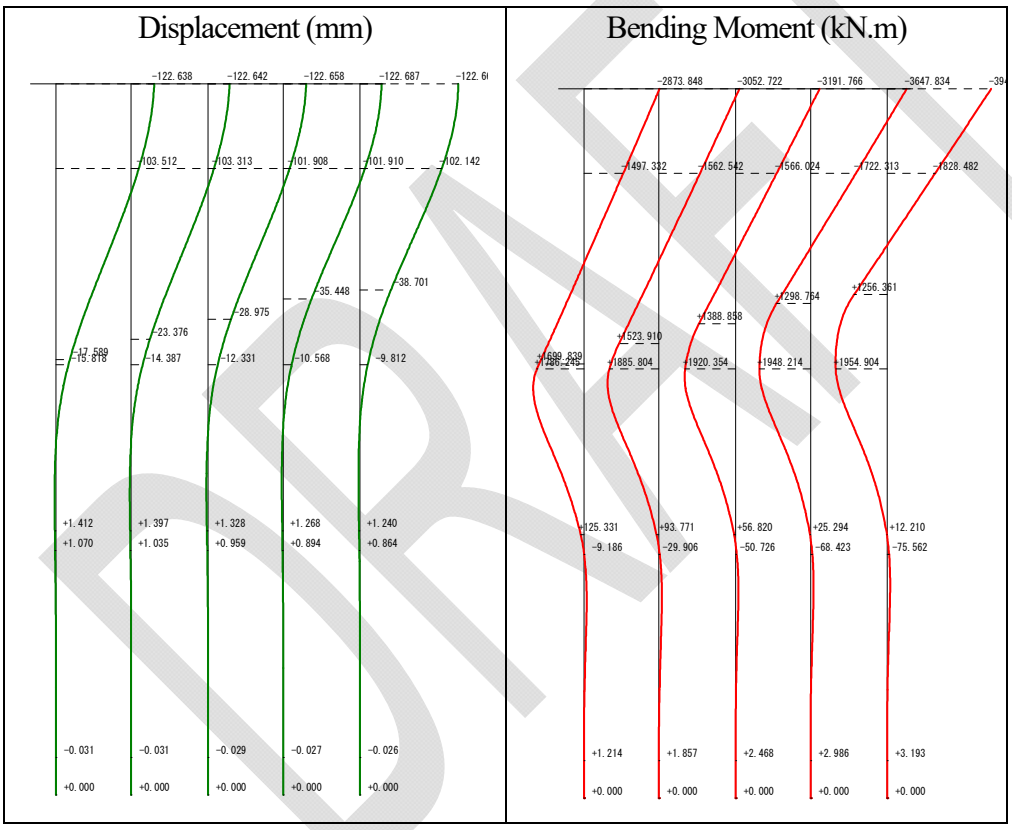

Figure 2.7- Distribution Diagram of Displacements and Bending Moments (Earthquake Ground Motion, Consideration of Crane, Sea-to-Land)

2-6. Verification of Pile Stress and Bearing Capacity

(1) Verification of Pile Stress

The axial compressive yield stress of each pile is shown in Table 2.8. Additionally, examples of the assessment results for the stress intensity of the piles are presented in Table 2.9 and 2.10. The factor of safety against the applied load is at maximum 0.854 for the five-row piles (harbor (land) side piles) during earthquake motion.

Table 2.8- Reduction Coefficients of Axial Compressive Yield Stress

Pile Row	Pile	Material	L (m)	r (m)	L/r	Axial Compressive Stress (MPa)	γ_{ed}
Row 1	D1200×19t	SPP490	23.464	0.418	56.1	230.895	0.733
Row 2	D1200×19t	SPP490	22.527	0.418	53.9	235.305	0.747
Row 3	D1200×19t	SPP490	21.573	0.418	51.6	240.345	0.763
Row 4	D1200×19t	SPP490	20.636	0.418	49.4	244.755	0.777
Row 5	D1200×19t	SPP490	20.212	0.418	48.4	246.960	0.784

Table 2.9- Example Verification Results of Pile Stress (Earthquake Motion, Crane Consideration, Sea-to-Land)

Pile Head: $\gamma_S = 1.00$, $\gamma_R = 1.00$, $m = 1.12$						
Items		**Row 1**	**Row 2**	**Row 3**	**Row 4**	**Row 5**
Material		SPP490	SPP490	SPP490	SPP490	SPP490
Axial Force, N	(kN)	299.101	1,093.191	1,953.834	2,771.670	2,643.220
Bending Moment, M	(kNm)	2,873.848	3,052.722	3,191.766	3,647.834	3,945.416
$1/\beta$	(m)	5.214	5.602	5.998	6.386	6.562
L	(m)	23.464	22.527	21.573	20.636	20.212
r	(m)	0.418	0.418	0.418	0.418	0.418
L/r		56.1	53.9	51.6	49.4	48.4
γ_{ed}		0.733	0.747	0.763	0.777	0.784
Section Area, A	(cm^2)	704.9	704.9	704.9	704.9	704.9
Section Modulus, Z	(cm^3)	20,500	20,500	20,500	20,500	20,500
Stress, σ_{cd}, σ_{td}	(N/mm^2)	4.243	15.508	27.716	39.318	37.496
Stress, σ_{bd}	(N/mm^2)	140.188	148.913	155.696	177.943	192.459
S_k	(N/mm^2)	145.977	169.673	192.021	228.545	240.286
R_k	(N/mm^2)	315.000	315.000	315.000	315.000	315.000
S_d	(N/mm^2)	145.977	169.673	192.021	228.545	240.286
R_d	(N/mm^2)	315.000	315.000	315.000	315.000	315.000
$m(S_d/R_d)$		0.519	0.603	0.683	0.813	0.854
Judgement		O.K.	O.K.	O.K.	O.K.	O.K.
Above Seabed: $\gamma_S = 1.00$, $\gamma_R = 1.00$, $m = 1.12$						
Items		**Row 1**	**Row 2**	**Row 3**	**Row 4**	**Row 5**
Material		SPP490	SPP490	SPP490	SPP490	SPP490
Axial Force, N	(kN)	398.162	1,123.587	1,984.231	2,802.066	2,673.617
Bending Moment, M	(kNm)	1,699.839	1,562.542	1,566.024	1,722.313	1,828.482
$1/\beta$	(m)	5.214	5.602	5.998	6.386	6.562
L	(m)	23.464	22.527	21.573	20.636	20.212
r	(m)	0.417	0.417	0.417	0.417	0.417
L/r		56.3	54.0	51.7	49.5	48.5
γ_{ed}		0.731	0.747	0.762	0.777	0.783
Section Area, A	(cm^2)	667.3	667.3	667.3	667.3	667.3
Section Modulus, Z	(cm^3)	19,400	19,400	19,400	19,400	19,400
Stress, σ_{cd}, σ_{td}	(N/mm^2)	5.967	16.839	29.737	41.993	40.068
Stress, σ_{bd}	(N/mm^2)	87.621	80.543	80.723	88.779	94.252
S_k	(N/mm^2)	95.784	103.085	119.748	142.824	145.424

R_k	(N/mm^2)	315.000	315.000	315.000	315.000	315.000
S_d	(N/mm^2)	95.784	103.085	119.748	142.824	145.424
R_d	(N/mm^2)	315.000	315.000	315.000	315.000	315.000
$m(S_d/R_d)$		0.341	0.367	0.426	0.508	0.517
Judgement		O.K.	O.K.	O.K.	O.K.	O.K.
In ground: $\gamma_S = 1.00$, $\gamma_R = 1.00$, $m = 1.12$						
Items		**Row 1**	**Row 2**	**Row 3**	**Row 4**	**Row 5**
Material		SPP490	SPP490	SPP490	SPP490	SPP490
Axial Force, N	(kN)	402.881	1,198.866	2,061.826	2,874.402	2,743.472
Bending Moment, M	(kNm)	1,926.536	1,958.064	1,940.290	1,948.617	1,959.291
$1/\beta$	(m)	5.214	5.602	5.998	6.386	6.562
L	(m)	23.464	22.527	21.573	20.636	20.212
r	(m)	0.418	0.418	0.418	0.418	0.418
L/r		56.1	53.9	51.6	49.4	48.4
γ_{ed}		0.733	0.747	0.763	0.777	0.784
Section Area, A	(cm^2)	699.3	699.3	699.3	699.3	699.3
Section Modulus, Z	(cm^3)	20,300	20,300	20,300	20,300	20,300
Stress, σ_{cd}, σ_{td}	(N/mm^2)	5.761	17.144	29.485	41.105	39.232
Stress, σ_{bd}	(N/mm^2)	94.903	96.456	95.581	95.991	96.517
S_k	(N/mm^2)	102.762	119.406	134.225	148.893	146.558
R_k	(N/mm^2)	315.000	315.000	315.000	315.000	315.000
S_d	(N/mm^2)	102.762	119.406	134.225	148.893	146.558
R_d	(N/mm^2)	315.000	315.000	315.000	315.000	315.000
$m(S_d/R_d)$		0.365	0.425	0.477	0.529	0.521
Judgement		O.K.	O.K.	O.K.	O.K.	O.K.

Table 2.10- Example Assessment Results of Stress Intensity for Piles (Earthquake Motion, Crane Consideration, Land-to-Sea)

Pile Head: $\gamma_S = 1.00$, $\gamma_R = 1.00$, $m = 1.12$						
Items		**Row 1**	**Row 2**	**Row 3**	**Row 4**	**Row 5**
Material		SPP490	SPP490	SPP490	SPP490	SPP490
Axial Force, N	(kN)	5,188.857	2,352.567	992.990	489.543	-213.689
Bending Moment, M	(kNm)	2,461.868	2,883.882	3,460.150	3,824.490	3,838.816
$1/\beta$	(m)	5.214	5.602	5.998	6.386	6.562
L	(m)	23.464	22.527	21.573	20.636	20.212
r	(m)	0.418	0.418	0.418	0.418	0.418
L/r		56.1	53.9	51.6	49.4	48.4
γ_{ed}		0.733	0.747	0.763	0.777	———
Section Area, A	(cm^2)	704.9	704.9	704.9	704.9	704.9
Section Modulus, Z	(cm^3)	20,500	20,500	20,500	20,500	20,500
Stress, σ_{cd}, σ_{td}	(N/mm^2)	73.607	33.373	14.086	6.944	-3.031
Stress, σ_{bd}	(N/mm^2)	120.091	140.677	168.788	186.560	187.259
S_k	(N/mm^2)	220.510	185.353	187.249	195.497	190.290
R_k	(N/mm^2)	315.000	315.000	315.000	315.000	315.000
S_d	(N/mm^2)	220.510	185.353	187.249	195.497	190.290
R_d	(N/mm^2)	315.000	315.000	315.000	315.000	315.000
$m(S_d/R_d)$		0.784	0.659	0.666	0.695	0.677

Judgement		O.K.	O.K.	O.K.	O.K.	O.K.
Above Seabed: γ_S = 1.00, γ_R = 1.00, m = 1.12						
Items		**Row 1**	**Row 2**	**Row 3**	**Row 4**	**Row 5**
Material		SPP490	SPP490	SPP490	SPP490	SPP490
Axial Force, N	(kN)	5,287.918	2,444.436	1,023.386	519.940	-183.292
Bending Moment, M	(kNm)	1,710.044	1,580.716	1,707.691	1,799.998	1,731.895
$1/\beta$	(m)	5.214	5.602	5.998	6.386	6.562
L	(m)	23.464	22.527	21.573	20.636	20.212
r	(m)	0.417	0.417	0.417	0.417	0.417
L/r		56.3	54.0	51.7	49.5	48.5
γ_{ed}		0.731	0.747	0.762	0.777	———
Section Area, A	(cm^2)	667.3	667.3	667.3	667.3	667.3
Section Modulus, Z	(cm^3)	19,400	19,400	19,400	19,400	19,400
Stress, σ_{cd}, σ_{td}	(N/mm^2)	79.247	36.633	15.337	7.792	-2.747
Stress, σ_{bd}	(N/mm^2)	88.147	81.480	88.025	92.783	89.273
S_k	(N/mm^2)	196.556	130.520	108.152	102.811	92.020
R_k	(N/mm^2)	315.000	315.000	315.000	315.000	315.000
S_d	(N/mm^2)	196.556	130.520	108.152	102.811	92.020
R_d	(N/mm^2)	315.000	315.000	315.000	315.000	315.000
$m(S_d/R_d)$		0.699	0.464	0.385	0.366	0.327
Judgement		O.K.	O.K.	O.K.	O.K.	O.K.
In ground: γ_S = 1.00, γ_R = 1.00, m = 1.12						
Items		**Row 1**	**Row 2**	**Row 3**	**Row 4**	**Row 5**
Material		SPP490	SPP490	SPP490	SPP490	SPP490
Axial Force, N	(kN)	5,293.105	2,458.514	1,100.923	592.306	-121.167
Bending Moment, M	(kNm)	1,908.519	1,996.493	2,069.034	2,054.007	2,017.066
$1/\beta$	(m)	5.214	5.602	5.998	6.386	6.562
L	(m)	23.464	22.527	21.573	20.636	20.212
r	(m)	0.418	0.418	0.418	0.418	0.418
L/r		56.1	53.9	51.6	49.4	48.4
γ_{ed}		0.733	0.747	0.763	0.777	———
Section Area, A	(cm^2)	699.3	699.3	699.3	699.3	699.3
Section Modulus, Z	(cm^3)	20,300	20,300	20,300	20,300	20,300
Stress, σ_{cd}, σ_{td}	(N/mm^2)	75.693	35.157	15.743	8.470	-1.733
Stress, σ_{bd}	(N/mm^2)	94.016	98.349	101.923	101.183	99.363
S_k	(N/mm^2)	197.281	145.413	122.556	112.084	101.096
R_k	(N/mm^2)	315.000	315.000	315.000	315.000	315.000
S_d	(N/mm^2)	197.281	145.413	122.556	112.084	101.096
R_d	(N/mm^2)	315.000	315.000	315.000	315.000	315.000
$m(S_d/R_d)$		0.701	0.517	0.436	0.399	0.359
Judgement		O.K.	O.K.	O.K.	O.K.	O.K.

(2) Verification of Pile Bearing Capacity

The verification of the pile bearing capacity under seismic ground motion will be conducted refer to the Equation (1.23).

$$m \cdot \frac{S_d}{R_d} \leq 1.0 \quad R_d = \gamma_R R_k \quad S_d = \gamma_S S_k$$

Where:

m : adjustment factor
S : characteristic value of load term (kN/m)
R : characteristic value of resistance term (kN/m)
γ_S : partial factor that is to be multiplied with the load term
γ_R : partial factor that is to be multiplied with the resistance term

Verification target	Type of piles	Partial factor to be multiplied with resistance term: γ_R	Partial factor to be multiplied with load term: γ_S	Adjustment factor: m
Bearing capacity of the open-type wharves on vertical piles (variable situation for surcharges during ship actions)	Pulling pile	- (1.00)	- (1.00)	3.00
	Pushing pile	- (1.00)	- (1.00)	2.50
Bearing capacity of the open-type wharves on vertical piles (variable situation for storm, high waves, and Level 1 earthquake ground motion)	Pulling pile	- (1.00)	- (1.00)	2.50
	Pushing pile (bearing pile)	- (1.00)	- (1.00)	1.50
	Pushing pile (friction pile)	- (1.00)	- (1.00)	2.00

$$R_k = R_{pk} + R_{fk}$$

Where:

R_{tk} : characteristic value of the pushing resistance force of a pile in its axial direction (kN)
R_{pk} : characteristic value of the base resistance force of a pile (kN)
R_{fk} : characteristic value of the skin friction force of a pile (kN)

1) Characteristic Value of End Bearing Resistance (R_{pk})

$$R_{pk} = 300N \times \alpha \times A_p$$

Where:

$N_1 = 50$

$N_2 = (2.30 \times 20 + 2.5 \times 50) / (4 \times 1.2) = 35.6$

$N = (N_1 + N_2) / 2 = (50 + 35.6) / 2 = 42.8$

$A_p = \pi \times 1.1997^2 / 4 = 1.13$ (m^2)

α: pile toe closure ratio (Based on adjacent work experience, assumed as 0.50)

Therefore,

$R_{pk} = 300 \times 42.8 \times 1.13 \times 0.5 = 7{,}254.6$ (kN)

2) Characteristic Value of Skin Friction Resistance (R_{fk})

$$R_{fk} = \sum \overline{\gamma_{fki}} \times A_{si} = 2 \sum \overline{N_i} \times A_{si}$$

Where:

$A_{si} = \pi \times 1.1997 \times l_i = 3.769 \times l_i$ (m^2)

- Frictional resistance of the Row 1 piles

$R_{fk} = (2\times2\times0.350 + 2\times8\times11.0 + 2\times20\times15.0 + 2\times50\times2.5) \times3.769$
$= 3{,}872.3$ (kN)

- Frictional resistance of the Row 2 piles

$R_{fk} = (2\times2\times1.675 + 2\times8\times11.0 + 2\times20\times15.0 + 2\times50\times2.5) \times3.769$
$= 3{,}892.2$ (kN)

- Frictional resistance of the Row 3 piles

$R_{fk} = (2\times2\times3.025 + 2\times8\times11.0 + 2\times20\times15.0 + 2\times50\times2.5) \times3.769$
$= 3{,}912.6$ (kN)

- Frictional resistance of the Row 4 piles

$R_{fk} = (2\times2\times4.350 + 2\times8\times11.0 + 2\times20\times15.0 + 2\times50\times2.5) \times3.769$
$= 3{,}932.6$ (kN)

- Frictional resistance of the Row 5 piles

$R_{fk} = (2\times2\times4.950 + 2\times8\times11.0 + 2\times20\times15.0 + 2\times50\times2.5) \times3.769$
$= 3{,}941.6$ (kN)

3) Characteristic Value of Axial Resistance Force of Piles (R_{tk})

- Axial resistance of the Row 1 piles: (compression)

$R_{tk} = 7{,}254.6 + 3{,}872.3 = 11{,}126.9$ (kN)

- Axial resistance of the Row 2 piles: (compression)

$R_{tk} = 7{,}254.6 + 3{,}892.2 = 11{,}146.8$ (kN)

- Axial resistance of the Row 3 piles: (compression)

$R_{tk} = 7{,}254.6 + 3{,}912.6 = 11{,}167.2$ (kN)

- Axial resistance of the Row 4 piles: (compression)

$R_{tk} = 7{,}254.6 + 3{,}932.6 = 11{,}187.2$ (kN)

- Axial resistance of the Row 5 piles: (compression)

$R_{tk} = 7{,}254.6 + 3{,}941.6 = 11{,}196.2$ (kN)

The design values of axial resistance force are calculated from the base bearing resistance and skin friction resistance of each pile, and the verification results regarding pile capacity are indicated in Table 2.11.

Table 2.11- Verification Results regarding the Bearing Capacity of Piles

Conditions	Pile Row	Case	m	Load Term (kN)	Resistance Term (kN)	$m(S_d/R_d)$	Judgement
Operation (Surcharge)	Row 1	Push	2.50	1,173.461	11,126.9	0.264	O.K.
	Row 2	Push	2.50	1,292.912	11,146.8	0.290	O.K.
	Row 3	Push	2.50	1,334.265	11,167.2	0.299	O.K.
	Row 4	Push	2.50	1,296.786	11,187.2	0.290	O.K.
	Row 5	Push	2.50	1,180.870	11,196.2	0.264	O.K.
Earthquake (Sea-to-Land)	Row 1	Push	2.00	744.477	11,126.9	0.134	O.K.
	Row 2	Push	2.00	1,013.083	11,146.8	0.182	O.K.
	Row 3	Push	2.00	1,096.353	11,167.2	0.196	O.K.

	Row 4	Push	2.00	1,137.619	11,187.2	0.203	O.K.
	Row 5	Push	2.00	1,286.762	11,196.2	0.230	O.K.
Earthquake (Land-to-Sea)	Row 1	Push	2.00	1,235.325	11,126.9	0.222	O.K.
	Row 2	Push	2.00	1,157.840	11,146.8	0.208	O.K.
	Row 3	Push	2.00	1,140.734	11,167.2	0.204	O.K.
	Row 4	Push	2.00	1,039.502	11,187.2	0.186	O.K.
	Row 5	Push	2.00	704.894	11,196.2	0.126	O.K.
Operating +Crane (Sea-to-Land)	Row 1	Push	2.50	2,562.140	11,126.9	0.576	O.K.
	Row 2	Push	2.50	2,023.092	11,146.8	0.454	O.K.
	Row 3	Push	2.50	2,047.527	11,167.2	0.458	O.K.
	Row 4	Push	2.50	2,362.660	11,187.2	0.528	O.K.
	Row 5	Push	2.50	2,043.891	11,196.2	0.456	O.K.
Operating +Crane (Land-to-Sea)	Row 1	Push	2.50	3,884.206	11,126.9	0.873	O.K.
	Row 2	Push	2.50	2,364.257	11,146.8	0.530	O.K.
	Row 3	Push	2.50	1,803.018	11,167.2	0.404	O.K.
	Row 4	Push	2.50	1,758.399	11,187.2	0.393	O.K.
	Row 5	Push	2.50	1,229.430	11,196.2	0.275	O.K.
Earthquake + Crane (Sea-to-Land)	Row 1	Push	2.00	554.760	11,126.9	0.100	O.K.
	Row 2	Push	2.00	1,348.849	11,146.8	0.242	O.K.
	Row 3	Push	2.00	2,209.493	11,167.2	0.396	O.K.
	Row 4	Push	2.00	3,027.328	11,187.2	0.541	O.K.
	Row 5	Push	2.00	2,898.879	11,196.2	0.518	O.K.
Earthquake + Crane (Land-to-Sea)	Row 1	Push	2.00	5,444.516	11,126.9	0.979	O.K.
	Row 2	Push	2.00	2,608.226	11,146.8	0.468	O.K.
	Row 3	Push	2.00	1,248.648	11,167.2	0.224	O.K.
	Row 4	Push	2.00	745.202	11,187.2	0.133	O.K.
	Row 5	Push	2.00	41.970	11,196.2	0.007	O.K.
	Row 5	Pull	2.50	(-)213.689	3,941.6	0.054	O.K.
Mooring	Row 1	Push	2.50	1,410.274	11,126.9	0.317	O.K.
	Row 2	Push	2.50	1,207.453	11,146.8	0.271	O.K.
	Row 3	Push	2.50	1,153.970	11,167.2	0.258	O.K.
	Row 4	Push	2.50	1,003.796	11,187.2	0.224	O.K.
	Row 5	Push	2.50	502.801	11,196.2	0.112	O.K.
Berthing	Row 1	Push	2.50	814.462	11,126.9	0.183	O.K.
	Row 2	Push	2.50	1,188.731	11,146.8	0.267	O.K.
	Row 3	Push	2.50	1,304.011	11,167.2	0.292	O.K.
	Row 4	Push	2.50	1,369.176	11,187.2	0.306	O.K.
	Row 5	Push	2.50	1,601.915	11,196.2	0.358	O.K.
Storm (Sea-to-Land)	Row 1	Push	2.00	866.541	11,126.9	0.156	O.K.
	Row 2	Push	2.00	1,380.209	11,146.8	0.248	O.K.
	Row 3	Push	2.00	2,062.332	11,167.2	0.369	O.K.
	Row 4	Push	2.00	2,678.749	11,187.2	0.479	O.K.
	Row 5	Push	2.00	2,318.405	11,196.2	0.414	O.K.
Storm (Land-to-Sea)	Row 1	Push	2.00	3,723.872	11,126.9	0.669	O.K.
	Row 2	Push	2.00	2,105.634	11,146.8	0.378	O.K.
	Row 3	Push	2.00	1,434.684	11,167.2	0.257	O.K.
	Row 4	Push	2.00	1,278.752	11,187.2	0.229	O.K.
	Row 5	Push	2.00	763.293	11,196.2	0.136	O.K.

2-7. Verification of Structural Members

(1) Design Conditions

1) Material Conditions

Since the materials that can be procured vary depending on the construction conditions, this casebook applies the materials specified in OCDI 2020. Therefore, consultants shall verify the applicable materials.

i) Concrete
- Design characteristic strength f'_{ck} = 30 N/mm²
- Design compressive strength $f'_{cd} = f'_{ck}/\gamma_c$ = 30/1.3 = 23.1 N/mm²
- Young's modulus E_c = 28 kN/mm²

ii) Reinforcement (SD345)
- Design tensile yield strength f_{yd} = 345 N/mm²
- Young's modulus E_s = 200 kN/mm²

2) Load Conditions

i) Dead Load
- Unreinforced Concrete γ_c = 22.6 kN/m³
- Reinforced Concrete γ_c = 24.0 kN/m³
- Pavement Concrete γ_c = 24.0 kN/m³
  (Assumed to be the same as reinforced concrete due to integral construction with the deck.)

ii) Live Load
- Permanent: 20 kN/m²
- Earthquake: 10 kN/m²

iii) Moving Load
- Vehicle (truck) load
- Vehicle (trailer) load
- Forklift load
- Crane load

Description omitted as it is included in the basic design conditions.

(2) Load Combinations and Load Factors

The load combinations and load factors for the standard block are provided below.

Table 2.12- Load Factors

Verification of cross-sectional failure	Verification of serviceability	Verification of fatigue failure
1.1(0.9)*D*+1.2(0.8)*S*	1.0*D*+0.5*S*	-
1.1(0.9)*D*+1.2(0.8)*L*	1.0*D*+0.5*L*	1.0*D*+1.0*L*
1.1(0.9)*D*+1.2(0.8)*S*+1.2(0.8)*B*	1.0*D*+0.5*S*+0.5*B*	-
0.9(1.1)*D*+1.0*U*	-	-
1.0*D*+1.0*S*+1.0*L*+1.0*E*	-	-

The values in parentheses for the verification of cross-sectional failure indicate the effective action against the design load.

The factor 0.5 multiplied by the variable load (live load, moving load, etc.) accounts for the effect of corrosion of steel due to crack width caused by permanent loads. It is a constant (k_y) to consider the impact of crack width caused by permanent loads on the corrosion of steel.

The list of loads acting on the superstructure is presented in Table 2.13. The combinations of actions to be verified are as shown in Table 2.14.

In this example, the verification of fatigue failure is omitted because the stress ratio when the moving load is applied during operation is small and not dominant as a result of verification of cross-sectional failure and verification of serviceability.

Table 2.13- List of Acting Loads

<table>
<tr><td colspan="3">Item</td><td>Symbol</td></tr>
<tr><td colspan="3">Permanent Load</td><td>A</td></tr>
<tr><td colspan="2" rowspan="2">Surcharge Load</td><td>Operation</td><td>B</td></tr>
<tr><td>Earthquake</td><td>C</td></tr>
<tr><td colspan="3">Vehicle Load</td><td>D</td></tr>
<tr><td colspan="2" rowspan="2">Crane Load</td><td>Operation</td><td>E</td></tr>
<tr><td>Earthquake</td><td>F</td></tr>
<tr><td rowspan="7">Bending Moment at Pile Head</td><td colspan="2">Operating Crane</td><td>G</td></tr>
<tr><td rowspan="3">Earthquake</td><td>Permanent Load</td><td>H</td></tr>
<tr><td>Permanent + Surcharge</td><td>I</td></tr>
<tr><td>Crane Load</td><td>J</td></tr>
<tr><td colspan="2">Storm (Crane Load)</td><td>K</td></tr>
<tr><td colspan="2">Berthing Load</td><td>L</td></tr>
<tr><td colspan="2">Mooring Load</td><td>M</td></tr>
<tr><td colspan="3">Uplift Load</td><td>N</td></tr>
</table>

Table 2.14- Verification Cases

Case	Combinations	Transverse Beam		
		Cross-sectional failure	Serviceability	Fatigue failure
Case-1	A+B	○	○	
Case-2	A+B+G	○	○	
Case-3	A+D	○	○	
Case-4	A+E	○	○	
Case-5	A+D+G	○	○	
Case-6	A+B+L	○	○	
Case-7	A+C+I+J	○		
Case-8	A+M	○	○	
Case-9	A+N	○		

(3) Allowable Crack Width

The verification of serviceability generally ensures that the crack width of the member resulting from the design values of the load in its ultimate state does not exceed the limit crack width.

Table 2.15- Limit Values of Crack Width

Environmental classification	Minimum cover, c (mm)	Crack width limit value (mm)
Particularly severe corrosion environment	70	0.0035c

Corrosion environment	50	0.0040c
Ordinary environment	50	0.0050c

2-8. Example of Structural Verification of Beam

(1) Typical Model

The typical span of superstructure is as shown in Figure 2.8. In this example, the TB2 beam in the cross-sectional direction is considered for the verification.

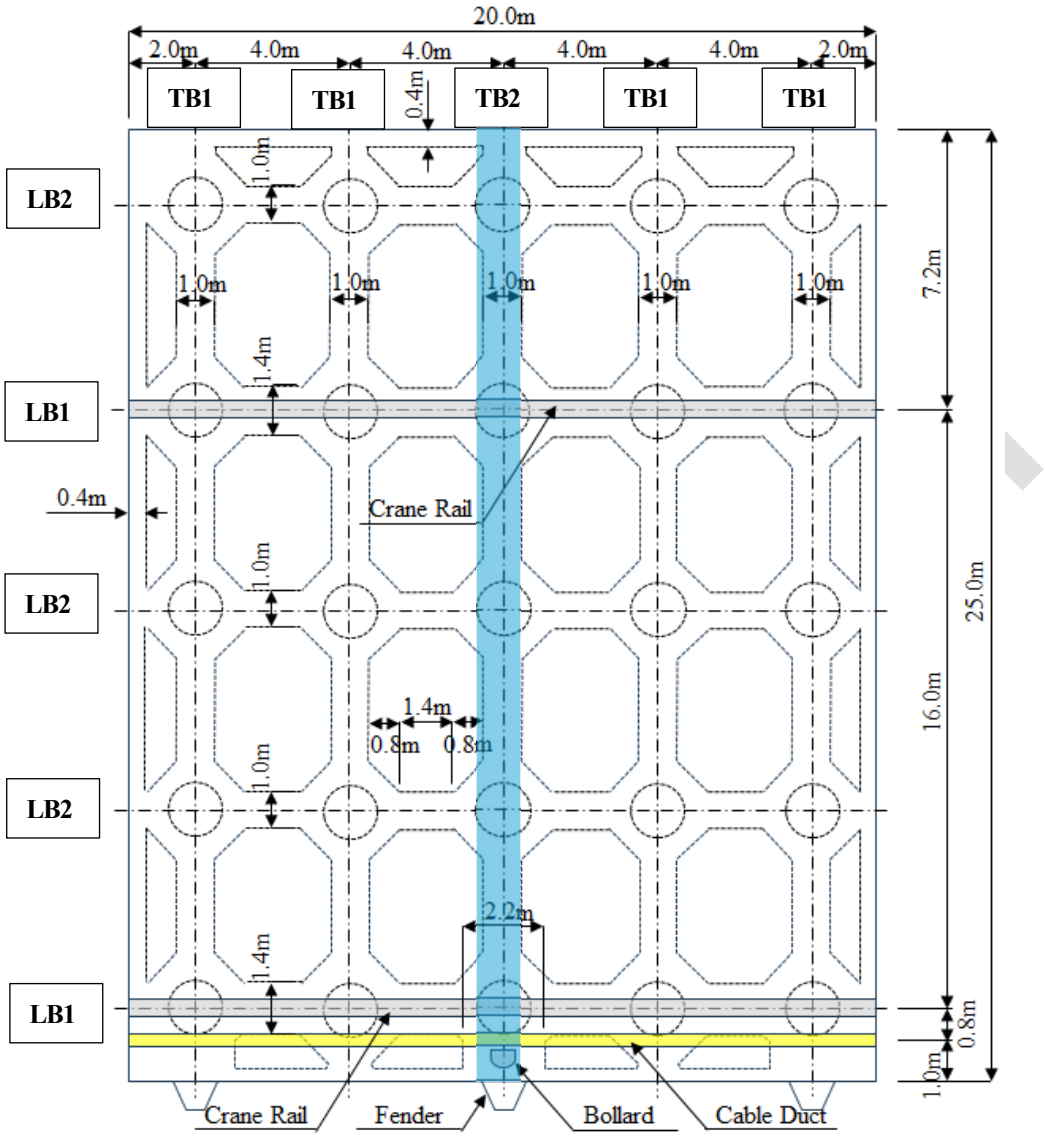

Figure 2.8- Typical Span of Superstructure

(2) Design Values of Sectional Forces

The combinations of actions to be verified for TB2 beam are as shown in Table 2.16.

Table 2.16- Verification Cases

Case	Combinations	Transverse Beam		
		Cross-sectional failure	Serviceability	Fatigue failure
Case-1	A+B+G	○	○	
Case-2	A+D+G	○	○	

Case-3	A+B+L	○	○	
Case-4	A+M	○	○	
Case-5	A+C+I+J	○		

The design values of bending moment and shear force are estimated from characteristics values against each load and load factors. The calculated design values are presented in Table 2.17 and 2.18.

Table 2.17- Design Values of Bending Moment (Beam TB2)
(Verification of Cross-sectional Failure)

Design Moment - ULS		Support 1	Support 2	Support 3	Support 4	Support 5
Max	(+)	3,326.9	3,014.2	1,985.8	2,234.7	2,816.7
Min	(-)	-2,493.7	-2,173.9	-2,643.2	-4,143.3	-5,296.7

Design Moment - ULS		Span 1	Span 2	Span 3	Span 4
Max	(+)	1,585.0	1,090.8	1,063.3	1,203.1
Min	(-)	-786.0	-169.9	-628.7	-1,769.9

(Verification of Serviceability)

Design Moment - SLS		Support 1	Support 2	Support 3	Support 4	Support 5
Max	(+)	1,224.8	1,140.9	715.5	830.6	1,038.2
Min	(-)	-1,156.4	-991.6	-1,183.3	-1,813.5	-2,324.3

Design Moment - SLS		Span 1	Span 2	Span 3	Span 4
Max	(+)	699.7	516.3	498.2	580.6
Min	(-)	-282.1	0.0	-177.3	-667.1

Table 2.18- Design Values of Shear Force (Beam TB2)
(Verification of Cross-sectional Failure)

Design Shear Force - ULS		Support 1	Support 2	Support 3	Support 4	Support 5
Max	(+)	1,319.4	1,320.3	1,309.6	1,320.8	1,259.7
Min	(-)	-1,259.7	-1,309.7	-1,573.1	-1,563.1	-1,544.8

Design Shear Force - ULS		Span 1	Span 2	Span 3	Span 4
Max	(+)	557.1	641.1	704.6	657.9
Min	(-)	-835.3	-1,034.8	-1,143.3	-1,113.9

(Verification of Serviceability)

Design Shear Force - SLS		Support 1	Support 2	Support 3	Support 4	Support 5
Max	(+)	661.6	658.7	650.1	652.3	613.4
Min	(-)	-613.4	-692.8	-762.7	-757.7	-757.5

Design Shear Force - SLS		Span 1	Span 2	Span 3	Span 4
Max	(+)	238.5	267.8	292.4	269.1

Min	(-)	-338.4	-430.4	-477.2	-470.1

(3) Structural Analysis of Members

Regarding negative bending moments at supports (pile location), as introduced by the Equation (2.1), reduction is allowed. Therefore, for negative bending moments at supports in this design case, the design value of $0.9M_d$ is applied.

The reduced design moment M_d can be calculated by the following equation:

TCVN 11820 Part11: 2025 Equation (4.2.3)

$$M_d = M_{od} - rv^2/8 \qquad (2.1)$$
$$M_d \geq 0.9M_{od}$$

Where:

M_d : reduced design moment at intermediate support
M_{od} : design moment at intermediate support calculated as support
r : R_{od}/v
R_{od} : design support reaction force at intermediate support
v : hypothetical distribution width of support reaction force along centroidal axis of member

1) Safety Verification

i) Effective height of members is as follows:

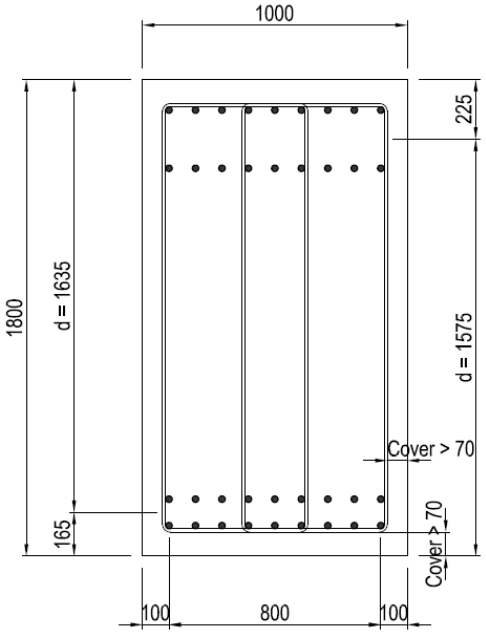

Figure 2.9- Typical Span of Superstructure Beam

ii) Verification of bending moment

The safety verification for bending moment is conducted by ensuring that the design value of bending moment capacity (M_{ud}) exceeds the design value of bending moment (M_d).

$$\frac{\gamma_i \cdot M_d}{M_{ud}} \leq 1.0 \qquad (2.2)$$

The area of reinforcement (A_{sn}) when $\gamma_i M_d/M_{ud} = 1.0$ is calculated using the following formula:

$$A_{sn}=\frac{A_n\left(d-\sqrt{d^2-\frac{4\gamma_b\gamma_i M_d}{A_n}}\right)}{2f_{yd}} \quad (2.3)$$

Where:

d : effective height of the beam (mm)
γ_b : member factor (1.10)
γ_c : material factor for concrete (1.3)
γ_s : material factor for reinforcement steel (1.0)
γ_i : structure factor
1.0 for accidental load
1.1 for other cases
A_n : $A_n = 1.7 b_w f'_{cd}$
b_w : width of the member's web (mm)
f'_{cd} : design compressive strength of concrete
$f'_{cd}=f'_{ck}/\gamma_c=30/1.3=23.1$ N/mm^2
f'_{yd} : design yield strength of tensile reinforcement
$f'_{yd}=f'_{yk}/\gamma_s=345/1.0=345$ N/mm^2

The design value of bending moment capacity (M_{ud}) is calculated as follows:

$$M_{ud}=A_s f_{yd} d\left(1-\frac{p_w}{1.7}\times\frac{f_{yd}}{f'_{cd}}\right)/\gamma_b \quad (2.4)$$

TCVN 11820 Part11: 2025 Equation (4.1.7)

Where:

A_s : area of tension reinforcement (mm^2)
p_w : reinforcement ratio ($=A_s/(b_w.\, d)$)

Example: Examination of Support 1 of Beam TB2

- Design value of bending moment:

  Upper side: $-M_1 = -2{,}493.7$ kN.m
  Lower side: $+M_1 = 3{,}326.9$ kN.m

- Effective height of member:

  Upper side: $d = 1{,}575$ mm
  Lower side: $d = 1{,}635$ mm

- $A_n = 1.7 b_w f'_{cd} = 1.7\times1{,}000\times23.1 = 39{,}270$ N/mm

- Verification of upper side

$$A_{sn}=\frac{39{,}270\left(1{,}575-\sqrt{1{,}575^2-\frac{4\times1.1\times1.0\times2{,}493.7}{39{,}270\times10^{-6}}}\right)}{2\times345.0}=5{,}199.2 \text{ mm}^2$$

Reinforcement: 2-layer reinforcement at 10cm intervals
Layer 1: 9 bars × D32

Layer 2: 9 bars × D25
Total: A_s = 11,708.1 mm^2
p_w = 11,708.1/ (1,000 × 1,575) = 0.007434

Design value of bending moment capacity:

$$M_{ud}=11,708.1\times345\times1,575\times\left(1-\frac{0.007434}{1.7}\times\frac{345}{23.1}\right)/1.1$$

M_{ud} = 0.54058×10^6 N.mm = 5,405.8 kN.m

Verification for bending moment:

1.0×2,493.7/ 5,405.8 = 0.461 ≤ 1.0 OK

- Verification of lower side

$$A_{sn}=\frac{39,270\left(1,635-\sqrt{1,635^2-\frac{4\times1.1\times1.0\times3,326.9}{39,270\times10^{-6}}}\right)}{2\times345.0}=6,731.6\ \text{mm}^2$$

Reinforcement: 2-layer reinforcement at 10cm intervals
Layer 1: 9 bars × D25
Layer 2: 6 bars × D25
Total: A_s = 7,600.5 mm^2
p_w = 7,600.5 / (1,000×1,635) = 0.004649

Design value of bending moment capacity:

$$M_{ud}=7,600.5\times345\times1,635\times\left(1-\frac{0.004649}{1.7}\times\frac{345}{23.1}\right)/1.1$$

M_{ud} = 0.37382×10^6 N.mm = 3,738.2 kN.m

Verification for bending moment:

1.0×3,326.9 / 3,738.2 = 0.890 ≤ 1.0 OK

Further calculations are performed similarly for each point, and the results for the beam are shown in Table 2.19.

Table 2.19- Verification Results of Bending Moment
Verification of Cross-sectional Failure (Beam TB2)

Design for Bending Moment		Support 1		Support 2		Support 3		Support 4		Support 5	
		Upper Side	Lower Side	Upper Side	Lower Side	Upper Side	Lower Side	Upper Side	Lower Side	Upper Side	Lower Side
Beam Width	b (mm)	1000	1000	1000	1000	1000	1000	1000	1000	1000	1000
Effective Depth	d (mm)	1575	1635	1575	1635	1575	1635	1575	1635	1575	1635
Design Moment	M_d(kN・m)	2493.7	3326.9	2173.9	3014.2	2643.2	1985.8	4143.3	2234.7	5296.7	2816.7
Necessary Rebar Area	A_{sn}(mm^2)	5199.2	6731.6	4514.6	6076.5	5521.0	3956.7	8822.2	4465.2	11455.3	5665.5
Member Coefficient	γ_b	1.1	1.1	1.1	1.1	1.1	1.1	1.1	1.1	1.1	1.1
Structural Coefficient	γ_i	1.0	1.0	1.0	1.0	1.0	1.0	1.0	1.0	1.0	1.0
Layer 1	(D x Bars)	D32 x 9 bars	D25 x 9 bars	D32 x 9 bars	D25 x 9 bars	D32 x 9 bars	D25 x 9 bars	D32 x 9 bars	D25 x 9 bars	D32 x 9 bars	D25 x 9 bars
Layer 2	(D x Bars)	D25 x 9 bars	D25 x 6 bars	D25 x 9 bars	D25 x 6 bars	D25 x 9 bars	D25 x 6 bars	D25 x 9 bars	D25 x 6 bars	D25 x 9 bars	D25 x 6 bars
Design Rebar Area	A_s(mm^2)	11708.1	7600.5	11708.1	7600.5	11708.1	7600.5	11708.1	7600.5	11708.1	7600.5
Rebar Area Ratio	pw	0.007434	0.004649	0.007434	0.004649	0.007434	0.004649	0.007434	0.004649	0.007434	0.004649
Design Strength of Concrete	f'_{cd}(N/mm^2)	23.1	23.1	23.1	23.1	23.1	23.1	23.1	23.1	23.1	23.1
Design Strength of Steel	f_{yd}(N/mm^2)	345	345	345	345	345	345	345	345	345	345
Ultimate Moment of the Section	M_{ud}(kN・m)	5405.45	3738.171	5405.45	3738.171	5405.45	3738.171	5405.45	3738.171	5405.45	3738.171
$\gamma_i \cdot M_d/M_{ud}$		0.461	0.89	0.402	0.806	0.489	0.531	0.767	0.598	0.98	0.754
Examination Results		O.K.	O.K.	O.K.	O.K.	O.K.	O.K.	O.K.	O.K.	O.K.	O.K.

Design for Bending Moment		Span 1		Span 2		Span 3		Span 4	
		Upper Side	Lower Side	Upper Side	Lower Side	Upper Side	Lower Side	Upper Side	Lower Side
Beam Width	b (mm)	1000	1000	1000	1000	1000	1000	1000	1000
Effective Depth	d (mm)	1575	1635	1575	1635	1575	1635	1575	1635
Design Moment	M_d(kN・m)	786.0	1585.0	169.9	1090.8	628.7	1063.3	1769.9	1203.1
Necessary Rebar Area	A_{sn}(mm^2)	1605.5	3144.2	344.7	2370.1	1281.9	2309.5	3657.7	2617.6
Member Coefficient	γ_b	1.1	1.1	1.1	1.1	1.1	1.1	1.1	1.1
Structural Coefficient	γ_i	1.0	1.0	1.0	1.1	1.0	1.1	1.0	1.1
Layer 1	(D x Bars)	D32 x 9 bars	D25 x 9 bars	D32 x 9 bars	D25 x 9 bars	D32 x 9 bars	D25 x 9 bars	D32 x 9 bars	D25 x 9 bars
Layer 2	(D x Bars)	D25 x 9 bars	D25 x 6 bars	D25 x 9 bars	D25 x 6 bars	D25 x 9 bars	D25 x 6 bars	D25 x 9 bars	D25 x 6 bars
Design Rebar Area	A_s(mm^2)	11708.1	7600.5	11708.1	7600.5	11708.1	7600.5	11708.1	7600.5
Rebar Area Ratio	pw	0.007434	0.004649	0.007434	0.004649	0.007434	0.004649	0.007434	0.004649
Design Strength of Concrete	f'_{cd}(N/mm^2)	23.1	23.1	23.1	23.1	23.1	23.1	23.1	23.1
Design Strength of Steel	f_{yd}(N/mm^2)	345	345	345	345	345	345	345	345
Ultimate Moment of the Section	M_{ud}(kN・m)	5405.5	3738.2	5405.5	3738.2	5405.5	3738.2	5405.5	3738.2
$\gamma_i \cdot M_d/M_{ud}$		0.145	0.424	0.031	0.321	0.116	0.313	0.327	0.354
Examination Results		O.K.	O.K.	O.K.	O.K.	O.K.	O.K.	O.K.	O.K.

vi) Verification of shear force

The safety verification of shear force is conducted by ensuring that the design value of shear capacity (V_{yd}) exceeds the design value of shear force (V_d) multiplied by the structure factor (γ_i).

$$V_{yd}=V_{cd}+V_{sd}$$
$$V_{cd}=\beta_d\beta_p f_{vcd} b_w d/\gamma_b \quad (2.5)$$

TCVN 11820 Part11: 2025 Equation (4.1.8) (4.1.9) (4.1.10)

Where:

V_{cd} : design value of the shear capacity of concrete (N)

$$f_{vcd}=0.20\times(f_{cd})^{1/3},(\text{N/mm}^2)\ ,\ f_{vcd}\le 0.72\ (\text{N/mm}^2)$$

$$\beta_d=(1000/d)^{1/4},(d;\text{mm})$$

When β_d >1.5, β_d should be taken as 1.5.

$$\beta_p=(100p_w)^{1/3}$$

When β_p>1.5, β_p should be taken as 1.5.

M_d : design bending moment (N·m)

M_0 : limiting bending moment causing tensile stress in the section (N·m)

b_w : width of web (mm)

d : effective height (mm)

p_w : $p_w = A_s/(b_w \cdot d)$)
A_s : cross-sectional area of tensile reinforcement (mm²)
f'_{cd} : design compressive strength of concrete (N/mm²)
γ_b : member factor (1.3 for shear)

$$V_{sd} = \left\{ A_w f_{wyd} (\sin a_s + \cos a_s)/s_s \right\} z/\gamma_b \qquad (2.6)$$

TCVN 11820 Part11: 2025 Equation (4.1.11)

Where:

V_{sd} : design value of shear capacity provided by the shear reinforcing bars (N)
A_w : total cross-sectional area of the shear reinforcing bars in interval s_S (mm²)
f_{wyd} : design yield strength of the shear reinforcing bars (≤ 400 N/mm²)
z : distance from the acting position of the resultant force of compressive stress to the centroid of the tensile reinforcing bar (can be taken as d/1.15)
α_s : Angle between the shear reinforcing bars and the structural member axis
s_S : spacing in arrangement of the shear reinforcing bars (mm)
γ_b : member factor (may generally be set to 1.10)

Design diagonal compressive failure capacity V_{wcd} with respect to shear in web concrete may be calculated using the following Equation.

$$V_{wcd} = f_{wcd} b_w d/\gamma_b$$
$$f_{wcd} = 1.25 f'^{1/2}_{cd} \qquad (2.7)$$

TCVN 11820 Part11: 2025 Equation (4.1.12)

Where:

γ_b : member factor (may generally be set to 1.3)

Example: Examination of Support 1 of Beam TB2

- Design value of shear force:

  Upper side: S_1 = 1,259.7 kN
  Lower side: S_1 = 1,319.4 kN

- Effective height of member:

  Upper side: d = 1,575 mm; p_w = 0.007434
  Lower side: d = 1,635 mm; p_w = 0.004649

- Upper side

  Design value of shear capacity by concrete:

  $f_{vcd} = 0.2 \times 23.1^{1/3} = 0.569$

  $\beta_d = (100/157.5)^{1/4} = 0.893$

  $\beta_p = (100 \times 0.007434)^{1/3} = 0.906$

V_{cd} = 0.893×0.906×0.569×1,000×1,575/ 1.3 = 557,736 N = 557.7 kN

Design value of shear capacity supported by shear reinforcement:
Arrangement of stirrups: D13@200 x 02 set
A_s = 506.7 mm^2
$f_{wyd} = f_{wyk}/\gamma_s$ = 345/1.0 = 345 N/mm^2
z = 1,575/ 1.15 = 1,370 mm
α_s = 90 degree

V_{sd} ={506.7×345×(sin90+cos90)/200}×1,370/1.1 = 1,088,598 N =1,088.5 kN

Design value of shear capacity:
V_{yd} = 557.7 + 1,088.5 = 1,646.2 kN

Verification for shear force:

1.1×1,259.7 / 1,646.2 = 0.842 ≤ 1.0 OK

Consideration of diagonal compression failure of core concrete:
f_{wyd} = 1.25/23.1$^{1/2}$ = 6.005 N/mm^2

V_{wcd} = 6.005×1,000×1,575/1.3 = 7,275,288 N = 7,275.3 kN

Verification for diagonal compression failure:

1.1×1,259.7 / 7,275.3 = 0.190 ≤ 1.0 OK

- Lower side

  Design value of shear capacity by concrete:

  f_{vcd} = 0.2×23.1$^{1/3}$ = 0.569

  β_d = (100/163.5)$^{1/4}$ = 0.884

  β_p = (100×0.004649)$^{1/3}$ = 0.775

  V_{cd} = 0.884×0.775×0.569×1,000×1,635/ 1.3 = 490,276 N = 490.3 kN

  Design value of shear capacity supported by shear reinforcement:
  Arrangement of stirrups: D13@200 x 02 set
  A_s = 506.7 mm^2
  $f_{wyd} = f_{wyk}/\gamma_s$ = 345/1.0 = 345 N/mm^2
  z = 1,635/ 1.15 = 1,422 mm
  α_s = 90 degree

  V_{sd} ={506.7×345×(sin90+cos90)/200}×1,422/1.1 = 1,129,917 N =1,129.9 kN

  Design value of shear capacity:
  V_{yd} = 490.3 + 1,129.9 = 1,620.2 kN

  Verification for shear force:

$1.1 \times 1{,}319.4 / 1{,}620.2 = 0.896 \leq 1.0$ OK

Consideration of diagonal compression failure of core concrete:

$f_{wyd} = 1.25/23.1^{1/2} = 6.005$ N/mm^2

$V_{wcd} = 6.005 \times 1{,}000 \times 1{,}635/1.3 = 7{,}552{,}442$ N $= 7{,}552.4$ kN

Verification for diagonal compression failure:

$1.1 \times 1{,}319.4 / 7{,}552.4 = 0.192 \leq 1.0$ OK

Further calculations are performed similarly for each point, and the results for the beam are shown in Table 2.20.

Table 2.20- Verification Results of Shear Force
Verification of Cross-sectional Failure (Beam TB2)

Design for Shear Force	Support 1		Support 2		Support 3		Support 4		Support 5	
	Upper Side	Lower Side	Upper Side	Lower Side	Upper Side	Lower Side	Upper Side	Lower Side	Upper Side	Lower Side
Beam Width b (mm)	1000	1000	1000	1000	1000	1000	1000	1000	1000	1000
Effective Depth d (mm)	1575	1635	1575	1635	1575	1635	1575	1635	1575	1635
Design Shear Force V_d(kN)	1259.7	1319.4	1309.7	1320.3	1573.1	1309.6	1563.1	1320.8	1544.8	1259.7
Design Rebar Area A_s(mm^2)	11708.1	7600.5	11708.1	7600.5	11708.1	7600.5	11708.1	7600.5	11708.1	7600.5
Rebar Area Ratio pw	0.007434	0.004649	0.007434	0.004649	0.007434	0.004649	0.007434	0.004649	0.007434	0.004649
β_d	0.893	0.884	0.893	0.884	0.893	0.884	0.893	0.884	0.893	0.884
β_p	0.906	0.775	0.906	0.775	0.906	0.775	0.906	0.775	0.906	0.775
β_n	1.0	1.0	1.0	1.0	1.0	1.0	1.0	1.0	1.0	1.0
f'_{vcd}(N/mm^2)	0.569	0.569	0.569	0.569	0.569	0.569	0.569	0.569	0.569	0.569
f_{wyd}(N/mm^2)	345	345	345	345	345	345	345	345	345	345
Member Coefficient γ_b	1.3	1.3	1.3	1.3	1.3	1.3	1.3	1.3	1.3	1.3
Structural Coefficient γ_i	1.1	1.1	1.1	1.1	1.0	1.1	1.0	1.1	1.0	1.1
Rebar Diameter and Interval	D13 @200 mm	D13 @200 mm	D13 @200 mm	D13 @200 mm	D13 @200 mm	D13 @200 mm	D13 @200 mm	D13 @200 mm	D13 @200 mm	D13 @200 mm
Shear Rebar Area A_w(mm^2)	506.8	506.8	506.8	506.8	506.8	506.8	506.8	506.8	506.8	506.8
Angle to Member Axis α_s(deg)	90	90	90	90	90	90	90	90	90	90
Shear Reinfocement Member Coefficient γ_b	1.1	1.1	1.1	1.1	1.1	1.1	1.1	1.1	1.1	1.1
Shear Strength of Reinforcement V_{sd}(kN)	1088.5	1129.9	1088.5	1129.9	1088.5	1129.9	1088.5	1129.9	1088.5	1129.9
Shear Strength of Concrete V_{cd}(kN)	557.7	490.3	557.7	490.3	557.7	490.3	557.7	490.3	557.7	490.3
Shear Strength of the Section V_{yd}(kN)	1646.2	1620.2	1646.2	1620.2	1646.2	1620.2	1646.2	1620.2	1646.2	1620.2
$\gamma_i \cdot V_d/V_{yd}$	0.842	0.896	0.875	0.896	0.956	0.889	0.949	0.897	0.938	0.855
Examination Results	O.K.	O.K.	O.K.	O.K.	O.K.	O.K.	O.K.	O.K.	O.K.	O.K.
f_{wcd}(N/mm^2)	6.005	6.005	6.005	6.005	6.005	6.005	6.005	6.005	6.005	6.005
Diagonal Compression Failure Force V_{wcd}(kN)	7275.3	7552.4	7275.3	7552.4	7275.3	7552.4	7275.3	7552.4	7275.3	7552.4
$\gamma_i \cdot V_d/V_{wcd}$	0.19	0.192	0.198	0.192	0.216	0.191	0.215	0.192	0.212	0.183
Examination Results	O.K.	O.K.	O.K.	O.K.	O.K.	O.K.	O.K.	O.K.	O.K.	O.K.

Design for Shear Force	Span 1		Span 2		Span 3		Span 4	
	Upper Side	Lower Side	Upper Side	Lower Side	Upper Side	Lower Side	Upper Side	Lower Side
Beam Width b (mm)	1000	1000	1000	1000	1000	1000	1000	1000
Effective Depth d (mm)	1575	1635	1575	1635	1575	1635	1575	1635
Design Shear Force V_d(kN)	835.3	557.1	1034.8	641.1	1143.3	704.6	1113.9	657.9
Design Rebar Area A_s(mm^2)	11708.1	7600.5	11708.1	7600.5	11708.1	7600.5	11708.1	7600.5
Rebar Area Ratio pw	0.007434	0.004649	0.007434	0.004649	0.007434	0.004649	0.007434	0.004649
β_d	0.893	0.884	0.893	0.884	0.893	0.884	0.893	0.884
β_p	0.906	0.775	0.906	0.775	0.906	0.775	0.906	0.775
β_n	1.0	1.0	1.0	1.0	1.0	1.0	1.0	1.0
f'_{vcd}(N/mm^2)	0.569	0.569	0.569	0.569	0.569	0.569	0.569	0.569
f_{wyd}(N/mm^2)	345	345	345	345	345	345	345	345
Member Coefficient γ_b	1.3	1.3	1.3	1.3	1.3	1.3	1.3	1.3
Structural Coefficient γ_i	1.0	1.1	1.0	1.0	1.0	1.0	1.0	1.1
Rebar Diameter and Interval	D13 @200 mm	D13 @200 mm	D13 @200 mm	D13 @200 mm	D13 @200 mm	D13 @200 mm	D13 @200 mm	D13 @200 mm
Shear Rebar Area A_w(mm^2)	506.8	506.8	506.8	506.8	506.8	506.8	506.8	506.8
Angle to Member Axis α_s(deg)	90	90	90	90	90	90	90	90
Shear Reinfocement Member Coefficient γ_b	1.1	1.1	1.1	1.1	1.1	1.1	1.1	1.1
Shear Strength of Reinforcement V_{sd}(kN)	1088.5	1129.9	1088.5	1129.9	1088.5	1129.9	1088.5	1129.9
Shear Strength of Concrete V_{cd}(kN)	557.7	490.3	557.7	490.3	557.7	490.3	557.7	490.3
Shear Strength of the Section V_{yd}(kN)	1646.2	1620.2	1646.2	1620.2	1646.2	1620.2	1646.2	1620.2
$\gamma_i \cdot V_d/V_{yd}$	0.507	0.378	0.629	0.396	0.695	0.435	0.677	0.447
Examination Results	O.K.	O.K.	O.K.	O.K.	O.K.	O.K.	O.K.	O.K.
f_{wcd}(N/mm^2)	6.005	6.005	6.005	6.005	6.005	6.005	6.005	6.005
Diagonal Compression Failure Force V_{wcd}(kN)	7275.3	7552.4	7275.3	7552.4	7275.3	7552.4	7275.3	7552.4
$\gamma_i \cdot V_d/V_{wcd}$	0.115	0.081	0.142	0.085	0.157	0.093	0.153	0.096
Examination Results	O.K.	O.K.	O.K.	O.K.	O.K.	O.K.	O.K.	O.K.

2) Serviceability Verification

The serviceability verification is primarily conducted by ensuring that the crack width of the member resulting from the design response values at its limit state is below the limit value of crack width.

i) Serviceability verification by bending moment

The calculation of the crack width (w) is performed using the following formula:

$$w = 1.1 \times k_1 \times k_2 \times k_3 \times \{4 \times c + 0.7 \times (c_s - \varphi)\} \times (\sigma_{se} / E_s + \varepsilon'_{csd}) \qquad (2.8)$$

TCVN 11820 Part 1: 2025 Equation (I.10)

Where:

- w : design response value of the crack width (mm)
- k_1 : coefficient expressing the influence of the surface profile of reinforcing bars on crack width (when deformed bars = 1.0)
- k_2 : coefficient expressing the influence of concrete quality on crack width
  $k_2 = 15/(f_c' + 20) + 0.7 = 15/(30 + 20) + 0.7 = 1.0$
- f_c' : compressive strength of concrete (= 30N/mm^2)
  It can normally be the design value of the compressive strength f_{cd}'

TCVN 11820 Part11: 2025 Equation (4.1.20)

- k_3 : coefficient expressing the influence of the number of layers on the tensile bars, $k_3 = 5(n + 2)/(7n + 8)$
- n : number of layers of tension bars
- c : concrete cover (mm)
- c_s : distance between the centers of reinforcing bars (mm)
- φ : diameter of the tension reinforcing bar, nominal diameter of the smallest reinforcing bar (mm)
- E_s : Young's modulus of reinforcing bars (200 kN/mm^2)
- ε'_{csd} : value for considering the increase in crack width due to concrete shrinkage and creep (for structures mostly submerged in water (=0), atmospheric structures (=0.00010)).
- σ_{se} : stress increment of the reinforcing bars near the surface:
  $\sigma_{se} = M_s / (A_s j.d)$

TCVN 11820 Part 1: 2025 Equation (I.11)

- M_s : design value of the bending moment (kNmm)
- A_s : cross-sectional area of reinforcing bars (mm^2)
- j : j=1-k/3
- k : neutral axis ratio

$$k = \sqrt{2np_w + (np_w)^2} - np_w$$

- n : Young's modules ratio

$$n = \frac{E_s}{E_c} = \frac{2.0 \times 10^6}{2.8 \times 10^5} = 7.1$$

TCVN 11820 Part11: 2025 Equation (4.1.21)

- p_w : Reinforcing bar ratio

$$p_w = \frac{A_s}{b \times d}$$

- b_w : width of the member (mm)
- d : Effective height (mm)

The limit value of crack width w_a for the upper and lower sections is as follows:

Upper reinforcement section (corrosive environment)

$w_a = 0.0040 \times c = 0.0040 \times 84 = 0.336$ mm

Lower reinforcement section (particularly severe corrosive environment)

$w_a = 0.0035 \times c = 0.0035 \times 87 = 0.305$ mm

Example: Examination of Support 1 of Beam TB2

- Design value of bending moment:

  Upper side: $-M_1 = -1{,}156.4$ kN.m
  Lower side: $+M_1 = 1{,}224.8$ kN.m

- Effective height of member:

  Upper side: $d = 1{,}575$ mm
  Lower side: $d = 1{,}635$ mm

- Upper side

  Reinforcement: 2-layer reinforcement at 10cm intervals
  Layer 1: 9 bars × D32
  Layer 2: 9 bars × D25
  Total: $A_s = 11{,}708.1$ mm^2

  $k_3 = 5(2 + 2)/ (7 \times 2 + 8) = 0.909$

  $p_w = 11{,}708.1/ (1{,}000 \times 1{,}575) = 0.007434$

  $k = \{2 \times 7.1 \times 0.007434 + (7.1 \times 0.007434)^2\}^{1/2} - 7.1 \times 0.007434 = 0.277$

  $j = 1 - 0.277/3 = 0.908$

  $\sigma_{se} = 1{,}156.4 \times 10^6 / (11{,}708.1 \times 0.908 \times 1{,}575) = 69.06$ N/mm^2 $= 0.069$ kN/mm^2

  Verification for crack width:

  $w = 1.1 \times 1.0 \times 1.0 \times 0.909 \times \{4 \times 84 + 0.7 \times (100 - 32)\} \times (69.06/(200 \times 10^3) + 0.0001)$

  $= 0.173$ mm ≤ 0.336 mm OK

- Lower side

  Reinforcement: 2-layer reinforcement at 10cm intervals
  Layer 1: 9 bars × D25
  Layer 2: 6 bars × D25
  Total: $A_s = 7{,}600.5$ mm^2

  $k_3 = 5(2 + 2)/ (7 \times 2 + 8) = 0.909$

  $p_w = 7{,}600.5 / (1{,}000 \times 1{,}635) = 0.004649$

$k = \{2\times7.1\times0.004649 + (7.1\times0.004649)^2\}^{1/2} - 7.1\times0.004649 = 0.227$

$j = 1 - 0.227/3 = 0.924$

$\sigma_{se} = 1{,}224.8\times10^6/(7{,}600.5\times0.924\times1{,}635) = 106.67\ \text{N/mm}^2 = 0.107\ \text{kN/mm}^2$

Verification for crack width:

$w = 1.1\times1.0\times1.0\times0.909\times\{4\times87 + 0.7\times(100-25)\}\times(106.7/(200\times10^3) + 0.0001)$

$= 0.254\ \text{mm} \le 0.305\ \text{mm}$ OK

The crack width calculation is performed similarly for each point. The calculation results for the beam are shown in Table 2.21.

Table 2.21- Verification Results of Bending Crack Width
Verification of Serviceability (Beam TB2)

Examination of Bending Crack Width	Support 1		Support 2		Support 3		Support 4		Support 5	
	Upper Side	Lower Side	Upper Side	Lower Side	Upper Side	Lower Side	Upper Side	Lower Side	Upper Side	Lower Side
Beam Width b (mm)	1000	1000	1000	1000	1000	1000	1000	1000	1000	1000
Effective Depth d (mm)	1575	1635	1575	1635	1575	1635	1575	1635	1575	1635
Design Moment M_d(kN · m)	1156.4	1224.8	991.6	1140.9	1183.3	715.5	1813.5	830.6	2324.3	1038.2
Design Rebar Area A_s(mm^2)	11708.1	7600.5	11708.1	7600.5	11708.1	7600.5	11708.1	7600.5	11708.1	7600.5
Layer 1 (D x Bars)	D32 x 9 bars	D25 x 9 bars	D32 x 9 bars	D25 x 9 bars	D32 x 9 bars	D25 x 9 bars	D32 x 9 bars	D25 x 9 bars	D32 x 9 bars	D25 x 9 bars
Layer 2 (D x Bars)	D25 x 9 bars	D25 x 6 bars	D25 x 9 bars	D25 x 6 bars	D25 x 9 bars	D25 x 6 bars	D25 x 9 bars	D25 x 6 bars	D25 x 9 bars	D25 x 6 bars
k_1	1.000	1.000	1.000	1.000	1.000	1.000	1.000	1.000	1.000	1.000
k_2	1.000	1.000	1.000	1.000	1.000	1.000	1.000	1.000	1.000	1.000
k_3	0.909	0.909	0.909	0.909	0.909	0.909	0.909	0.909	0.909	0.909
Pure Cover c (mm)	84	87	84	87	84	87	84	87	84	87
c_o(mm)	100	100	100	100	100	100	100	100	100	100
Rebar Area Ratio pw	0.00743	0.00465	0.00743	0.00465	0.00743	0.00465	0.00743	0.00465	0.00743	0.00465
Neutral Axis Ratio k	0.277	0.227	0.277	0.227	0.277	0.227	0.277	0.227	0.277	0.227
j = 1 - k / 3	0.908	0.924	0.908	0.924	0.908	0.924	0.908	0.924	0.908	0.924
Increased Tensile Stress σ_{se}(kN/mm^2)	0.069	0.107	0.059	0.099	0.071	0.062	0.108	0.072	0.139	0.09
Crack Width W (mm)	0.173	0.254	0.153	0.238	0.177	0.164	0.249	0.184	0.309	0.22
Allowable Crack Width W_{lim}(mm)	0.336	0.305	0.336	0.305	0.336	0.305	0.336	0.305	0.336	0.305
Examination Results	O.K.	O.K.	O.K.	O.K.	O.K.	O.K.	O.K.	O.K.	O.K.	O.K.

Examination of Bending Crack Width	Span 1		Span 2		Span 3		Span 4	
	Upper Side	Lower Side	Upper Side	Lower Side	Upper Side	Lower Side	Upper Side	Lower Side
Beam Width b (mm)	1000	1000	1000	1000	1000	1000	1000	1000
Effective Depth d (mm)	1575	1635	1575	1635	1575	1635	1575	1635
Design Moment M_d(kN · m)	282.1	699.7	0.0	516.3	177.3	498.2	667.1	580.6
Design Rebar Area A_s(mm^2)	11708.1	7600.5	11708.1	7600.5	11708.1	7600.5	11708.1	7600.5
Layer 1 (D x Bars)	D32 x 9 bars	D25 x 9 bars	D32 x 9 bars	D25 x 9 bars	D32 x 9 bars	D25 x 9 bars	D32 x 9 bars	D25 x 9 bars
Layer 2 (D x Bars)	D25 x 9 bars	D25 x 6 bars	D25 x 9 bars	D25 x 6 bars	D25 x 9 bars	D25 x 6 bars	D25 x 9 bars	D25 x 6 bars
k_1	1.000	1.000	1.000	1.000	1.000	1.000	1.000	1.000
k_2	1.000	1.000	1.000	1.000	1.000	1.000	1.000	1.000
k_3	0.909	0.909	0.909	0.909	0.909	0.909	0.909	0.909
Pure Cover c (mm)	84	87	84	87	84	87	84	87
c_o(mm)	100	100	100	100	100	100	100	100
Rebar Area Ratio pw	0.00743	0.00465	0.00743	0.00465	0.00743	0.00465	0.00743	0.00465
Neutral Axis Ratio k	0.277	0.227	0.277	0.227	0.277	0.227	0.277	0.227
j = 1 - k / 3	0.90764	0.92446	0.90764	0.92446	0.90764	0.92446	0.90764	0.92446
Increased Tensile Stress σ_{se}(kN/mm^2)	0.017	0.061	0	0.045	0.011	0.043	0.04	0.051
Crack Width W (mm)	0.072	0.162	0.039	0.13	0.06	0.126	0.117	0.142
Allowable Crack Width W_{lim}(mm)	0.336	0.305	0.336	0.305	0.336	0.305	0.336	0.305
Examination Results	O.K.	O.K.	O.K.	O.K.	O.K.	O.K.	O.K.	O.K.

ii) Serviceability verification by shear force

When dealing with members subjected to shear force, if the design shear force V_d is less than 70% of the concrete shear capacity V_{cd}, there is no need to consider shear crack width. However, in this case, the member factor γ_b is generally taken as 1.0.

If consideration of shear crack width is necessary, it must be examined using appropriate methods.

If the design shear force V_d is greater than 70% of the concrete shear capacity V_{cd}, it is

sufficient to verify that the stress level of shear reinforcement σ_{se} is lower than the limit value of reinforcement stress increase shown in Table 2.22. Additionally, the stress level of stirrups can be determined using the following equation:

$$\sigma_{wpd} = \frac{(V_d + V_{rd} - k_r V_{cd}) \times s}{A_w z(\sin\alpha_s + \cos\alpha_s)} \times \frac{V_{pd} + V_{cd}}{V_d + V_{rd} + V_{cd}} \quad (2.9)$$

TCVN 11820 Part11: 2025 Equation (4.1.23)

Where:

σ_{wpd} : design stress in shear reinforcement due to permanent action
V_d : design shear force due to permanent load
V_{rd} : design shear force due to variable load
V_{cd} : design shear force acting on a bar member without shear reinforcement, where parameter γ_b may be taken as 1.0
A_w : total cross-sectional area of shear reinforcement in interval s
s : spacing in shear reinforcement
z : distance from the loading position of the resultant compressive stress to the centroid of the tension reinforcement. It may be taken as d/1.15
d : effective depth
a_s : angle between shear reinforcement and member axis
k_r : coefficient to take into account of the effects of variable loads. It may, in general, be taken as 0.5. However, it may be taken as 1.0 for members without significant effect of fatigue loads

Table 2.22- Limit Values of Reinforcement Stress Intensity (N/mm²)

Reinforcement Type	The limit value of stress intensity
Shaped rebar	120
Ordinary round steel	100
PC steel	100

Example: Examination of Support 1 of Beam TB2

- Design value of shear force:

  Upper side: V_d = 613.4 kN
  Lower side: V_d = 661.6 kN

- Effective height of member:

  Upper side: d = 1,575 mm
  Lower side: d = 1,635 mm

- Upper side

  Reinforcement: 2-layer reinforcement at 10cm intervals
  Layer 1: 9 bars × D32
  Layer 2: 9 bars × D25
  Total: A_s = 11,708.1 mm^2

  p_w = 11,708.1/ (1,000×1,575) = 0.007434

  Design value of concrete shear capacity:

$f_{vcd} = 0.2 \times 30.0^{1/3} = 0.621$

$\beta_d = (100/157.5)^{1/4} = 0.893$

$\beta_p = (100 \times 0.007434)^{1/3} = 0.906$

$V_{cd} = 0.893 \times 0.906 \times 0.621 \times 1{,}000 \times 1{,}575 / 1.0 = 791{,}319 \text{ N} = 791.3 \text{ kN}$

$0.7 \times V_{cd} = 0.7 \times 791.3 = 553.9 \text{ kN} < V_d = 613.4 \text{ kN}$

Therefore, the examination of the stress level of stirrups should be conducted.

Design stress intensity of shear reinforcing bars:

$$\sigma_{wpd} = \frac{(613.4 - 1.0 \times 791.3) \times 200}{506.8 \times 1{,}370(\sin 90 + \cos 90)} \frac{163.4+791.3}{613.4+791.3} \times 10^3$$

$= -34.85 \text{ N/mm}^2 < \sigma_{se} = 120 \text{ N/mm}^2$ OK

- Lower side

  Reinforcement: 2-layer reinforcement at 10cm intervals
  Layer 1: 9 bars × D25
  Layer 2: 6 bars × D25
  Total: $A_s = 7{,}600.5 \text{ mm}^2$

  $p_w = 7{,}600.5 / (1{,}000 \times 1{,}635) = 0.004649$

  Design value of concrete shear capacity:

  $f_{vcd} = 0.2 \times 30.0^{1/3} = 0.621$

  $\beta_d = (100/163.5)^{1/4} = 0.884$

  $\beta_p = (100 \times 0.004649)^{1/3} = 0.775$

  $V_{cd} = 0.884 \times 0.775 \times 0.621 \times 1{,}000 \times 1{,}635 / 1.0 = 695{,}606 \text{ N} = 695.6 \text{ kN}$

  $0.7 \times V_{cd} = 0.7 \times 695.6 = 486.9 \text{ kN} < V_d = 661.6 \text{ kN}$

  Therefore, the examination of the stress level of stirrups should be conducted.

  Design stress intensity of shear reinforcing bars:

$$\sigma_{wpd} = \frac{(661.6 - 1.0 \times 695.6) \times 200}{506.8 \times 1{,}422(\sin 90 + \cos 90)} \frac{206.4+695.6}{661.6+695.6} \times 10^3$$

  $= -6.277 \text{ N/mm}^2 < \sigma_{se} = 120 \text{ N/mm}^2$ OK

Similar calculations are performed for each point. The calculation results for the beam are shown in Table 2.23.

Table 2.23- Verification results of Shear Force
Verification of Serviceability (Beam TB2)

Design for Shear Force	Support 1		Support 2		Support 3		Support 4		Support 5	
	Upper Side	Lower Side	Upper Side	Lower Side	Upper Side	Lower Side	Upper Side	Lower Side	Upper Side	Lower Side
Beam Width b (mm)	1000	1000	1000	1000	1000	1000	1000	1000	1000	1000
Effective Depth d (mm)	1575	1635	1575	1635	1575	1635	1575	1635	1575	1635
Design Shear Force V_d(kN)	613.4	661.6	692.8	658.7	762.7	650.1	757.7	652.3	757.5	613.4
Design Rebar Area A_s(mm^2)	11708.1	7600.5	11708.1	7600.5	11708.1	7600.5	11708.1	7600.5	11708.1	7600.5
Rebar Area Ratio pw	0.00743	0.00465	0.00743	0.00465	0.00743	0.00465	0.00743	0.00465	0.00743	0.00465
β_d	0.893	0.884	0.893	0.884	0.893	0.884	0.893	0.884	0.893	0.884
β_p	0.906	0.775	0.906	0.775	0.906	0.775	0.906	0.775	0.906	0.775
β_n	1.000	1.000	1.000	1.000	1.000	1.000	1.000	1.000	1.000	1.000
f'_{vcd}(N/mm^2)	0.621	0.621	0.621	0.621	0.621	0.621	0.621	0.621	0.621	0.621
Shear Rebar Diameter and Interval	D13 @200	D13 @200	D13 @200	D13 @200	D13 @200	D13 @200	D13 @200	D13 @200	D13 @200	D13 @200
Shear Rebar Area A_w(mm^2)	506.8	506.8	506.8	506.8	506.8	506.8	506.8	506.8	506.8	506.8
Angle to Member Axis α_s(deg)	90	90	90	90	90	90	90	90	90	90
Shear Strength of Concrete V_{cd}(kN)	791.3	695.6	791.3	695.6	791.3	695.6	791.3	695.6	791.3	695.6
V_{cd}x 70% (kN)	553.9	486.9	553.9	486.9	553.9	486.9	553.9	486.9	553.9	486.9
Shear Force under Permanent Load V_{pd}(kN)	163.4	206.4	182.8	200.5	197.9	192.8	196.5	188.2	210.2	163.4
Coefficient considering the frequency of live loads k_2	1.000	1.000	1.000	1.000	1.000	1.000	1.000	1.000	1.000	1.000
Shear Reinfocement Stress σ_{wd}(N/mm^2)	-34.849	-6.277	-18.63	-6.774	-5.256	-8.339	-6.178	-7.885	-6.301	-14.979
Limit Value of Increase Stress (N/mm^2)	120	120	120	120	120	120	120	120	120	120
Examination Results	O.K.	O.K.	O.K.	O.K.	O.K.	O.K.	O.K.	O.K.	O.K.	O.K.

Design for Shear Force	Span 1		Span 2		Span 3		Span 4	
	Upper Side	Lower Side	Upper Side	Lower Side	Upper Side	Lower Side	Upper Side	Lower Side
Beam Width b (mm)	1000	1000	1000	1000	1000	1000	1000	1000
Effective Depth d (mm)	1575	1635	1575	1635	1575	1635	1575	1635
Design Shear Force V_d(kN)	338.4	238.5	430.4	267.8	477.2	292.4	470.1	269.1
Design Rebar Area A_s(mm^2)	11708.1	7600.5	11708.1	7600.5	11708.1	7600.5	11708.1	7600.5
Rebar Area Ratio pw	0.00743	0.00465	0.00743	0.00465	0.00743	0.00465	0.00743	0.00465
β_d	0.893	0.884	0.893	0.884	0.893	0.884	0.893	0.884
β_p	0.906	0.775	0.906	0.775	0.906	0.775	0.906	0.775
β_n	1.000	1.000	1.000	1.000	1.000	1.000	1.000	1.000
f'_{vcd}(N/mm^2)	0.621	0.621	0.621	0.621	0.621	0.621	0.621	0.621
Shear Rebar Diameter and Interval	D13 @200	D13 @200	D13 @200	D13 @200	D13 @200	D13 @200	D13 @200	D13 @200
Shear Rebar Area A_w(mm^2)	506.8	506.8	506.8	506.8	506.8	506.8	506.8	506.8
Angle to Member Axis α_s(deg)	90	90	90	90	90	90	90	90
Shear Strength of Concrete V_{cd}(kN)	791.3	695.6	791.3	695.6	791.3	695.6	791.3	695.6
V_{cd}x 70% (kN)	553.9	486.9	553.9	486.9	553.9	486.9	553.9	486.9
Shear Force under Permanent Load V_{pd}(kN)	0	11.818	0	1.306	1.846	0	10.973	0
Coefficient considering the frequency of live loads k_2	1.0	1.0	1.0	1.0	1.0	1.0	1.0	1.0
Shear Reinfocement Stress σ_{wd}(N/mm^2)	———	———	———	———	———	———	———	———
Limit Value of Increase Stress (N/mm^2)	———	———	———	———	———	———	———	———
Examination Results	———	———	———	———	———	———	———	———

- End -